MONSANTO RESEARCH CORPORATION

A SUBSIDIARY OF MONSANTO COMPANY

BOSTON
LABORATORY

EVERETT, MASSACHUSETTS 02149

FINAL REPORT
STUDY OF FUEL CELLS USING STORABLE ROCKET PROPELLANTS

Contract No. NAS3-2791
28 June 1963 to 27 January 1964

11 May 1964

MRC Report No. MRB5002F
NASA Report No. CR-54116

For

National Aeronautics and Space Administration
Lewis Research Center
Cleveland, Ohio

Authors

J. O. Smith

R. E. Chute
R. G. Gentile
D. L. Kavanaugh
E. A. McElhill
J. C. Orth
W. H. Power
R. H. M. Simon
G. B. Skinner
A. D. Snyder
S. P. Terpko

Contributors

M. L. Cook
G. S. Robinson
J. Sumrall

Technical Management

NASA - Lewis Research Center
APGO - Robert B. King

MONSANTO RESEARCH CORPORATION
BOSTON LABORATORY
Everett, Massachusetts 02149
Telephone: 617-389-0480

NOTICES

This report was prepared as an account of Government sponsored work. Neither the United States nor the National Aeronautics and Space Administration (NASA), nor any person acting on behalf of NASA:

A) Makes any warranty or representation, expressed or implied, with respect to the accuracy, completeness, or usefulness of the information contained in this report, or that the use of any information, apparatus, method, or process disclosed in this report may not infringe privately-owned rights; or

B) Assumes any liabilities with respect to the use of, or for damages resulting from the use of any information, apparatus, method or process disclosed in this report.

As used above, "person acting on behalf of NASA" includes any employee or contractor of NASA, or employee of such contractor, to the extent that such employee or contractor of NASA or employee of such contractor prepares, disseminates, or provides access to, any information pursuant to his employment or contract with NASA, or his employment with such contractor.

———o———

Copies of this report can be obtained from:

National Aeronautics and Space Administration
Office of Scientific and Technical Information
Washington 25, D.C.
Attention: AFSS-A

TABLE OF CONTENTS

TABLE OF CONTENTS (cont'd.)

TABLE OF CONTENTS (cont'd.)

TABLE OF CONTENTS (cont'd.)

LIST OF TABLES

LIST OF TABLES (cont.)

LIST OF FIGURES

LIST OF FIGURES (Cont.)

I. INTRODUCTION

The proposed use of storable rocket propellants for many space missions suggests the possibility of their utilization in a fuel cell to produce electrical energy.

A fuel cell using storable rocket propellants has the important advantage over the more conventional hydrogen-oxygen cell of eliminating the necessity for cryogenic facilities. Thus, problems of supply, storage, and handling are simplified or eliminated.

A. OBJECTIVE

The objective of this work was to perform a feasibility study of hydrazine-type fuels and dinitrogen tetroxide (N_2O_4) or chlorine trifluoride (ClF_3) oxidants for use in fuel cells. This was a preliminary investigation whose ultimate aim was to develop a fuel cell design that would operate relatively efficiently on a variety of storable rocket propellants such as may be used in space missions in the future. The work was conducted by combining theoretical and analytical studies with planned experimentation.

The literature provides free energy data from which the reversible potential of the oxidant and fuel electrode can be estimated. Also, the reversible energy-to-weight ratio for a given oxidant-reductant system can be calculated. Therefore, upper limits of performance can be predicted. The purpose of calculating the theoretical performance of fuel cells was threefold:

1. To provide a basis for comparing and choosing systems for study.

2. To provide a measure of our state of sophistication in building cells and predicting their performance.

3. To indicate areas where the mechanisms are not well understood so as to provide a scope for future investigations.

The theoretical calculations are, of course, valid only for the specific reversible reaction postulated.

The experimentation both in half cells and in full cells establishes the actual performance of the electrodes, the types of reactions taking place, and the extent of the various types of polarization (activation, concentration, and IR drop). The catalytic properties of the electrolytes and the stability of catalysts under different loads in the presence of different electrolytes can only be determined experimentally.

B. SCOPE OF THIS REPORT

Theoretical studies were made of the thermodynamic properties of the fuel cell systems under study. The potentials and energy density for the most probable reactions were calculated. The heat absorbed or evolved during the reversible operation of a fuel cell was calculated. Such data provide a base from which the theoretical performance of the various proposed systems can be defined.

This report contains the following experimental data:

- Polarization Studies

  -- The anodic oxidation of hydrazine and its derivatives in acid, basic, and neutral aqueous electrolytes, in anhydrous hydrogen fluoride systems, and in nonaqueous organic systems.

  -- The cathodic reduction of nitric acid and dinitrogen tetroxide in aqueous media, the cathodic reduction of dinitrogen tetroxide in anhydrous hydrogen fluoride and in nonaqueous organic solvents, and the cathodic reduction of chlorine trifluoride in anhydrous hydrogen fluoride systems.

  -- The construction and use of vapor transport electrodes for the oxidation of hydrazine.

- Full Cell Operation

  -- The construction and demonstration of the hydrazine-nitric acid and the hydrazine-dinitrogen tetroxide fuel cells.

II. SUMMARY

A. THERMODYNAMIC CALCULATIONS

The thermodynamic properties of storable propellants and the products of reaction were calculated for 25°C and 90°C. These properties (tabulated in Tables 1, 2, and 3 in Section IV) permit calculation of the reversible performance of selected electrochemical reactions in terms of voltage, energy per pound, reversible heat effects, and temperature sensitivity (Tables 4 and 5, Section IV).

Thermodynamic calculations have shown that a number of the fuel/oxidant systems investigated under this contract are endothermic when the electrochemical operations occur reversibly. Thus, hydrazine-dinitrogen tetroxide fuel cell systems, performing reversibly at 90°C, require that heat energy be supplied to the cell equivalent to 36% of the power output. Also, if certain fuels such as monomethylhydrazine (MMH), unsymmetrical dimethylhydrazine (UDMH), methanol, and propane can be reformed with water to yield hydrogen, the total operation, reforming plus using the hydrogen reversibly in a complete cell with nitric acid or dinitrogen tetroxide, will yield endothermic heat effects equal to 22-35% of the power output.

The endothermic property of those systems make them attractive for use in space vehicles where elimination of heat presents a problem and limits the module size of intrinsically exothermic fuel cell systems such as the hydrogen-oxygen system. An endothermic fuel cell also raises the possibility of using the cell as an electrochemical heat pump to absorb heat ($T \Delta S$) at the capsule temperature and reject the heat by radiation from a tungsten filament (5000°C) outside the capsule. Another contribution of thermodynamic calculations is the identification of phenomena that may contribute to energy loss.

Voltage losses due to the use of aqueous hydrazine (instead of pure hydrazine) and to the dissociation of nitrogen tetroxide ($N_2O_4 = 2NO_2$) are negligible (1 to 2%). However, the voltage loss due to the spontaneous thermal decomposition of hydrazine ($N_2H_4 \longrightarrow 2H_2 + N_2$) prior to the electrochemical reaction is not negligible and results in a loss of 0.44 volt from a possible 1.47 volts. A system that prevents this spontaneous decomposition, therefore, has a significant advantage (0.44 volt) over one in which the spontaneous decomposition takes place.

If a full cell is constructed such that a pH difference exists across an ion exchange membrane, this pH difference will not contribute to the full cell potential if the current is carried only by the H^+ or the OH^- ion. If ions other than those responsible for the pH difference carry the current, then the pH difference and the difference in chemical potential across the separator of the current carrying ions will contribute to the full-cell potential.

B. AQUEOUS SYSTEMS

1. Half-Cell Studies

a. Polarization Tests

N_2H_4 was found to be an excellent fuel in terms of electrochemical oxidation for short-term polarization tests. The fuel performed best in base with electroplated rhodium catalysts or chemically precipitated rhodium and ruthenium catalysts. In 5M H_3PO_4 electrolyte, chemically precipitated ruthenium catalysts proved superior.

Neither MMH nor UDMH showed promise as electrochemical fuels. MMH was better than UDMH. Polarization of 0.3 volt to 0.5 volt at 50 to 100 ma/cm^2, respectively, were found at 80°C in acid electrolyte.

HNO_3, either as 1M solution in 5M H_2SO_4 or 5M solution, was an excellent electrochemical oxidant in terms of polarization curves. For a cathodic current of 100 ma/cm^2, 0.20 volt polarization at 30°C and less than 0.10 volt at 90°C were found using a variety of catalyst/substrate systems. Uncatalyzed carbon (Pure Carbon porous FC-13 or -14) worked nearly as well as catalyzed electrodes and proved to be stable in up to 0.5M N_2H_4 at 90°C.

N_2O_4 showed promise as a source of HNO_3, as an aqueous solution of N_2O_4, or as a gas electrode, in various electrolytes. For low temperature work aqueous N_2O_4 tested better than HNO_3 at low H^+ concentration. With gaseous N_2O_4 as oxidant on an uncatalyzed porous carbon electrode, currents of over 100 ma/cm^2 could be obtained without severe polarization at 30°C and 60°C.

b. Stability Tests

The electrochemical oxidation of N_2H_4 was found to be unstable in long-term tests with most catalyst/electrode systems in either acid or base. For all electroplated catalyst/substrate systems, rapid deterioration occurred within 24 hours at either 30°C or 90°C. The 90°C results were better than those at 30°C. However, chemically precipitated catalysts gave significantly better results, and Ir (32%)-Ru(68%) at 30°C in 1M KOH and 1M N_2H_4 showed less than 0.1 volt deterioration over a 700-hour period. At 90°C in 1M KOH and 1M N_2H_4 the Ir-Ru catalyst deteriorated 0.2 volt after 300 hours, and a Ru catalyst in 3M N_2H_4 and 1M KOH started at a better potential and lasted over 300 hours, with a linear deterioration before reaching 0.2 volt polarization.

In 5M H_3PO_4, 1M N_2H_4 was not satisfactory in long-term tests. At 90°C, using chemically precipitated ruthenium catalysts in 2M N_2H_4 and 5M H_3PO_4, a quick initial polarization of 0.1 volt occurred; thereafter, negligible polarization took place for over 600 hours.

MMH and UDMH rapidly deteriorated under long-term electro-oxidation regardless of catalyst.

5M HNO_3 with Au/SS (stainless steel) catalyst at 30°C showed no deterioration in potential after 1000 hours of continuous operation at 100 ma/cm^2.

c. Mechanism Tests

N_2H_4 was found to be oxidized exclusively to N_2 in either acid or basic electrolyte within limits of experimental error.

MMH was found to be oxidized to CH_3OH and N_2 in 5M H_3PO_4, with a small amount of CH_3OH further oxidized.

UDMH was found to be oxidized to N_2 by a four-electron reaction in 5M H_3PO_4. In 5M H_2SO_4 a mixture of products appeared; initially a two-electron reaction probably produced a tetrazine, and as deterioration of potential occurred, a mixed reaction producing some N_2 was found. The maximum electron change was about three for overall tests when the electrode failed.

HNO_3, as either 5M HNO_3, or as 1M HNO_3 in 5M H_2SO_4, produced NO nearly exclusively. At 30°C a small amount of N_2 was produced at Au/C electrodes. At 90°C some N_2O_4 was produced initially, but NO was the only product after reaching steady state conditions.

2. Full Cell Studies

Full cell studies demonstrated the feasibility of using hydrazine and monomethylhydrazine as fuels, and HNO_3, N_2O_4, and H_2O_2 as oxidants. The electrolytes consisted of 5M H_2SO_4, 5M H_3PO_4 and KOH. Porous Teflon or Teflon-impregnated glass* vapor diffusion electrodes were demonstrated for both fuels and oxidants in combination with the above electrolytes.

A full cell was constructed using two porous Teflon electrodes pressed against a cation exchange membrane.** This cell delivered 1.1 volts at 25°C, 1 atmosphere and 17.5 ma/cm² for 30 hours.*** The IR free voltage was 1.4 volts. This type of electrode construction appears to be stable. Feasibility of using MMH directly at this anode was also demonstrated. A material balance indicated that $N_2H_5^+$ was the current carrying species when a cation exchange membrane was used, which accounts in part for the high open-circuit potential. Advantages of the porous Teflon electrode in combination with an ion exchange membrane are the virtual absence of spontaneous decomposition of reactants (allowing storage of the concentrated reactant in contact with the Teflon) and the elimination of reactant feeding problems. The possibility also exists of limiting the ionic species to H^+ if hydrogen is the fuel or OH^- if H_2O_2 is the oxidant, thus minimizing waste of reactants due to diffusion.

C. NONAQUEOUS SYSTEMS

1. Polarization Studies

The anodic oxidation of hydrazine dihydrogen fluoride (HDHF) ($N_2H_4 \cdot 2HF$) and the cathodic reduction of chlorine trifluoride (CTF) have been demonstrated in anhydrous hydrogen fluoride (AHF) and in AHF-KF melts. Current densities up to 5 ma/cm² were attained at carbon anodes in 1M HDHF in AHF at 0.5 volt polarization and at 3°C. Current densities of 20 ma/cm² were attained during the cathodic reduction of CTF in AHF at 3°C. Current densities as high as 100 ma/cm² were attained during the cathodic reduction of 1.0M dinitrogen tetroxide (N_2O_4) at ruthenized platinum electrodes in AHF, but potentials were too low to be of interest. Current densities up to 100 ma/cm² were attained at anodes in contact with 1M HDHF in a molten solution of $KF \cdot 3HF$ at 85°C and at anodic polarization of 0.5 volt. Cathodic current densities of 5 ma/cm² were demonstrated in the same electrolyte at 85°C and at the same polarization.

---

*A Pall membrane, which is a Teflon-impregnated porous glass material.

**Ionics, Inc. Cation exchange membrane 61 AZL-183. 85% $N_2H_4 \cdot H_2O$ fuel - 70% HNO_3 Oxidant

*** Test arbitrarily terminated after 30 hours.

2. Reactant Compatibility

Upper compatibility limits for solutions of hydrazine and chlorine trifluoride in anhydrous hydrogen fluoride were established. Solutions of these reactants in concentrations greater than 1 molar of oxidant or reductant reacted violently. Below this concentration, although there may be some reaction, it should be possible to design a cell with an efficient separator to prevent excessive heat generation due to chemical mixing.

3. Reference Electrodes in Anhydrous Hydrogen Fluoride

The silver, cadmium, and lead fluoride electrodes and the palladium-hydrogen reference electrode were constructed, and relative potentials were assigned in anhydrous hydrogen fluoride in 0.5M sodium fluoride at 3°C, and also in the composition KF.3HF at 85°C. (Table 34 and 35).

4. Organic Solvents

The anhydrous organic solvents, acetonitrile (AN), N,N-dimethyl-formamide (DMF), propylene carbonate, and pyridine, were investigated for the cathodic reduction of N_2O_4 and for the oxidation of HDHF with magnesium perchlorate, potassium thiocyanate, and tetramethyl ammonium chloride as conducting salts. The best combination of solvent and electrolyte for the anodic oxidation of hydrazine was DMF with tetramethyl ammonium chloride, which was used with a platinized steel electrode to give a current density of 10 ma/cm^2 at a polarization of 0.5 volt.

The best organic solvent for the cathodic reduction of N_2O_4 was AN with an electrolyte of magnesium perchlorate. This combination resulted in a cathodic current density of 70 ma/cm^2 at 0.5 volt polarization at the platinized steel electrode.

5. Solid Palladium Anode

A hydrazine solid palladium electrode was demonstrated as an anode and as a reference electrode in anhydrous hydrogen fluoride. An anodic current of 10 ma/cm^2 was carried at 3°C with a polarization of 0.5 volt.

III. CONCLUSIONS

A. THERMODYNAMIC CALCULATIONS

The endothermic properties of the reversible electrochemical reaction of dinitrogen tetroxide with hydrazine at 25°C (31.6% of the maximum free energy), with hydrogen (18.2%), with methanol (33.4%), and with propane (35.2%) make these systems potentially attractive for space vehicles where heat elimination is a problem. Thermal decomposition of hydrazine ($N_2H_4 = 2H_2 + N_2$) prior to the anodic reaction reduces the endothermicity to that of the hydrogen-dinitrogen tetroxide system.

The use of these fuel cell systems as heat pumps in space capsules to absorb heat ($T \Delta S$) at the capsule temperature and reject the heat by radiation from a tungsten filament outside the capsule is a possibility.

B. AQUEOUS SYSTEMS

Hydrazine was found to be an excellent electrochemical fuel. It is anodically oxidized exclusively to nitrogen and water in either acid or base. The best catalyst for long-term anodic oxidation of hydrazine was chemically precipitated iridium-ruthenium on a carbon substrate. This system gave an initial potential of +0.08 volt vs HE at 100 ma/cm^2 load; and after a 700-hour test period demonstrated a deterioration of potential of only 0.1 volt.

Unsymmetrical dimethylhydrazine and monomethylhydrazine gave poor initial electrochemical performance; potentials rapidly deteriorated under long-term testing regardless of catalyst type.

Nitric acid, either as 1M solution in 5M sulfuric acid or as 5M solution, was an excellent electrochemical oxidant, operating 1000 hours at +0.98 volts vs HE at 100 ma/cm^2. A gold-catalyzed stainless steel cathode showed no deterioration in potential during a 1000-hour test. The nitric acid was reduced nearly exclusively to nitric oxide.

Limited work done with dinitrogen tetroxide showed that it compares favorably with nitric acid as an electrochemical oxidant.

Full-cell studies have demonstrated the feasibility of using hydrazine fuel with nitric acid, dinitrogen tetroxide, or hydrogen peroxide as oxidants. A full cell using porous Teflon electrodes pressed against a cation exchange membrane delivered 1.1 volts at 17.5 ma/cm^2 at 25°C for 30 hours.

C. NONAQUEOUS SYSTEMS

Encouraging anode current densities as high as 100 ma/cm^2 at 0.48 volt vs HE were attained in electrodes in contact with hydrazine dihydrogen fluoride in a molten solution of $KF \cdot 3HF$ at 85°C. It appears that continued work on the hydrazine/chlorine trifluoride system in anhydrous hydrogen fluoride is justified.

With the nonaqueous organic electrolytes acetonitrile, N,N-dimethylformamide, propylene carbonate, and pyridine, half-cell tests demonstrated the cathodic reduction of dinitrogen tetroxide and anodic oxidation of hydrazine. The results are not sufficiently promising to warrant further work.

IV. THEORETICAL STUDIES

The purpose of obtaining thermodynamic properties by theoretical analysis is to permit calculation of the reversible performance of selected electrochemical reactions in terms of voltage, energy per pound, efficiency, and reversible heat effects and to determine the sensitivity of this performance to temperature changes.

The number of possible electrochemical reactions that can arbitrarily be written is large. To insure that the calculations will have meaning and to avoid confusion from detailing all the possible reactions, only those systems have been analyzed whose practicality can be supported by experimental evidence.

A. THERMODYNAMIC TABULATION

To calculate the potential of a fuel cell system, it is necessary to know the free energy of formation of the reactants and products.

Table 1 lists the thermodynamic properties for the pure chemical species at 298°K (25°C) and 1 atmosphere. For hydrazine, all the properties except free energy of formation of the liquid ($\Delta F^\circ_{f\ liq}$) were available in the literature. Since the liquids are not in equilibrium with the vapors at 298°K and 1 atm, $\Delta F^\circ_{f\ liq} \neq \Delta F^\circ_{f\ gas}$.

The difference in the ΔF°_f for liquid and gas results from the entropy change in compressing the vapor from its autogenous pressure to 1 atmosphere. This calculation is shown in Appendix A-1. For monomethylhydrazine and unsymmetrical dimethylhydrazine, the heat of formation (ΔH°_f) was calculated from literature values of the heat of combustion (ΔH°_c), which, in turn, permitted calculation of ΔF°_f through the relation $\Delta F = \Delta H - T\Delta S$.

The voltage of this fuel cell is determined from ΔF of the reaction:

$$\Delta F_{joules} = -nFE$$

where n is the number of electrons transferred, F = 96,500 coulombs, and E is the voltage.

Table 4 presents the energy yield and the open-circuit potentials for the various fuel-oxidant couples.

The fuel-cell potentials were calculated for reversible reactions. They represent, therefore, an upper limit of performance

Given the thermodynamic properties at 25°C (Table 1), these properties at 90°C were calculated from heat capacity data:

Table 1

THERMODYNAMIC PROPERTIES OF FUEL CELL REACTANTS AND PRODUCTS

	Liquid at 25°C and 1 Atmosphere				Ideal Gas at 25°C and 1 Atmosphere				
Compound	ΔH° combust Kcal/mole	ΔH° Kcal/mole	ΔF°_f Kcal/mole	S° cal deg mole	ΔH° vap Kcal/mole	ΔH°_f Kcal/mole	ΔF°_f Kcal/mole	S° cal deg mole	Source
N_2H_4	-148.62								(4)
		12.05		29.41	10.700	22.75	37.89	57.41	(3)
			35.54						Calculated
CH_3NHNH_2	-311.71								(4)
				39.66	9.648			66.61	(5)
		12.703	41.83			21.351*	43.44*		Calculated
$(CH_3)_2NNH_2$	-473.38								(7)
				47.86	8.366			72.82	(6)
		11.266	48.65			19.632	49.58		Calculated
ClF_3						-38.869	-29.542	68.034	(8)
		-45.587	-29.229	44.449	6.718				Calculated
F_2						0	0	48.447	(8)
Cl_2						0	0	53.289	(8)
HF						-64.500	-65.002	41.510	(8)
HCl						-21.970	-22.685	44.645	(8)
N_2O_4						2.309	23.491	72.73	(1)
HNO_3		-41.404	-19.100	37.19				63.62	(1)
NO						21.6	20.719	50.339	(1)
CH_3OH		-57.04	-39.17	30.3		-48.10	-38.70	56.8	(2)
CO						-26.42	-32.81	47.3	(2)
CO_2						-94.05	-94.26	51.6	(2)
H_2O		-68.317	-56.69	16.716		-57.798	-54.635	45.106	(1)
H_2						0	0	31.21	(2)
N_2						0	0	45.77	(2)
C graphite B		0	0	1.36					(2)
C_3H_8						-24.82	-5.61	64.51	(2)

*Calculated from spectroscopic data

Table 2

THERMODYNAMIC PROPERTIES OF FUELS

	Liquid					Ideal Vapor				
	$\frac{cal}{mole\ °K}$	kcal per gram mole			$\frac{kcal}{g\text{-}mole\ °K}$	kcal/gram mole			$\frac{kcal}{g\text{-}mole\ °K}$	
	C_p	$\Delta H°_{combust.}$	$\Delta H°_f$	$\Delta F°_f$	$S°$	ΔH_{evap}	$\Delta H°_f$	$\Delta F°_f$	$S°$	Source
N_2H_4 at 298°K 1 atm	23.62_{liq}	-148.62	12.05		29.41	10.70	22.75	37.89	57.41	(4) (3)
				35.54						Calculated
N_2H_4 at 363°K 1 atm	24.86_{liq}		12.278	40.634	34.177	10.040	22.318	41.235	60.177	Calculated
CH_3NHNH_2 at 298°K 1 atm	32.25_{liq}	-311.71			39.66	9.648			66.61	(4) (5)
			12.703	41.83			21.351	43.44		Calculated
CH_3NHNH_2 at 363°K 1 atm	33.10_{liq}		11.879	48.384	46.112	8.633	20.512	48.342	70.009	Calculated
$(CH_3)_2NNH_2$ at 298°K 1 atm	39.21_{liq}	-473.38			47.86	8.366			72.82	(7) (6)
			11.266	48.65			19.632	49.58		Calculated
$(CH_3)_2NNH_2$ at 363°K 1 atm	41.37_{liq}		11.266	56.796	55.805	7.483	18.748	56.188	78.092	Calculated

Table 3

THERMODYNAMIC PROPERTIES OF OXIDANTS AND REACTION PRODUCTS

	C_p cal/mole °C	Liquid at 1 atm: Kcal per gram mole $\Delta H^\circ_{combust}$	ΔH°_f	ΔF°	cal/g-mole °C S°	Ideal Vapor at 1 atm: Kcal per gram mole ΔH_{evap}	ΔH°_f	ΔF°_f	cal/g-mole °C S°	Source
N_2O_4 at 25°C	15.68_{gas}						2.309	23.491	72.73	(1) (9)
N_2O_4 at 90°C	16.81_{gas}						1.99	28.146	75.935	Calculated
N_2 at 25°C	6.95_{gas}						0	0	45.77	(2)
N_2 at 90°C	6.98_{gas}						0	0	47.144	Calculated (10)
NO at 25°C	7.16_{gas}						21.6	20.719	50.339	(1)
NO at 90°C	7.17_{gas}						21.607	20.527	51.747	Calculated (11)
H_2O at 25°C	17.98_{liq}		-68.317	-56.69	16.716		-57.798	-54.635	45.106	(1) (12)
H_2O at 90°C	18.09_{liq}		-67.744	-54.196	20.471		-57.929	-53.933	46.767	Calculated (12)
O_2 at 25°C	7.02_{gas}						0	0	49.003	Latimer (1)
O_2 at 90°C	7.17_{gas}						0	0	50.402	Calc from Cp (10)
H_2 at 25°C	6.88_{gas}						0	0	31.21	(2)
H_2 at 90°C	6.91_{gas}						0	0	32.571	Calculated (10)

Table 4

ENERGY YIELD AND CELL POTENTIALS FOR
REVERSIBLE REACTIONS AT 25°C AND 1 ATMOSPHERE

	Watt-hr/lb	Full Cell volts
$3N_2H_4 + 4HNO_3 \longrightarrow 8H_2O + 4NO + 3N_2$	610	1.45
$5N_2H_4 + 4HNO_3 \longrightarrow 7N_2 + 12H_2O$	1000	1.7
$N_2H_4 + N_2O_4 \longrightarrow N_2 + 2NO + 2H_2O$	557	1.42
$2N_2H_4 + N_2O_4 \longrightarrow 3N_2 + 4H_2O$	1080	1.74
$N_2H_4 + ClF_3 \longrightarrow N_2 + HCl + 3HF$	950	2.42
$3CH_3NHNH_2 + 4HNO_3 \longrightarrow 3CH_3OH + 3N_2 + 4NO + 5H_2O$	495	1.33
$CH_3NHNH_2 + 2HNO_3 \longrightarrow CO_2 + 2N_2 + 4H_2O$	1000	1.41
$3CH_3NHNH_2 + 10HNO_3 \longrightarrow 3CO_2 + 3N_2 + 10NO + 14H_2O$	550	1.16
$CH_3NHNH_2 + N_2O_4 \longrightarrow CH_3OH + 2NO + N_2 + H_2O$	460	1.30
$3(CH_3)_2NNH_2 + 16HNO_3 \longrightarrow 6CO_2 + 3N_2 + 16NO + 20H_2O$	535	1.09
$5(CH_3)_2NNH_2 + 16HNO_3 \longrightarrow 10CO_2 + 13N_2 + 28H_2O$	1000	1.34
$(CH_3)_2NNH_2 + 4N_2O_4 \longrightarrow 2CO_2 + N_2 + 8NO + 4H_2O$	480	1.06

Basis:

Liquid Phase - All Fuels
HNO_3
CH_3OH
H_2O

Gas Phase - N_2O_4
NO
HCl
HF

$$1.\quad \Delta H_{363} = \Delta H_{298} + \int_{298}^{363} \Delta C_p dT$$

$$2.\quad S_{363} = S_{298} + \int_{298}^{363} \frac{C_p}{T}\, dT$$

In some cases the heat capacity data were provided in the form

$$C_p = a + bT + cT^2 + dT^3$$

In other cases the C_p was tabulated versus temperature. These data were then fitted to the form

$$C_p = a + bT + cT^2.$$

If ΔC_p is in the form:

$$\Delta C_p = \Delta a + \Delta bT + \Delta cT^2 + \Delta dT^3$$

the formula for calculating ΔH_T° at any temperature is:

$$3.\quad \Delta H_T^\circ = I_H + \Delta aT + \frac{\Delta b}{2} T^2 + \frac{\Delta c}{3} T^3 + \frac{\Delta d}{4} T^4$$

Then from the Gibbs-Helmholtz equation:

$$4.\quad \frac{\Delta F_T^\circ}{T} = -\int \frac{\Delta H_T^\circ}{T^2}\, dT$$

$$5.\quad \frac{\Delta F_T^\circ}{T} = \frac{I_H}{T} + I_F - \Delta a \ln T - \frac{\Delta b}{2} T - \frac{\Delta c}{6} T^2 - \frac{\Delta d}{12} T^3$$

where I_H and I_G are constants of integration which may be evaluated by equations 3 and then 5 if ΔH° and ΔF° are known at any one temperature.

In order to insure that the calculated data were consistent and that arithmetic errors had not been made, the data in Tables 2 and 3 were tested for consistency by the equation

$$\Delta F = \Delta H - T \Delta S$$

B. <u>THERMODYNAMIC CALCULATIONS FOR THE N_2O_4-N_2H_4 CELL</u>

Table 5 shows the calculated results obtained with the reaction

$$N_2H_{4liq} + N_2O_{4gas} \longrightarrow N_{2gas} + 2NO_{gas} + 2H_2O_{gas}$$

at 25°C and 90°C.

An important consideration concerning the reversible electrochemical reaction:

$$N_2H_4 + N_2O_4 \longrightarrow N_2 + 2NO + 2H_2O \text{ (gas at 90°C and 1 atm)}$$

$$\Delta F = \Delta H - T \Delta S$$

$$-135.6 \text{ Kcal} = -86.9 \text{ Kcal} - 48.7 \text{ Kcal}$$

is the fact that heat must be supplied to the cell to maintain the temperature. This fact has two important consequences.

Table 5

THEORETICAL PERFORMANCE FOR THE FULL CELL REACTION:

$$N_2H_4\ (Liq) + N_2O_4\ (Gas) \longrightarrow N_2 + 2NO\ (Gas) + 2H_2O\ (Gas)$$

	25°C at 1 atm	90°C at 1 atm
ΔH kcal/mole reaction	-86.75	-86.92
ΔF kcal/mole	-126.86	-135.61
ΔS cal/mole/deg	134.52	134.06
ΔC_p cal/mole/deg	17.93	16.06
$-T\Delta S$ kcal/mole	-40.11	-48.69
Voltage	1.37	1.47
Watt-hours/lb	537	575
Reversible Heat Effects = $-T\Delta S$ Btu/lb	-582.2 (endothermic)	-706.7
dE/dT = volts/°C	1.45×10^{-3}	1.45×10^{-3}

1. The cell must be supplied with heat to maintain the cell temperature. Referring to the equations above, 48.6 Kcal must be supplied for every 135.6 Kcal electrical output, or for every 100 watts electrical output, 36 watts of heat input to the cell is necessary.

2. If reversible potentials near 1.47 volts are achieved and the $T\Delta S$ heat is supplied by the I^2R losses in the separator, a separator with a resistance of 5.28 ohms/cm^2 would be required at a current density of 0.1 amp/cm^2. The IR loss would be 0.53 volt, which would leave a useful potential of 0.99 volt. (See Appendix A: I^2R loss necessary to sustain the cell temperature.)

An important aspect of our fuel cell development work is the ability to define which phenomenon presents problems of sufficient magnitude to be worth investigating. Phenomena that can decrease the attainable voltage and that can be investigated on paper are (1) The use of aqueous hydrazine (versus pure hydrazine), (2) the dissociation of dinitrogen tetroxide ($N_2O_4=2NO_2$), and (3) the spontaneous thermal decomposition of hydrazine ($N_2H_4 \rightarrow 2H_2 + N_2$) at the catalyst surface prior to the electrochemical reaction.

The free energy loss due to the solution of hydrazine in water is equal to:

$$RT \ln\left(\frac{\text{partial pressure in soln.}}{\text{pure vapor pressure}}\right)$$

The vapor pressure of hydrazine in the pure state is known and the partial pressure of hydrazine aqueous solutions can be calculated from knowledge of the activity coefficients. The activity coefficient is obtained from azeotropic data. Use of these data in the van Laar and Gilliland equations* gives a description of the activity coefficient as a function of composition and temperature. These calculations appear in Appendix A.

The free energy loss due to the reduction of the hydrazine vapor pressure is 1.04 Kcal, which, compared to an over-all free energy of 135.6 Kcal available from a system operating with pure hydrazine, represents a 0.77% loss in free energy or voltage. It is thus a negligible effect.

The free energy loss due to the dissociation of dinitrogen tetroxide ($N_2O_4 \rightleftharpoons 2NO_2$) is obtained by:

1. Calculating the standard free energy change from knowledge of the equilibrium constant: $-\Delta F^\circ = RT\ln K$

---

* Ref. 33, pp. 56-59.

2. The equilibrium constant is known as a function of temperature (see Figure 1) and allows calculation of the partial pressures of N_2O_4 and NO_2 in equilibrium.

3. Since the total pressure is one atmosphere, the N_2O_4 and NO_2 are not in their standard state (one atm) and due allowance for this effect in the free energy loss must be taken into account.

The results of these calculations, shown in Appendix A, is that at 90°C and one atmosphere, the free energy loss due to dissociation of dinitrogen tetroxide is 1.72 Kcal, which is a negligible percentage (1.27%) of the 135.6 Kcal (free energy available from the hydrazine-dinitrogen tetroxide electrochemical reaction).

If spontaneous thermal decomposition of hydrazine ($N_2H_4 \longrightarrow N_2 + 2H_2$) takes place prior to the electrochemical reaction, hydrogen is then the fuel and the attainable free energy from the system:

$$2H_2 + \underset{\text{Gas}}{N_2O_4} \longrightarrow 2NO + \underset{\text{Gas}}{2H_2O}$$

is 94.96 Kcal or 1.03 volts. This represents a loss of 0.44 volts or a 29.9% decrease in voltage from the 1.47 volts available when N_2H_4 is electrochemically decomposed to N_2 and $4H^+$. (see Table 5)

However, the over-all endothermic effect (including the exotherm from decomposition) is still 8.5% of the power output. The chief disadvantage of the spontaneous decomposition of hydrazine prior to electrochemical reaction is the resultant decrease in voltage and power per pound. On the plus side is the remaining endothermic effect and the fact that hydrogen is a clean fuel.

C. REFORMING

Calculation and tabulation of the thermodynamic properties permitted another set of interesting calculations. Hydrogen is a clean and easily oxidized fuel compared to other fuels. However, these "other" fuels can in theory be reformed with steam to yield hydrogen and other gaseous products. The electrochemical reaction between hydrogen and dinitrogen tetroxide or nitric acid is endothermic as shown below. However, the reforming operation of the potential fuels further augments the effect since it is endothermic itself. Calculations below show the various reforming operations in combination with the electrochemical use of hydrogen. Note that the calculations assume the use and formation of water vapor at 25°C and 1 atmosphere. This temperature was chosen since data for CH_3OH, CO_2, and C_3H_8 are tabulated only at 25°C. However, the $T\Delta S$ for the electrochemical reaction increases

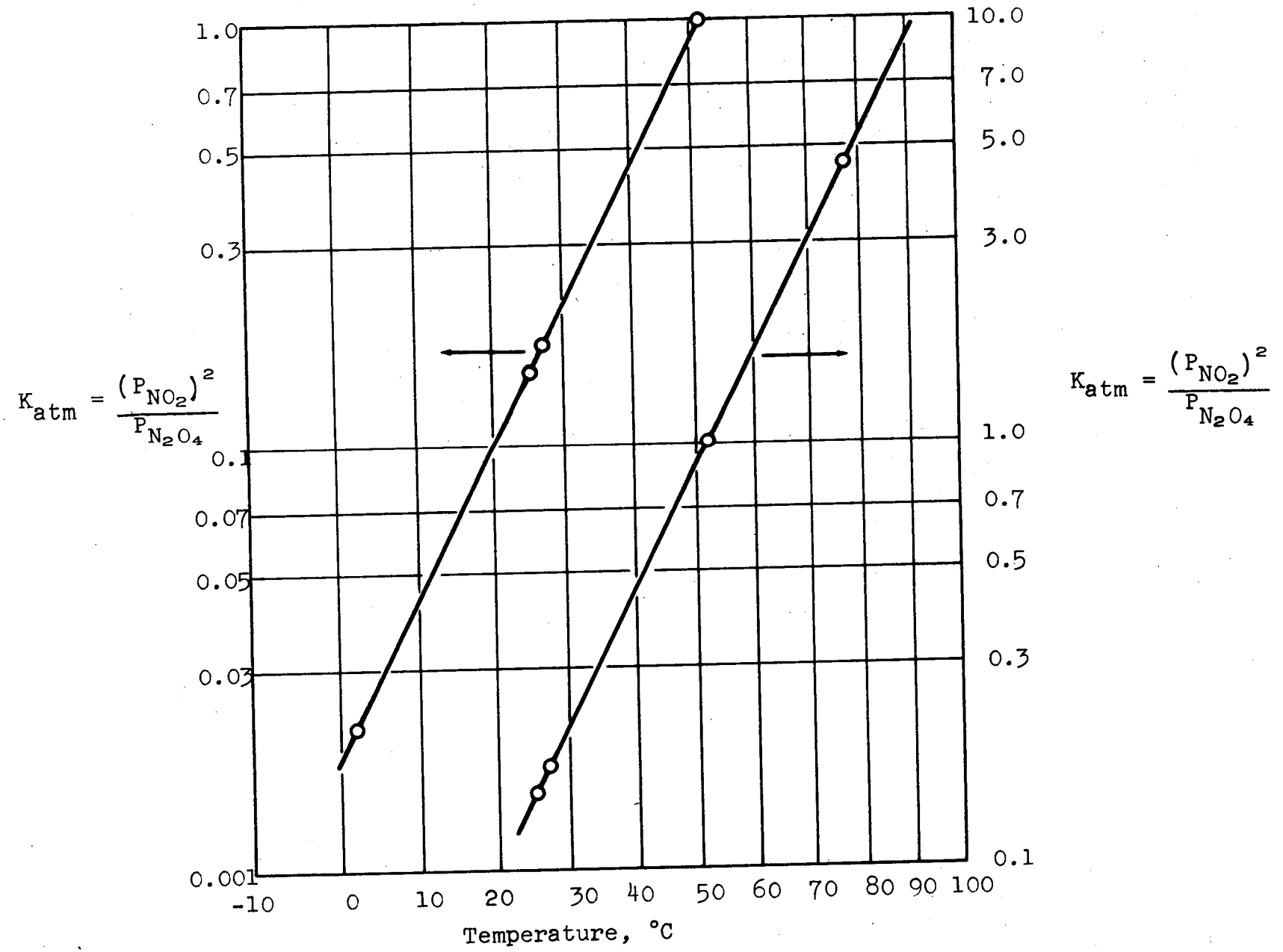

Figure 1. Equilibrium Constant for $N_2O_4 \rightleftharpoons 2NO_2$
[Ref. J. Phys. Chem., 65, 2252 (1961)]

with temperature, and for the reforming operation

$$\Delta H_T = \Delta H_{25} + \sum (C_{prod} - C_{react})\,\Delta T,$$

which indicates that ΔH becomes more endothermic with increasing temperature since the heat capacity of the simple molecules resulting from the reforming is greater than for the larger molecules. Therefore, the endothermic effect would increase as the operating temperature rises above 25°C.

$2H_2 + N_2O_4 \longrightarrow 2NO + 2H_2O$ gas

$\Delta F = -91.33$ Kcal/4 equivalents

$T\Delta S = 16.62$ Kcal/4 equivalents(endothermic)

$= 18.2\%$ of power output

$2H_2 + O_2 \longrightarrow 2H_2O$ gas

$\Delta F = -109.28$ Kcal/4 equivalents

$T\Delta S = -6.32$ Kcal/4 equivalents(exothermic)

$= -5.8\%$ of power output

The endothermic advantage is increased by combining the electrochemical reaction with hydrogen production by reforming various fuels:

Theoretically, at 25°C and one atmosphere

$2/3\ CH_3OH + 2/3\ H_2O$ gas $\xrightarrow{\text{reform}}$ $2/3\ CO_2 + 2H_2$ $\Delta H = 13.9$ Kcal/4 equivalents

Subsequently,

$2H_2 + N_2O_4 \longrightarrow 2NO + 2H_2O$ gas $T\Delta S = 16.62$ Kcal/4 equivalents

Total endothermic effect = 30.52 Kcal/4 equivalents
$\Delta F = -91.33$ Kcal/4 equivalents

$\therefore$ Endothermicity = 33.4% of power output

$1/3\ C_3H_8 + 2/3\ H_2O(gas) \xrightarrow{\text{reforming}} 1/3\ CO_2 + 2H_2$ $\Delta H = 15.46$ Kcal/4 equivalents

Subsequently,

$2H_2 + N_2O_4 \longrightarrow 2NO + 2H_2O$ (gas) $T\Delta S = 16.62$ Kcal/4 equivalents.

Total endothermic effect = 32.08 Kcal/4 equivalents

= 35.2% of power output

$2/5\ CH_3NHNH_2 + 4/5\ H_2O\ (gas) \longrightarrow 2/5\ CO_2 + 2H_2 + 2/5\ N_2$

ΔH = 3.54 Kcal/4 equivalents

Subsequently,

$2H_2 + N_2O_4 \longrightarrow 2NO + 2H_2O\ (gas)$ $T\Delta S$ = 16.62 Kcal/4 equivalents

Total endothermic effect = 20.16 Kcal/4 equivalents

= 22.1% of power output

$1/4\ (CH_3)_2N\cdot NH_2 + H_2O\ (gas) \longrightarrow 1/2\ CO_2 + 2H_2 + 1/4\ N_2$ ΔH = 7.96 Kcal/4 equivalents.

Subsequently,

$2H_2 + N_2O_4 \longrightarrow 2NO + 2H_2O\ (gas)$ $T\Delta S$ = 16.62 Kcal/4 equivalents

Total endothermic effect = 24.58 Kcal/4 equivalents

= 26.9% of power output

D. USE OF FUEL CELL AS A HEAT PUMP

The endothermic property of these systems presents the intriguing possibility of their use as an electrochemical heat pump. If $\Delta F = \Delta H - T\Delta S$ is the electrical output (ΔF is negative for power output) from a fuel cell, $T\Delta S$ is the heat absorbed from the surroundings that contributes directly to the power output. Therefore, if ΔF is expended as I^2R loss through a tungsten radiator at 5000°C outside the space capsule, the effect is to pump $T\Delta S$ by expending ΔF. This concept of pumping heat is not limited by Carnot efficiency or the temperatures involved, nor is there danger of losing working fluid from meteorite punctures of heat exchange tubes.

As opposed to the system described in the previous paragraph, if W is the work supplied to a conventional heat pump, the heat pumped from T_1 to T_2 is

$$Q = W \frac{T_1}{T_2 - T_1}$$

Since heat radiation depends on the fourth power of the temperature a high temperature (T_2) is required to cause a high radiant heat flux. Therefore with $T_2 >> T_1$ the heat pump efficiency $\left(\frac{Q}{W}\right)$ approaches zero.

E. ELECTROLYTE JUNCTION POTENTIALS

Another phenomenon that will influence the full cell potential is the existence of a difference in chemical potential (such as pH) of ionic species across the separators. To illustrate the argument, consider the following half cell reactions (subscripts L and R and left and right):

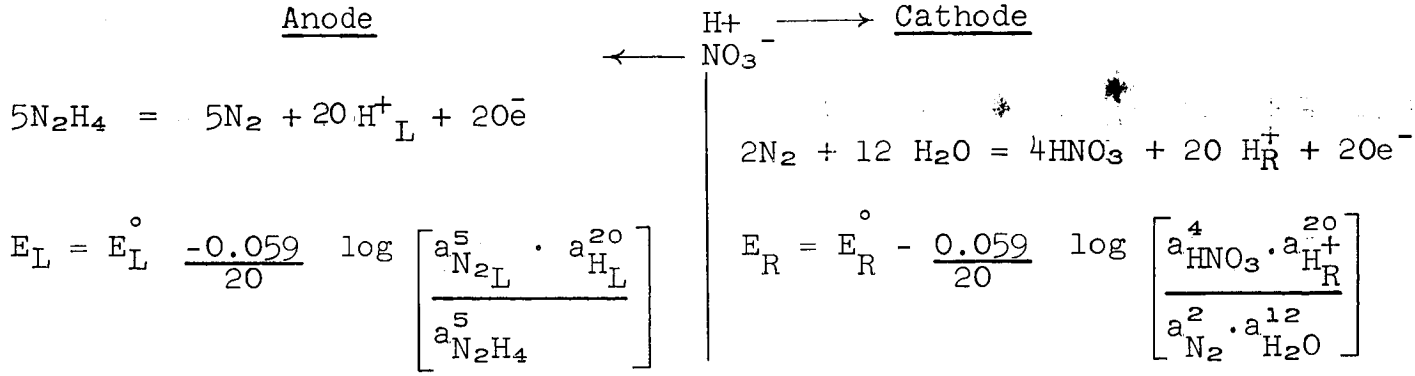

To simplify the argument, assume reactants and products are in their standard states; i.e., $a_{N_2H_4} = a_{HNO_3} = a_{H_2O} = a_{N_2} = 1$

so,

$$E_L = E^\circ_L - 0.059 \log a_{H^+_L} \qquad E_R = E^\circ_R - 0.059 \log a_{H^+_R}$$

In addition to the above half cell potentials, a potential will exist across the separator owing to the free energy change accompanying the transport of ions from one activity to another. The reaction occurring across the separators using the same conventions as for the half cells, i.e., oxidation occurs from left to right and is spontaneous if E is positive (this is the convention of the Electrochemical Society) is:

$$t_+H^+_L + t_-NO^-_{3R} \longrightarrow t_+H^+_R + t_-NO^-_{3L}$$

For 1 faraday t_+ and t_- are transport numbers or fraction of current carried by the respective ions

$$E_J = -0.059 \log \left[\frac{a^{t_+}_{H^+_R} \cdot a^{(1-t_+)}_{NO^-_{3L}}}{a^{t_+}_{H^+_L} \cdot a^{(1-t_+)}_{NO^-_{3R}}} \right]$$

The full cell potential will be the difference between oxidation potentials of the left and right half cells plus the junction potential (ref. 12-A).

$$E = E_L - E_R + E_J = \overset{\circ}{E_L} - \overset{\circ}{E_R} - 0.059 \log \left[\frac{a_{H^+_L} \cdot a^{t_+}_{HR} \cdot a^{(1-t_+)}_{NO_{3L}^-}}{a_{H^+_L} \cdot a^{t_+}_{H^+_L} \cdot a^{(1-t)}_{NO_{3R}^-}} \right]$$

Simplifying:

$$E = \overset{\circ}{E_L} - \overset{\circ}{E_R} - 0.059 \log \left[\frac{a_{H^+_L} \cdot a_{NO_{3L}^-}}{a_{H^+_R} \cdot a_{NO_{3R}^-}} \right]^{(1-t_+)} \qquad (1)$$

$\overset{\circ}{E_L} - \overset{\circ}{E_R}$ has already been calculated for the over-all reaction and is equal to 1.70 volts at 25°C and 1 atmosphere.

These calculations lead to the following conclusions:

1. When ions on both sides of a membrane are at unit activity, or when the activities are the same on each side, $E = E_L^{\circ} - E_R^{\circ} = 1.7$ volts irrespective of the value of t_+. This is true since the activity terms of Equation (1) become unity, and the log term becomes zero. If no concentration difference of current-carrying ions across the membrane exists, the liquid junction potential is still zero, since the activity ratio of Equation (1) is unity.

2. Even though ion activities are not unity or are not equal on each side of the membrane, the liquid junction potential will be zero if the membrane is permeable to only hydrogen ion $[(1-t_+) = 0]$. This assumption is not entirely valid if cations other than hydrogen ion carry appreciable current.

3. If the ion exchange membrane is not sufficiently selective to cations the liquid junction potential can vary from zero to unpredictible values, either positive or negative depending on the value of t^+ and on the activities of H^+ and NO_3^- on each side.

4. The above three conclusions and the liquid junction equations are valid only if H^+ and NO_3^- ions are the only ions present. However, we also have a very large possibility that $N_2H_5^+$ is formed and carries a large percentage of the current. If this is true the above liquid junction equation is not valid.
If $N_2H_5^+$ carried all the current, the following stoichiometric equation would hold:

$N_2H_4 \longrightarrow N_2 + 4H^+ + 4e^-$	electrode reaction
$4H^+ + 4N_2H_4 \longrightarrow 4N_2H_5^+$	chemical reaction
$4N_2H_5^+{}_L \longrightarrow 4N_2H_5^+{}_R$	current transfer

Thus we would then get a high potential, since qualitatively it can be seen that this liquid junction would add to the potential, at the sacrifice of only 20% utilization of our fuel.

V. EXPERIMENTAL-AQUEOUS SYSTEMS

A. HALF CELL POLARIZATION STUDIES

The open circuit voltage (OCV), the specific energy, and the potential available at various current densities are the most important parameters of any fuel cell system. The OCV and the specific energy can be calculated from thermodynamic data if the electrochemical reactions and hence the reaction products are known. The electrode polarization under load, being a kinetic phenomenon, cannot be predicted from thermodynamic considerations, and it is therefore calculable only in very special and rigidly defined cases.

The validity of the results presented in Table 4 of the previous section is based on the assumption that only the postulated reactions take place in the cell.

The objective of the work reported in this section was to verify those assumptions, to provide guidelines from which second approximation calculations can be made, and to provide criteria for the selection of suitable oxidant-reductant couples. Most of the experimental work was performed in half cells (see Appendix A-3, Figs. A-2, A-3, A-4 and A-5).

Half-cell measurements are based on the fact that in an electrochemical cell the potential at one electrode is independent of the reaction at the opposite electrode. For example, an electrode at which the principal reaction is:

$$NO_3^- + 6H^+ + 5e^- = 1/2N_2 + 3H_2O$$

will have the same potential whether the reaction at the opposite electrode is:

$$H_2NNH_2 = N_2 + 4H^+ + 4e^-$$

or:

$$H_2O = 1/2O_2 + 2H^+ + 2e^-$$

The potentials are recorded versus the reversible hydrogen electrode at the same temperature and pH. With this method of presentation, the full-cell potential, without IR drop, with any combination of anodic and cathodic half cells at the same pH, temperature, and current density can be found merely by subtracting the anode potential from the cathode potential. When the pH is different, an extra potential must be added for the H^+ concentration cell potential as follows:

30°C: Full cell potential = $E_{ox.} - E_{fuel} - 0.060(pH_{ox.} - pH_{fuel})$

90°C Full cell potential = $E_{ox.} - E_{fuel} - 0.072(pH_{ox.} - pH_{fuel})$

All liquid junction potentials are assumed to be negligible. Table 6 gives the pH values for the fuel solutions studied.

1. Fuel-Electrode-Catalyst-Electrolyte Systems

a. Soluble Systems

The electrochemical oxidation of hydrazines at catalyzed electrodes was studied in various electrolytes at 30°C and 90°C. The catalysts were put on the electrode substrate using two different techniques: (1) electroplating, and (2) chemical precipitation (see Appendix A-2). When using the precipitation technique, alloys or mixtures of catalysts were tested because of reports (ref. 13) of increased catalytic activity with some alloys of Ir, Ru, Pt and Au. Precipitated catalysts necessarily used a porous carbon material* as the electrode substrate, while with electroplated catalysts, stainless steel, nickel, and graphite substrates were used.

While the actual measurements were made versus a saturated calomel electrode (SCE) maintained at the same temperature as the electrolyte, the potentials are reported versus a reversible hydrogen electrode at the pH and temperature of the particular run. The use of this voltage scale permits a comparison of the fuels in relation to the open-circuit potential of a reversible hydrogen electrode (HE). Furthermore, if the anodic oxidation of hydrazine proceeds in aqueous media by an intermediate hydrogen mechanism, the potential of HE is an upper limit of performance. It is apparent then that the best fuels have the least overvoltage.

(1) Hydrazine

Aqueous solutions of hydrazine were studied in six different electrolytes using a large number of different electroplated catalyst-substrate systems (Table 7). The best short-term polarization test at 100 ma/cm² was obtained in 1M KOH at 30° with Rh/Ni electrode.

*Pure Carbon Co., FC-14 grade Pure Carbon

Table 6

pH VALUES OF FUEL SOLUTIONS
(At 30°C)

Fuel	Conc.	1M KOH	1M Buffer	1M H_3PO_4	5M HNO_3	1M KNO_3	5M H_3PO_4
N_2H_4	1M	~ 14	8.8	4.8	~0	11.1	0.7
N_2H_4	2M	--	--	--	--	--	1.2
MMH	1M	~ 14	8.6	4.3 4.4	~0	10.75	0.6
	2.5M	~ 14					
UDMH	1M	< 14	7.9 8.5	3.8 4.2	~0	11.1	0.6
	2.5M	~ 14					
N_2H_4 (50/50) MMH	0.5M 0.5M	~ 14	8.6	4.2	~0	11.3	0.6
N_2H_4 (50/50) UDMH	0.5M 0.5M	< 14	8.4	4.3	~0	11.9	
N_2H_4 UDMH	0.1M 1M	< 14	--	5.3	~0	--	
N_2H_4 UDMH	0.3M 1M	< 14	--	6.4	~0	--	

Table 7

ANODIC OXIDATION OF 1M N_2H_4

Catalyst	Sub-strate	Current Density ma/cm²	Potential vs HE at Same pH and Temperature, Volts*											
			Buffer		1M KNO_3		5M HNO_3		1M H_3PO_4		1M KOH		5M H_3PO_4	
			30°C	90°C	30°C	90°C	30°C	90°C	30°C	90°C	30°C	90°C	30°C	90°C
Pt	C	1	0.10	0.16	0.17	0.23	0.40	0.40	0.20	0.19	-	-	-	-
Pt	C	50	0.23	0.28	0.36	0.42	0.53	0.46	0.58	0.40	-	-	-	-
Pt	C	100	0.32	0.33	0.45	0.54	0.54	0.48	0.75	0.50	-	-	-	-
Pt	Ni	1	0.03	0.08	0.15	0.17	-	-	0.18	0.12	0.02	0.08	-	-
Pt	Ni	50	0.30	0.21	0.37	0.29	-	-	0.44	0.26	0.03	0.09	-	-
Pt	Ni	100	0.39	0.39	0.46	0.33	-	-	0.34	0.32	0.06	0.11	-	-
Pt	SS	1	-	-	-	-	0.37	0.34	0.15	0.12	0.07	0.15	0.18	0.06
Pt	SS	50	-	-	-	-	0.53	0.41	0.41	0.23	0.14	0.24	0.35	0.23
Pt	SS	100	-	-	-	-	0.56	0.44	0.49	0.33	0.18	0.26	0.37	0.28
Au	C	1	-	-	-	-	0.83	0.56	0.49	0.46	-	-	-	-
Au	C	50	-	-	-	-	0.96	0.78	1.2	0.85	-	-	-	-
Au	C	100	-	-	-	-	0.98	0.81	1.3	1.2	-	-	-	-
Au	Ni	1	-	-	0.17	0.10	-	-	-	-	-0.04	0.06	-	-
Au	Ni	50	-	-	0.57	0.49	-	-	-	-	0.04	0.11	-	-
Au	Ni	100	-	-	0.72	0.63	-	-	-	-	0.09	0.15	-	-
Au	SS	1	-	-	-	-	0.49	0.54	-	-	-	-	-	-
Au	SS	50	-	-	-	-	0.94	0.73	-	-	-	-	-	-
Au	SS	100	-	-	-	-	0.99	0.80	-	-	-	-	-	-
Rh	C	1	-	-	-	-	0.51	0.57	0.02	0.02	-	-	-	-
Rh	C	50	-	-	-	-	0.84	0.79	0.27	0.08	-	-	-	-
Rh	C	100	-	-	-	-	0.99	0.88	0.29	0.15	-	-	-	-
Rh	Ni	1	0.01	0.06	0.07	0.08	-	-	0.00	-0.02	-0.05	0.04	-	-
Rh	Ni	50	0.19	0.12	0.23	0.21	-	-	0.24	0.11	-0.04	0.05	-	-
Rh	Ni	100	0.31	0.18	0.33	0.28	-	-	0.30	0.19	-0.04	0.06	-	-
Rh	SS	1	-	-	-	-	0.63	0.57	-	-	-	-	-	-
Rh	SS	50	-	-	-	-	0.94	0.78	-	-	-	-	-	-
Rh	SS	100	-	-	-	-	1.04	0.86	-	-	-	-	-	-

*E° for reaction: $N_2H_4 \longrightarrow N_2 + 4H^+ + 4e^-$ = -0.38 at 30°C and -0.47 at 90°C.

This system operated at a potential 0.04 volt better than a reversible H_2 electrode at the same temperature and pH. However, it is improbable that either N_2O_4 or HNO_3 could be coupled with this fuel system in a full cell, thus limiting it to O_2 or H_2O_2 for a full cell couple.

The best system compatible with N_2O_4 and HNO_3 is H_3PO_4 at 90°C using a platinum-catalyzed stainless steel (Pt/SS) electrode. A potential + 0.30 volt from HE (or poorer than reversible H_2) was obtained at 100 ma/cm^2.

Table 8 lists the data for tests of 1M N_2H_4 in 5M H_3PO_4 and 1M KOH using precipitated catalysts and catalyst mixtures, at 30°C and 80°C.

In 1M KOH at 30°C a ruthenium catalyst performed best, but rhodium by itself was nearly as good. The best electrode was identical in potential to the best electroplated system at about the same current density.

At 80°C in 1M KOH a rhodium catalyst performed 0.02 volt worse than the Rh/Ni electroplated electrode system at 90°C. However, a precipitated ruthenium electrode performed slightly better than the electroplated Rh/Ni system.

With 5M H_3PO_4 electrolyte at 80°C, a precipitated ruthenium electrode was only 0.18 volt poorer than HE at 100 ma/cm^2; this was the best precipitated catalyst. The only other catalyst within 0.1 volt at the same current was an iridium (32%)-ruthenium (68%) electrode. The ruthenium electrode shows a 0.12 volt improvement over the best electroplated system.

The main reason for the investigation of the precipitated catalyst electrode was for information on catalysts and catalyst mixtures that were difficult to obtain by electroplating techniques. Catalyst-substrate systems that would give improved long-term characteristics were desired. In the section on long-term tests, it will be seen that vast improvements were found.

(2) Monomethylhydrazine and Unsymmetrical Dimethylhydrazine

Tables 9 and 10 list data on 1M MMH and 1M UDMH in seven different electrolytes including 5M H_2SO_4 in which N_2H_4 is not soluble. Of the electrolytes that would be CO_2 rejecting, MMH performs best in 5M H_3PO_4 with a Au/SS electrode, while UDMH performs best in 5M H_2SO_4 with a Au/SS electrode. The potentials are 0.2 to 0.3 volt worse than N_2H_4 potentials. This, coupled with poor efficiency due to incomplete reactions (CO_2 not produced, see analytical discussion), and very poor long-term stability (see long-term test section) indicates no further interest in the electrochemical oxidation of these fuels.

Table 7

ANODIC OXIDATION OF 1M N_2H_4

Catalyst	Substrate	Current Density ma/cm²	Potential vs HE at Same pH and Temperature, Volts*											
			Buffer		1M KNO_3		5M HNO_3		1M H_3PO_4		1M KOH		5M H_3PO_4	
			30°C	90°C	30°C	90°C	30°C	90°C	30°C	90°C	30°C	90°C	30°C	90°C
Pt	C	1	0.10	0.16	0.17	0.23	0.40	0.40	0.20	0.19	-	-	-	-
Pt	C	50	0.23	0.28	0.36	0.42	0.53	0.46	0.58	0.40	-	-	-	-
Pt	C	100	0.32	0.33	0.45	0.54	0.54	0.48	0.75	0.50	-	-	-	-
Pt	Ni	1	0.03	0.08	0.15	0.17	-	-	0.18	0.12	0.02	0.08	-	-
Pt	Ni	50	0.30	0.21	0.37	0.29	-	-	0.44	0.26	0.03	0.09	-	-
Pt	Ni	100	0.39	0.39	0.46	0.33	-	-	0.34	0.32	0.06	0.11	-	-
Pt	SS	1	-	-	-	-	0.37	0.34	0.15	0.12	0.07	0.15	0.18	0.06
Pt	SS	50	-	-	-	-	0.53	0.41	0.41	0.23	0.14	0.24	0.35	[illegible]
Pt	SS	100	-	-	-	-	0.56	0.44	0.49	0.33	0.18	0.26	[illegible]	[illegible]
Au	C	1	-	-	-	-	0.83	0.56	0.49	0.46	-	-	-	-
Au	C	50	-	-	-	-	0.96	0.78	1.2	0.85	-	-	-	-
Au	C	100	-	-	-	-	0.98	0.81	1.3	1.2	-	-	-	-
Au	Ni	1	-	-	0.17	0.10	-	-	-	-	-0.04	0.06	-	-
Au	Ni	50	-	-	0.57	0.49	-	-	-	-	0.04	0.11	-	-
Au	Ni	100	-	-	0.72	0.63	-	-	-	-	0.09	0.15	-	-
Au	SS	1	-	-	-	-	0.49	0.54	-	-	-	-	-	-
Au	SS	50	-	-	-	-	0.94	0.73	-	-	-	-	-	-
Au	SS	100	-	-	-	-	0.99	0.80	-	-	-	-	-	-
Rh	C	[illegible]	-	-	-	-	0.51	0.57	0.02	0.02	-	-	-	-
Rh	C	[illegible]	-	-	-	-	0.84	0.79	0.27	0.08	-	-	-	-
Rh	C	100	-	-	-	-	0.99	0.88	0.29	0.15	-	-	-	-
Rh	Ni	1	[illegible]	0.06	0.07	0.08	-	-	0.00	-0.02	-0.05	0.04	-	-
Rh	Ni	50	[illegible]	[illegible]	0.23	0.21	-	-	0.24	0.11	-0.04	0.05	-	-
Rh	Ni	100	[illegible]	[illegible]	0.33	0.28	-	-	0.30	0.19	-0.04	0.06	-	-
Rh	SS	1	-	-	-	-	0.63	0.57	-	-	-	-	-	-
Rh	SS	50	-	-	-	-	0.94	0.78	-	-	-	-	-	-
Rh	SS	100	-	-	-	-	1.04	0.86	-	-	-	-	-	-

*E° for reaction: $N_2H_4 \longrightarrow N_2 + 4H^+ + 4e^-$ = -0.38 at 30°C and -0.47 at 90°C.

This system operated at a potential 0.04 volt better than a reversible H_2 electrode at the same temperature and pH. However, it is improbable that either N_2O_4 or HNO_3 could be coupled with this fuel system in a full cell, thus limiting it to O_2 or H_2O_2 for a full cell couple.

The best system compatible with N_2O_4 and HNO_3 is H_3PO_4 at 90°C using a platinum-catalyzed stainless steel (Pt/SS) electrode. A potential + 0.30 volt from HE (or poorer than reversible H_2) was obtained at 100 ma/cm^2.

Table 8 lists the data for tests of 1M N_2H_4 in 5M H_3PO_4 and 1M KOH using precipitated catalysts and catalyst mixtures, at 30°C and 80°C.

In 1M KOH at 30°C a ruthenium catalyst performed best, but rhodium by itself was nearly as good. The best electrode was identical in potential to the best electroplated system at about the same current density.

At 80°C in 1M KOH a rhodium catalyst performed 0.02 volt worse than the Rh/Ni electroplated electrode system at 90°C. However, a precipitated ruthenium electrode performed slightly better than the electroplated Rh/Ni system.

With 5M H_3PO_4 electrolyte at 80°C, a precipitated ruthenium electrode was only 0.18 volt poorer than HE at 100 ma/cm^2, this was the best precipitated catalyst. The only other catalyst within 0.1 volt at the same current was an iridium (32%)-ruthenium (68%) electrode. The ruthenium electrode shows a 0.12 volt improvement over the best electroplated system.

The main reason for the investigation of the precipitated catalyst electrode was for information on catalysts and catalyst mixtures that were difficult to obtain by electroplating techniques. Catalyst-substrate systems that would give improved long-term characteristics were desired. In the section on long-term tests, it will be seen that vast improvements were found.

(2) Monomethylhydrazine and Unsymmetrical Dimethylhydrazine

Tables 9 and 10 list data on 1M MMH and 1M UDMH in seven different electrolytes including 5M H_2SO_4 in which N_2H_4 is not soluble. Of the electrolytes that would be CO_2 rejecting, MMH performs best in 5M H_3PO_4 with a Au/SS electrode, while UDMH performs best in 5M H_2SO_4 with a Au/SS electrode. The potentials are 0.2 to 0.3 volt worse than N_2H_4 potentials. This, coupled with poor efficiency due to incomplete reactions (CO_2 not produced, see analytical discussion), and very poor long-term stability (see long-term test section) indicates no further interest in the electrochemical oxidation of these fuels.

Table 8

ANODIC OXIDATION OF N_2H_4 AND MMH AT PRECIPITATED CATALYSTS

Substrate - FC-14 Porous Carbon, Electrolyte - 5M H_3PO_4

Potential vs HE at Same pH and Temperature, Volts

Catalyst	1M N_2H_4 in 5M H_3PO_4 30°C Cat. %	Current in ma/cm² 0	50	100	200	1M N_2H_4 in 5M H_3PO_4 80°C* Cat. %	Current in ma/cm² 0	50	100	200	1M N_2H_4 in 1M KOH 30°C Cat. %	Current in ma/cm² 10	50	100	200
Platinum	3.3	+0.22	+0.52	+0.60	+0.70	+0.09	+0.30	+0.34	+0.38	0.7					
Rhodium	2.4	+0.10	+0.35	+0.44	+0.55	+0.04	+0.21	+0.30	+0.40	3.0	-0.04	-0.03	-0.01	+0.02
Ruthenium	3.2					+0.09	+0.14	+0.18	+0.24	3.0	-0.08	-0.06	-0.03	0.0
Gold	1.0					+0.42	+0.81	-	-	1.0%				
Iridium	0.8					+0.39	+0.77	-	-	1.4	+0.14	+0.37	+0.41	+0.45
Nickel										1.0				
80% Platinum - 20% Ruthenium	2.7	+0.19	+0.52	+0.60	+0.68	+0.17	+0.26	+0.33	+0.40	1.7	-0.03	-0.01	+0.02	+0.06
60% Platinum - 20% Ruthenium - 20% Gold	2.9	+0.20	+0.54	+0.60	+0.66	+0.13	+0.26	+0.31	+0.38	2.9	-0.03	+0.06	+0.12	+0.22
32% Iridium - 68% Ruthenium	2.6	+0.16	+0.39	+0.50	+0.60	+0.12	+0.17	+0.22	+0.30	2.6	-0.09	-0.05	0.0	+0.06
80% Platinum - 20% Nickel	2.6	+0.20	+0.59	+0.66	+0.72	+0.18	+0.45	+0.52	+0.58	2.6	-0.02	+0.06	+0.10	+0.17
80% Rhodium - 20% Nickel	2.9	+0.12	+0.42	+0.50	+0.59	+0.08	+0.23	+0.28	+0.34	2.9	-0.03	-0.02	-0.01	0.0
40% Platinum - 40% Rhodium - 20% Gold	3.0	+0.07	+0.36	+0.44	+0.51	+0.10	+0.19	+0.25	+0.30	3.0	-0.04	+0.02	+0.05	+0.09
50% Gold - 50% Ruthenium														

Catalyst	1M N_2H_4 in 1M KOH 80°C* Cat. %	Current in ma/cm² 0	50	100	200	1M MMH in 5M H_3PO_4 30°C Cat. %	Current in ma/cm² 0	50	100	200	80°C* 0	50	100	200
Platinum	3.3	+0.09	+0.26	+0.38	+0.50	1.0	+0.38	+0.73	+0.80	+0.88	+0.27	+0.68	+0.76	+0.83
Rhodium	2.4	+0.01	+0.07	+0.08	+0.09	1.9	+0.34	+0.63	+0.69	+0.74	+0.22	+0.43	+0.48	+0.52
Ruthenium	3.2	-0.05	0.0	+0.02	+0.04	2.2	+0.38	+0.70	+0.85	-	+0.33	+0.41	+0.45	+0.51
Gold	1.0	+0.25	+0.49	+0.55	+0.58	7.0	+0.54	-	-	-	+0.45	+0.77	+0.78	+0.80
Iridium	0.8	+0.18	+0.31	+0.36	+0.41	1.2	+0.07	+0.90	-	-	+0.23	+0.72	+0.78	+0.85
Nickel		+0.05	+0.11	+0.15	+0.20									
80% Platinum - 20% Ruthenium	2.7	+0.05	+0.06	+0.06	+0.07	1.4	+0.34	+0.68	+0.82	+0.89	+0.27	+0.56	+0.63	+0.71
60% Platinum - 20% Ruthenium - 20% Gold	2.9	+0.06	+0.09	+0.13	+0.15	2.9	+0.34	+0.56	+0.65	+0.66	+0.28	+0.53	+0.57	+0.63
32% Iridium - 68% Ruthenium	2.6	0.0	+0.03	+0.06	+0.10	2.8	+0.37	+0.65	+0.88	-	+0.28	+0.46	+0.52	+0.60
80% Platinum - 20% Nickel	2.6	+0.10	+0.15	+0.20	+0.30	1.7	+0.35	+0.74	+0.83	+0.93	+0.17	+0.68	+0.75	+0.86
80% Rhodium - 20% Nickel	2.9	+0.05	+0.06	+0.07	+0.09	1.9	+0.35	+0.54	+0.62	+0.70	+0.26	+0.42	+0.45	+0.49
40% Platinum - 40% Rhodium - 20% Gold	3.0	+0.07	+0.09	+0.11	+0.13	2.6	+0.34	+0.55	+0.60	+0.65	+0.25	+0.44	+0.50	+0.55
50% Gold - 50% Ruthenium						3.3	+0.42	+0.67	+0.75	+0.81	+0.29	+0.42	+0.47	+0.51

*Tests run at 80°C instead of 90°C, due to rapid loss of fuels from vaporization.

Table 9

ANODIC OXIDATION OF 1M MMH

Catalyst	Sub-strate	Current Density ma/cm²	Potential vs HE at Same pH and Temperature, Volts													
			Buffer		1M KNO_3		5M HNO_3		1M H_3PO_4		1M KOH		5M H_3PO_4		5M H_2SO_4	
			30°C	90°C	30°C	90°C	30°C	90°C	30°C	90°C	30°C	90°C	30°C	90°C	30°C	90°C
Pt	C	1	0.64	0.48	-	-	0.29	0.67	0.63	0.55	0.48	0.56	-	-	-	-
Pt	C	50	1.10	0.96	-	-	0.80	0.81	1.09	0.95	1.13	1.12	-	-	-	-
Pt	C	100	1.23	1.05	-	-	0.90	0.87	1.25	1.02	1.3	1.19	-	-	-	-
Pt	Ni	1	0.59	0.37	-	0.43	-	-	0.52	0.17	0.53	0.33	-	-	-	-
Pt	Ni	50	1.09	0.84	-	0.84	-	-	1.08	0.94	0.96	0.90	-	-	-	-
Pt	Ni	100	1.23	1.07	-	0.93	-	-	1.23	1.06	1.08	1.04	-	-	-	-
Pt	SS	1	-	-	-	-	0.28	0.56	0.61	0.57	-	-	-		0.[illegible]7	0.43
Pt	SS	50	-	-	-	-	0.71	0.77	1.04	0.97	-	-	-		0.[illegible]2	0.73
Pt	SS	100	-	-	-	-	0.82	0.81	1.17	1.05	-	-	-		0.96	0.78
Au	C	1	-	-	-	-	0.74	0.60	0.60	0.56	-	-	-	-	-	-
Au	C	50	-	-	-	-	1.06	0.75	0.80	0.65	-	-	-	-	-	-
Au	C	100	-	-	-	-	1.11	0.78	0.84	0.78	-	-	-	-	-	-
Au	Ni	1	0.55	0.33	-	0.23	-	-	0.32	0.16	0.34	0.33	-	-	-	-
Au	Ni	50	0.96	0.51	-	0.70	-	-	0.78	0.62	0.53	0.63	-	-	-	-
Au	Ni	100	1.21	0.56	-	0.78	-	-	0.90	0.73	0.55	0.72	-	-	-	-
Au	SS	1	-	-	-	0.28	0.62	0.53	-	-	-	-	0.48	0.28	0.44	0.29
Au	SS	50	-	-	-	0.77	0.98	0.71	-	-	-	-	0.60	0.35	0.75	0.54
Au	SS	100	-	-	-	0.95	1.07	0.75	-	-	-	-	0.61	0.39	0.83	0.62
Rh	C	1	-	-	-	-	0.50	0.60	-	-	-	-	-	-	-	-
Rh	C	50	-	-	-	-	0.78	0.76	-	-	-	-	-	-	-	-
Rh	C	100	-	-	-	-	0.88	0.82	-	-	-	-	-	-	-	-
Rh	Ni	1	0.77	0.46	-	0.29	-	-	0.59	0.14	0.53	0.37	-	-	-	-
Rh	Ni	50	1.31	0.96	-	1.09	-	-	1.05	0.85	1.06	0.99	-	-	-	-
Rh	Ni	100	1.49	1.10	-	1.3	-	-	1.3	0.95	1.10	1.06	-	-	-	-
Rh	SS	1	-	-	-	-	0.50	0.55	0.38	0.38	-	-	-	-	-	-
Rh	SS	50	-	-	-	-	0.80	0.73	0.96	0.84	-	-	-	-	-	-
Rh	SS	100	-	-	-	-	0.89	0.79	1.3	0.94	-	-	-	-	-	-

Table 10

ANODIC OXIDATION OF 1M UDMH

Catalyst	Sub-strate	Current Density ma/cm²	Potential vs HE at Same pH and Temperature, Volts													
			Buffer		1M KNO_3		5M HNO_3		1M H_3PO_4		1M KOH		5M H_3PO_4		5M H_2SO_4	
			30°C	90°C	30°C	90°C	30°C	90°C	30°C	90°C	30°C	90°C	30°C	90°C	30°C	90°C
Pt	C	1	0.61	0.49	-	-	0.65	0.59	0.81	0.52	-	-	-	-	-	-
Pt	C	50	0.97	0.77	-	-	0.84	0.72	1.2	1.03	-	-	-	-	-	-
Pt	C	100	1.01	0.97	-	-	0.94	0.80	1.3	1.19	-	-	-	-	-	-
Pt	Ni	1	0.57	0.43	-	0.57	-	-	0.76	0.81	0.54	0.49	-	-	-	-
Pt	Ni	50	1.02	0.66	-	0.79	-	-	1.2	1.0	0.91	0.86	-	-	-	-
Pt	Ni	100	1.17	0.73	-	0.88	-	-	1.3	1.2	0.99	0.99	-	-	-	-
Pt	SS	1	-	-	-	-	0.62	0.58	0.73	0.53	0.67	0.53	-	-	0.51	0.44
Pt	SS	50	-	-	-	-	0.89	0.72	1.3	1.2	1.2	1.05	-	-	1.03	0.97
Pt	SS	100	-	-	-	-	0.94	0.78	1.4	1.3	1.3	1.09	-	-	1.23	1.10
Au	C	1	-	-	-	-	0.61	0.54	0.65	0.47	-	-	-	-	-	-
Au	C	50	-	-	-	-	0.79	0.72	1.10	0.87	-	-	-	-	-	-
Au	C	100	-	-	-	-	0.84	0.76	1.3	1.03	-	-	-	-	-	-
Au	Ni	1	0.50	0.44	-	0.57	-	-	0.51	0.51	0.56	0.56	-	-	-	-
Au	Ni	50	0.76	0.56	-	0.81	-	-	0.78	0.66	0.81	0.62	-	-	-	-
Au	Ni	100	0.97	0.59	-	0.89	-	-	0.92	0.76	1.1	0.64	-	-	-	-
Au	SS	1	-	-	-	0.54	0.60	0.53	0.57	0.57	0.42	-	-	0.36	0.54	0.36
Au	SS	50	-	-	-	1.3	0.74	0.57	0.89	0.74	0.74	-	-	0.71	0.64	0.49
Au	SS	100	-	-	-	1.4	0.84	0.59	0.94	0.89	0.89	-	-	0.86	0.70	0.57
Rh	C	1	-	-	-	-	0.61	0.73	0.72	0.26	-	-	-	-	-	-
Rh	C	50	-	-	-	-	0.84	0.88	1.2	1.08	-	-	-	-	-	-
Rh	C	100	-	-	-	-	1.3	0.94	1.3	1.3	-	-	-	-	-	-
Rh	Ni	1	0.70	0.54	-	0.50	-	-	0.71	0.27	0.72	0.49	-	-	-	-
Rh	Ni	50	1.21	0.97	-	1.4	-	-	1.2	1.10	1.2	1.07	-	-	-	-
Rh	Ni	100	1.49	1.05	-	1.5	-	-	1.3	1.3	1.3	1.12	-	-	-	-
Rh	SS	1	-	-	-	-	0.61	0.58	-	-	-	-	-	-	-	-
Rh	SS	50	-	-	-	-	1.3	0.82	-	-	-	-	-	-	-	-
Rh	SS	100	-	-	-	-	1.3	1.20	-	-	-	-	-	-	-	-

Table 8 lists data obtained with precipitated catalyst systems for MMH in 5M H_3PO_4. Potentials about 0.1 volt better than with electroplated catalysts were obtained. Interestingly, gold was no longer effective when precipitated, and the best potentials were obtained with ruthenium and 80% rhodium-20% nickel. However, the evaluation of MMH given above for electroplated catalyst systems still would hold true.

(3) Mixtures of N_2H_4 with MMH or UDMH

Since the above mixtures were possible fuels for future rocket systems, they were tested with electroplated catalyst-substrate systems with most of the electrolytes previously mentioned.

Tables 11 and 12 list the data for these tests. In general the mixtures are poorer by 0.1 to 0.2 volt than the same concentration of N_2H_4. This is compatible with the data for N_2H_4 and the methylated hydrazines alone. Hydrazine may be preferentially oxidized and a steady state with a low N_2H_4 concentration is eventually reached, after which the potential deteriorates.

To investigate the above possibility, tests were made with 1M UDMH while the N_2H_4 concentration was varied (Table 13). For all electrodes except Rh/Ni at 90°C in 1M KOH, the potentials rapidly deteriorated with lowered N_2H_4 concentration. It would seem that Rh/Ni is such a specific catalyst for N_2H_4, that as low as 0.1M N_2H_4 can be utilized at 90°C. Thus, it might be possible to use a flow-through system that would discard the unused fuel, and thus use 90% of the N_2H_4 in the mixture. However, such an electrode would be highly inefficient, and would not be compatible with HNO_3 or N_2O_4 because of the basic electrolyte requirement.

b. Vapor Transport Electrodes

Electrodes of this type might also be classed as porous electrodes. Our porous electrodes are of the type described in Appendix A-2. The usefulness of a porous Teflon vapor electrode is thoroughly discussed in Section D. Here half-cell data from the cell pictured in Figure A-5 (Appendix A-3) is presented. Since the Luggin capillary must be too far from the electrode for IR drops to be negligible, the data obtained in Table 14 were derived from Kordesch-Marko bridge measurements. (For a description of the Kordesch-Marko bridge and its circuit, see Appendix A-3.) These tests were made in conjunction with physical optimization studies on the Teflon electrodes and will be discussed further in the Section D.

Table 11

ANODIC OXIDATION OF 50/50 0.5M N_2H_4 + 0.5M MMH

Catalyst	Sub-strate	Current Density ma/cm^2	Potential vs HE at Same pH and Temperature, Volts											
			Buffer		1M KNO_3		5M HNO_3		1M H_3PO_4		1M KOH		5M H_3PO_4	
			30°C	90°C	30°C	90°C	30°C	90°C	30°C	90°C	30°C	90°C	30°C	90°C
Pt	C	1	0.17	0.22	-	-	0.47	0.52	0.58	0.62	-	-	-	-
Pt	C	50	0.60	0.57	-	-	0.64	0.69	0.99	0.78	-	-	-	-
Pt	C	100	0.88	0.88	-	-	0.71	0.76	1.16	0.96	-	-	-	-
Pt	Ni	1	0.11	0.12	0.13	0.17	-	-	0.14	0.11	-0.02	0.10	-	-
Pt	Ni	50	0.80	0.28	0.99	0.63	-	-	0.70	0.57	+0.90	0.20	-	-
Pt	Ni	100	0.94	0.68	1.3	0.90	-	-	0.90	0.77	0.98	0.53	-	-
Pt	SS	1	-	-	-	-	0.46	0.46	0.31	0.23	-	-	0.24	0.10
Pt	SS	50	-	-	-	-	0.61	0.58	0.84	0.88	-	-	0.52	0.41
Pt	SS	100	-	-	-	-	0.66	0.63	0.95	0.97	-	-	0.56	0.45
Au	C	1	-	-	-	-	0.70	0.50	0.60	0.43	-	-	-	-
Au	C	50	-	-	-	-	1.07	0.66	0.93	0.73	-	-	-	-
Au	C	100	-	-	-	-	1.3	0.73	1.06	0.82	-	-	-	-
Au	Ni	1	0.14	0.26	0.32	0.19	-	-	0.23	0.05	-0.01	0.10	-	-
Au	Ni	50	0.78	0.54	0.77	0.60	-	-	0.71	0.53	0.88	0.20	-	-
Au	Ni	100	0.94	0.61	0.87	0.75	-	-	0.78	0.65	0.91	0.57	-	-
Au	SS	1	0.15	0.24	-	-	0.70	0.52	0.38	0.15	-	-	0.53	0.13
Au	SS	50	0.68	0.51	-	-	1.09	0.72	0.82	0.59	-	-	0.64	0.36
Au	SS	100	0.78	0.55	-	-	1.3	0.74	0.83	0.68	-	-	0.65	0.37
Rh	C	1	0.20	0.00	0.06	0.16	0.57	0.58	0.20	0.01	-0.02	0.10	-	-
Rh	C	50	0.17	0.23	0.43	0.36	0.80	0.75	1.05	0.29	0.20	0.20	-	-
Rh	C	100	0.84	0.31	0.98	0.48	0.90	0.83	1.30	0.82	1.06	0.30	-	-
Rh	Ni	1	0.05	0.01	0.08	0.18	-	-	0.05	0.00	-0.02	0.08	-	-
Rh	Ni	50	0.42	0.16	0.40	0.36	-	-	0.77	0.32	0.12	0.16	-	-
Rh	Ni	100	1.05	0.24	1.2	0.48	-	-	1.0	0.69	0.18	0.22	-	-
Rh	SS	1	-	-	-	-	0.43	0.56	-	-	-	-	-	-
Rh	SS	50	-	-	-	-	0.75	0.70	-	-	-	-	-	-
Rh	SS	100	-	-	-	-	0.85	0.78	-	-	-	-	-	-

Table 12

ANODIC OXIDATION OF 50/50 0.5M UDMH + 0.5M N_2H_4

Catalyst	Sub-strate	Current Density ma/cm²	Potential vs HE at Same pH and Temperature, Volts									
			Buffer		1M KNO_3		5M HNO_3		1M H_3PO_4		1M KOH	
			30°C	90°C	30°C	90°C	30°C	90°C	30°C	90°C	30°C	90°C
Pt	C	1	0.36	0.25	-	-	0.48	0.46	0.37	0.37	-	-
Pt	C	50	0.86	0.45	-	-	0.96	0.68	0.73	0.99	-	-
Pt	C	100	1.02	0.51	-	-	1.05	0.78	1.03	1.12	-	-
Pt	Ni	1	0.29	0.15	0.13	0.19	-	-	0.17	0.10	-0.04	0.09
Pt	Ni	50	0.57	0.41	0.60	0.52	-	-	0.75	0.54	+0.06	0.15
Pt	Ni	100	0.91	0.47	0.76	0.65	-	-	1.02	0.64	0.11	0.20
Pt	SS	1	-	-	-	-	0.45	0.44	0.34	0.22	-	-
Pt	SS	50	-	-	-	-	.65	0.54	0.74	0.63	-	-
Pt	SS	100	-	-	-	-	.89	0.60	0.83	0.77	-	-
Au	C	1	-	-	-	-	0.62	0.53	0.39	0.48	-	-
Au	C	50	-	-	-	-	0.86	0.59	1.11	1.06	-	-
Au	C	100	-	-	-	-	0.90	0.64	1.17	1.22	-	-
Au	Ni	1	0.18	0.25	0.24	0.26	-	-	0.27	0.09	-0.04	0.05
Au	Ni	50	0.84	0.59	0.88	0.75	-	-	0.79	0.66	0.04	0.10
Au	Ni	100	0.98	0.65	1.05	0.90	-	-	0.94	0.92	0.13	0.15
Au	SS	1	0.32	0.26	-	-	0.60	0.52	-	-	-	-
Au	SS	50	0.82	0.59	-	-	0.89	0.59	-	-	-	-
Au	SS	100	0.94	0.67	-	-	0.93	0.61	-	-	-	-
Rh	C	1	0.15	0.17	0.23	0.25	0.39	0.59	-	-	-0.05	0.08
Rh	C	50	0.57	0.33	0.66	0.48	0.87	0.76	-	-	0.03	0.15
Rh	C	100	1.08	0.44	0.88	0.58	1.13	0.94	-	-	0.13	0.20
Rh	Ni	1	0.10	0.13	0.07	0.21	-	-	0.06	0.02	-0.05	0.07
Rh	Ni	50	0.52	0.41	0.26	0.40	-	-	0.54	0.38	-0.01	0.11
Rh	Ni	100	0.95	0.51	0.30	0.49	-	-	0.67	0.53	0.03	0.15
Rh	SS	1	-	-	-	-	0.38	0.58	0.46	0.25	-	-
Rh	SS	50	-	-	-	-	0.91	0.77	1.2	0.75	-	-
Rh	SS	100	-	-	-	-	1.24	0.97	1.3	0.95	-	-

Table 13

EFFECT OF RATIO CHANGE ON UDMH-N_2H_4 MIXTURES

Electrolyte	Catalyst/ Substrate	Current Density ma/cm²	Potential vs HE at Same pH and Temperature, Volts													
			Ratio Concentrations of N_2H_4								Comparison Data					
			0.1M		0.3M		0.5M		0.75M		1M UDMH		50/50 Mixture		1M N_2H_4	
			30°C	90°C	30°C	90°C	30°C	90°C	30°C	90°C	30°C	90°C	30°C	90°C	30°C	90°C
1M KOH	Rh/Ni	1	-0.03	0.10	-0.01	0.08	-	-	-	-	0.72	0.49	-0.05	0.07	-0.05	0.04
		50	0.04	0.15	0.08	0.15	-	-	-	-	1.2	1.07	-0.01	0.11	-0.04	0.05
		100	0.68	0.20	0.23	0.20	-	-	-	-	1.3	1.12	0.03	0.16	-0.04	0.06
1M KOH	Au/Ni	1	-0.01	0.08	0.03	0.07	-	-	-	-	0.56	0.56	-0.04	0.05	-0.04	0.06
		50	0.58	0.19	0.22	0.20	-	-	-	-	0.81	0.62	0.04	0.10	0.04	0.11
		100	0.68	0.25	0.35	0.34	-	-	-	-	1.1	0.64	0.13	0.15	0.09	0.15
1M H_3PO_4	Rh/Ni	1	0.12	0.07	0.14	0.08	-	-	-	-	0.71	0.27	0.06	0.02	0.00	0.02
		50	1.2	0.67	0.66	0.29	-	-	-	-	1.2	1.1	0.54	0.38	0.24	0.11
		100	1.3	1.12	1.10	0.46	-	-	-	-	1.3	1.3	0.67	0.53	0.30	0.19
1M H_3PO_4	Au/Ni	1	0.28	0.17	0.30	0.14	-	-	-	-	0.51	0.51	0.27	0.09	-	-
		50	1.07	0.80	0.99	0.59	-	-	-	-	0.78	0.66	0.79	0.66	-	-
		100	1.3	1.2	1.3	0.80	-	-	-	-	0.92	0.76	0.94	0.92	-	-
5M HNO_3	Pt/SS	1	0.46	0.47	-	-	-	-	-	-	0.62	0.58	0.45	0.44	0.37	0.34
		50	0.81	0.65	-	-	-	-	-	-	0.89	0.72	0.63	0.54	0.53	0.41
		100	0.92	0.69	-	-	-	-	-	-	0.94	0.78	0.89	0.60	0.56	0.44
5M HNO_3	Au/SS	1	0.60	0.56	0.63	0.57	0.59	0.56	0.67	0.56	0.60	0.53	0.60	0.52	0.49	0.54
		50	0.72	0.61	0.94	0.75	0.74	0.69	0.83	0.69	0.74	0.57	0.89	0.59	0.94	0.73
		100	0.89	0.70	0.98	0.79	0.85	0.73	0.89	0.72	0.84	0.59	0.93	0.61	0.99	0.88

Table 14

ANODIC STUDIES WITH POROUS TEFLON ELECTRODES

Pt (black) Powder Catalyst; 18μ; 10-15 mil Porous Teflon

Electrode	Am't Cat. Mg/ Cm^2	T °C	P psi	Time min	Test at 60°C Test Electrolyte	Test Fuel	OCV vs SHE*	Voltage at 100 ma/cm^2 vs SHE*	Voltage at max. Current/ density vs SHE*	Notes
49811	25	225	5100	15	$1MH_2SO_4$	H_2	+0.02	+0.06	+0.13 at 160 ma/cm^2	H_2 not bubbling through electrode at max. current.
					$5MH_3PO_4$	85% $N_2H_4.H_2O$	+0.12	--	+0.34 at 60 ma/cm^2	
49812	50	225	5100	15	$1MH_2SO_4$	H_2	+0.005	+0.02	+0.13 at 280 ma/cm^2	
					$5MH_3PO_4$	85% $N_2H_4.H_2O$	+0.16	--	+0.25 at 40 ma/cm^2	
49816	50	225	3200	15	$1MH_2SO_4$	H_2	+0.005	+0.025	+0.07 at 200 ma/cm^2	Couldn't try higher currents due to exp. difficulties.
					$5MH_3PO_4$	85% $N_2H_4.H_2O$	+0.11	--	+0.24 at 30 ma/cm^2	
49817	50	225	7000	15	$1MH_2SO_4$	H_2	+0.005	+0.04	+0.115 at 320 ma/cm^2	
					$5MH_3PO_4$	85% $N_2H_4.H_2O$	+0.15	--	+0.20 at 40 ma/cm^2	

* SHE = Standard hydrogen electrode

(1) Hydrazine

The feasibility of using N_2H_4 in vapor feed from concentrated $N_2H_4 \cdot H_2O$ solutions was demonstrated; a current density of 60 ma/cm² was obtained at 60°C with platinum black powder as a catalyst. This current density is fairly close to that obtained using soluble N_2H_4 solutions in direct contact with platinum catalysts. Further improvements in the half cell might be made by using more specific catalysts such as rhodium or ruthenium and by increasing the porosity of the electrode system. The latter change will improve the hydrazine electrode by providing more rapid transport of the vapor to the catalyst surface, since the N_2H_4 vapor pressure will not be variable over too wide a range. The vapor electrode must be used at 60°C and above to provide usable vapor pressures.

(2) Hydrogen

Since sufficient hydrogen pressure can be maintained to provide mass transport to the electrode, the porosity of the electrode should not be critical. The hydrogen fuel data thus shows nearly opposite behavior from that of N_2H_4, improving with increased catalyst concentration and with more homogeneous construction of the electrode. Anodic currents of 300 ma/cm² were obtained at +0.12 volt vs HE at 30°C in 1M H_2SO_4 with the best hydrogen electrode so far constructed.

2. Oxidant-Electrode-Catalyst-Electrolyte Systems

Nitric acid and dinitrogen tetroxide (N_2O_4) were the oxidants studied. HNO_3 was combined with various acid electrolytes. N_2O_4 was studied as a soluble oxidant in acid electrolytes, and as a gas electrode in 1M KOH, pH 6 buffer, and in a number of acid electrolytes.

a. Nitric Acid

Table 15 presents half-cell data obtained with electroplated catalyst systems for general acidic electrolytes. Table 16 presents data obtained for an intensive investigation of H_2SO_4-HNO_3 systems, which seem to be the best overall electrolyte for HNO_3.

Table 15

CATHODIC REDUCTION OF HNO_3

HNO_3 Conc.	Electrolyte	Conc.	Current Density ma/cm²	Potential vs. H.E. at Same pH and Temperature*											
				Platinum Catalyst				Rhodium Catalyst				Gold Catalyst			
				On S.S.		on Carbon		on S.S.		on Carbon		on S.S.		on Carbon	
				30°C	90°C	30°C	90°C	30°C	90°C	30°C	90°C	30°C	90°C	30°C	90°C
2.5M	HNO_3	2.5M	1	+0.41	+1.08	-	-	+0.44	+1.07	+0.42	+1.06	+0.19	+1.05	-	+1.05
			50	neg	+1.02	-	-	+0.18	+1.02	+0.12	+0.99	+0.04	+1.01	-	+1.00
			100	neg	+1.01	-	-	+0.14	+1.00	+0.06	+0.95	neg	+0.99	-	+0.98
5M	HNO_3	5M	1	+1.12	+1.14	-	-	+1.11	+1.15	+1.14	+1.15	+1.15	+1.14	+1.11	+1.14
			50	+1.08	+1.10	-	-	+1.05	+1.09	+1.07	+1.09	+1.09	+1.09	+1.06	+1.09
			100	+1.06	+1.08	-	-	+1.04	+1.06	+0.98	+1.06	+1.08	+1.07	+1.04	+1.05
1M	H_2SO_4	1M	1	+0.30	+1.03	-	-	+0.33	+1.06	-	-	+0.22	+1.03	+0.10	+1.06
			50	neg	+0.96	-	-	neg	+1.00	-	-	neg	+0.97	neg	+0.99
			100	neg	+0.93	-	-	neg	+0.98	-	-	neg	+0.95	neg	+0.96
1M	H_2SO_4	5M	1	+1.07	+1.10	-	-	+1.08	+1.12	-	-	+1.09	+1.11	+1.08	+1.12
			50	+1.02	+1.06	-	-	+1.03	+1.07	-	-	+1.02	+1.05	+1.00	+1.07
			100	+0.97	+1.05	-	-	+0.99	+1.06	-	-	+1.00	+1.04	+0.92	+1.04
2M	H_2SO_4	4M	1	-	-	-	-	+1.11	+1.14	-	-	+1.12	+1.14	-	-
			50	-	-	-	-	+1.06	+1.09	-	-	+1.07	+1.09	-	-
			100	-	-	-	-	+1.04	+1.08	-	-	+1.06	+1.08	-	-
1M	H_3PO_4	1M	1	+0.29	+0.99	-	-	+0.33	+0.99	-	-	+0.18	+1.01	+0.10	+1.01
			50	neg	+0.93	-	-	neg	+0.91	-	-	neg	+0.93	neg	+0.93
			100	neg	+0.13	-	-	neg	+0.29	-	-	neg	+0.90	neg	+0.86
1M	H_3PO_4	5M	1	+0.32	+1.00	-	-	+0.46	+1.02	-	-	neg	+1.01	neg	+1.03
			50	neg	+0.90	-	-	neg	+0.95	-	-	neg	+0.93	neg	+0.94
				neg	+0.09	-	-	neg	+0.91	-	-	neg	+0.88	neg	+0.89
2M	H_3PO_4	4M	1	-	-	-	-	+0.49	+1.02	-	-	+0.21	+1.09	-	-
			50	-	-	-	-	+0.18	+1.02	-	-	neg	+1.02	-	-
			100	-	-	-	-	neg	+0.99	-	-	neg	+1.01	-	-

* E° for reaction: $HNO_3 + 3H^+ + 3e^- \longrightarrow NO + 2H_2O = +1.06$ V versus HE at 30°C.

Table 16

CATHODIC REDUCTION OF HNO_3 IN H_2SO_4 ELECTROLYTE

HNO_3 Conc.	H_2SO_4 Conc.	Current Density ma/cm²	Uncatalyzed Carbon 30°C	Uncatalyzed Carbon 90°C	Potential vs HE at Same pH and Temperature, Volts: Pt/SS 30°C	Pt/SS 90°C	Rh/SS 30°C	Rh/SS 90°C	Au/SS 30°C	Au/SS 90°C
1M	5M	1	-- not	--	+1.07	+1.10	+1.08	+1.12	+1.09	+1.11
		50	-- tested	--	+1.02	+1.06	+1.03	+1.07	+1.02	+1.05
		100	--	--	+0.97	+1.05	+0.99	+1.06	+1.00	+1.04
1M	2.5M	1	--	+1.08	+0.49	+1.05	+0.41	+1.09	+0.24	+1.08
		50	--	+1.01	--	+1.01	--	+1.03	--	+1.03
		100	--	+0.99	--	+1.00	--	+1.01	--	+1.02
1M	1M H_2SO_4	1	-- not	--	+0.30	+1.03	+0.33	+1.06	+0.22	+1.03
		50	-- tested	--	--	+0.96	--	+1.00	--	+0.97
		100	--	--	--	+0.93	--	+0.98	--	+0.95
0.5M	5M	1	+1.04	+1.09	+1.10	+1.09	+1.09	+1.09	+1.10	+1.10
		50	--	+1.02	+1.00	+1.04	+1.00	+1.04	+1.05	+1.04
		100	--	+1.00	+0.94	+1.02	+0.92	+1.03	+0.96	+1.03
0.5M	2.5M	1	0.0	+1.01	+0.49	+1.05	+0.39	+1.03	+0.29	+1.10
		50	--	+0.94	--	+0.97	--	+0.96	--	+1.03
		100	--	+0.89	--	+0.95	--	+0.94	--	+1.01
0.25	2.5M	1	--	+1.02	--	+1.06	--	+1.10	--	+1.06
		50	--	--	--	+0.95	--	+0.97	--	+0.96
		100	--	--	--	--	--	--	--	--
0.1M	5M	1	--	+1.07	+0.47	+1.06	+0.40	+1.06	+0.34	+1.06
		50	--	+0.93	--	+0.99	--	+0.74	--	+0.96
		100	--	--	--	+0.90	--	--	--	+0.88

With HNO_3 as electrolyte and oxidant, a high HNO_3 concentration was found to be necessary for high reduction potentials. At 30°C, 5M HNO_3 was required. However, at 90°C, 2.5M HNO_3 gave an acceptable potential. The catalyst used made very little difference.

With H_3PO_4 electrolyte, 1M HNO_3 was not reduced at 30°C regardless of the H_3PO_4 concentration. At 90°C, generally only gold catalysts reduced nitric acid regardless of H_3PO_4 concentration*. When 2M HNO_3 was used, the half-cell potentials at 30°C and 90°C were equivalent to the 2.5M HNO_3 electrolyte half-cell potentials.

When H_2SO_4 was used as electrolyte, 1M HNO_3 at 90°C in 1M H_2SO_4 gave high positive potentials vs HE. In 5M H_2SO_4, however, the potentials were high even at 30°C. The catalyst seemed to make little difference.

The use of nitric acid and sulfuric acid mixtures was investigated to find the lowest usable HNO_3 concentration at 30°C and 90°C in both 5M H_2SO_4 and 2.5M H_2SO_4. The reason for interest in this mixture is apparent from the full-cell studies, where N_2H_4 contamination quickly deteriorated the oxidant half cell if 5M HNO_3 solutions were used, while with 1M HNO_3 and 5M H_2SO_4, the N_2H_4 precipitated as hydrazine sulfate without impairing the oxidant half-cell potential.

The following trends were noted:

1. At 30°C only 1M HNO_3-5M H_2SO_4 will maintain useful potentials at 100 ma/cm^2.

2. In general, the best catalyst electrode combination of the four investigated for any mixture is Au on SS.

3. If the HNO_3 concentration is held constant, potentials become less positive with decreasing H_2SO_4 concentration.

4. With 5M H_2SO_4 at 90°C 0.2M HNO_3 is the lowest concentration that still gives useful potentials.

5. With 2.5M H_2SO_4 at 90°C, a concentration of about 0.35 to 0.4M HNO_3 is the lowest possible for useful potentials.

---

*An exception was 5M H_3PO_4 electrolyte at 90°C with rhodium catalyst.

b. Dinitrogen Tetroxide

Table 17 lists data for both aqueous and gaseous utilization of N_2O_4.

(1) Aqueous

Dinitrogen tetroxide was utilized in aqueous solution by bubbling the gas into distilled water at 25°C. Half-cell runs were made with gold catalysts and at the H^+ concentration found by titration of a solution sample. The blue color that appeared in solution could be made to disappear within a few hours by discontinuing N_2O_4 flow. Runs made at approximately the same H^+ concentration when the blue color was present and absent showed that reduction was easier when the blue color was present. This was also better than HNO_3 reduction at equivalent H^+ concentration and temperatures. The blue color has been noted by others (refs. 14 and 15) and seems to be caused by a mixture of NO and NO_2 in solution. Liquid N_2O_3 is blue. The potentials were generally good and the current carrying capabilities were very good.

(2) Vapor

These half cell tests were made with the porous electrode illustrated in Figure A-4, Appendix A-3. The tests were conducted with a sufficiently high pressure of N_2O_4 to prevent gross moisture from the electrolyte backing up in the electrode. The electrode was a porous carbon disk, uncatalyzed. Currents were held for five minutes with readings immediately after current was imposed, then 1, 2 and 5 minutes later. A great potential drop with time indicated electrode failure for a given current density.

(a) Acid Electrolytes

Since 5M H_3PO_4, 1M H_3PO_4, and 1M HNO_3 have been shown to have no oxidizing properties in themselves at 25°C, the electrochemical activity shown in Table 17 can be ascribed to N_2O_4 reduction. At 25°C both 5M H_3PO_4 and 1M HNO_3 electrolyte behaved the same for N_2O_4 reduction, holding 50 ma/cm^2 maximum at about +0.80 volt from HE. In 1M H_3PO_4 at 60°C better performance was found with 120 ma/cm^2 being maintained at +0.80 volt versus HE.

Utilizing N_2O_4 in this manner avoids the inherent waste associated with converting it to HNO_3 before use, since from:

$$N_2O_4\ (g) \rightarrow N_2O_4\ (aq) \quad \text{and then}$$

$$H_2O + N_2O_4\ (aq) \rightarrow HNO_3 + HNO_2$$

$$1/3\ H_2O + 4/3\ HNO_3 + 2/3\ NO \leftarrow$$

Table 17

CATHODIC REDUCTION OF N_2O_4-AQUEOUS AND GASEOUS AT 25°C AND 60°C

Aqueous				Gas Porous Carbon Electrode*											
H^+ Conc.	Current Density ma/cm²	Potential**** Cat. Au/C	Cat. Au/SS	Current Density ma/cm²	25°C Potential**** 5M H_3PO_4	1M HNO_3	5M HNO_3	Current Density ma/cm²	60°C Potential**** 1M KOH 1 min	1M KOH 5 min	pH 6 Buffer 1 min	pH 6 Buffer 5 min	1M H_3PO_4 1 min	1M H_3PO_4 5 min
1.4M	1	+0.92	-	O.C.**	+1.03	+1.01	+1.06	O.C.**	+1.74	+1.74	+1.53	+1.53	+1.06	+1.06
1.4M	36(max)***	+0.84	-	1	+1.03	+1.01	+1.06	2	+1.71	+1.71	+1.53	+1.52	+1.06	+1.06
2.3M	1	+0.97	-	5	+1.01	+1.00	+1.04	4	+1.70	+1.70	+1.51	+1.51	+1.06	+1.04
2.3M	50	+0.83	-	10	+0.99	+0.98	+1.02	8	+1.67	+1.65	+1.50	+1.50	+1.02	+1.02
2.3M	100	+0.64	-	30	+0.92	+0.92	+1.01	20	+1.61	+1.59	+1.45	+1.45	+0.99	+0.97
4.3M	1	+0.97	-	50	+0.78	+0.81	+0.98	40	+1.56	+1.54	+1.40	+1.39	+0.94	+0.91
4.3M	50	+0.89	-	100	+0.09	+0.56	+0.93	80	+1.46	+1.43	+1.31	+1.30	+0.87	+0.85
4.3M	100	+0.83	-					120	+1.36	+1.35	+1.22	+1.16	+0.81	+0.84
6.2M	1	+1.05	+1.04											
6.2M	50	+1.01	+1.02											
6.2M	100	+0.98q	+1.00											

*Source of carbon - FC-12 Disk- Pure Carbon Co.

**Open Circuit Potential - E° for reaction N_2O_4 (g) + $4e^-$ + $4H^+$ ⟶ 2NO + $2H_2O$ = +1.03 V versus HE at 30°C and 90°C.

***Maximum current obtainable with available voltage

****vs HE at same temperature and pH

one-third of the energy possible is wasted in NO (g) evolution. However, at low temperatures (25°C) the rate of HNO_2 reaction to HNO_3 and NO (g) is slow, and the HNO_2 might be utilized.

(b) Basic and Buffer Electrolytes

N_2O_4 gas in basic or neutral electrolytes offers little possibility of use as a gas electrode. This could be important since N_2H_4 performs better in basic and neutral electrolytes. Table 17 shows data for tests at 60°C in 1M KOH and in a pH 6 phosphate buffer. Currents of over 100 ma/cm² were maintained at very high potentials. However, the large positive potential versus HE, corrected for the pH and temperatures of the electrolyte used, indicates a local pH effect at the electrode surface, and thus eventual contamination of the electrolyte.

B. STABILITY STUDIES

1. Open-Circuit Studies

This section considers the amount of fuel lost from open-circuit decomposition at the catalyst from decomposition of the fuel. If the decomposition is very large, significant losses in coulometric efficiency could occur. Also studied is the effect of open-circuit storage on the electrochemical activity of the catalyst/substrate. These data are found in Table 18.

a. Decomposition at Electrode

(1) Hydrazine

5M HNO_3 electrolytes were not further tested due to slow reaction with N_2H_4. N_2H_4 in 5M H_3PO_4 showed negligible decomposition at 30°C and 90°C. In 1M KOH with Pt on SS electrodes, decomposition was also negligible after 7 days of storage.

(2) Monomethylhydrazine and Unsymmetrical Dimethylhydrazine

These showed very small gas volumes from decomposition at electrode at 90°C with Au on SS electrodes in both H_3PO_4 and HNO_3. But, if a reaction analogous to N_2H_4 is assumed, i.e.,

$$4H^+ + 3CH_3NHNH_2 \longrightarrow 3CH_3NH_3^+ + N_2 + NH_4^+ \quad \text{and}$$

$$4H^+ + 3(CH_3)_2NNH_2 \longrightarrow 3(CH_3)_2NH_2^+ + N_2 + NH_4^+$$

Table 18

DECOMPOSITION OF THE FUELS AT OPEN CIRCUIT

Fuel	Electrolyte	No. of Days Storage	Temp of Decomposition °C	Catalyst/ Substrate	Storage Solution	Rate of Decomposition in ml gas/ cm^2/min at 25°C	Rate in moles/cm^2/min of N_2H_4 Used	Assumed Decomposition Reaction*	Current which could be Supported by N_2H_4 Decomposed ma/cm^2	Coulometric Efficiency at 100 ma/cm^2 Assuming Decomposition Products Lost, %	Half-Cell Potentials in Volts vs H.E. at same pH and Temperature of Electrode Immediately After Decomposition Test			
												ma/cm^2		
											OC**	1	50	100
1M N_2H_4	1M KOH	0	25	Au/Ni	Cell soln	0.0094	1.285×10^{-7}	B	0.82	99.3	-0.04	-0.04	-0.02	-0.01
		1	25	Au/Ni	Cell soln	0.0025	0.34×10^{-7}	B	0.23	99.7	-0.04	-0.04	-0.02	-0.01
		0	25	Au/Ni	H_2O	0.0079	1.08×10^{-7}	B	0.69	99.4	-0.07	-0.06	-0.03	-0.03
		1	25	Au/Ni	H_2O	0.0040	0.55×10^{-7}	B	0.35	99.6	-0.01	-0.01	+0.03	+0.04
		5	30	Au/Ni	H_2O	0.0049	0.67×10^{-7}	B	0.43	99.5	0.0	0.0	+0.02	+0.02
		0	90	Au/Ni	Cell soln	0.336	46.5×10^{-7}	B	29.9	77.0	+0.05	+0.05	+0.05	+0.05
		1	90	Au/Ni	Cell soln	0.056	7.7×10^{-7}	B	4.6	95.7	+0.05	+0.05	+0.05	+0.06
		5	90	Au/Ni	Cell soln	0.054	7.4×10^{-7}	B	4.4	95.8	+0.07	+0.07	+0.07	+0.07
1M N_2H_4	1M KOH	0	30	Pt/SS	Cell soln	0.020	2.7×10^{-7}	B	1.8	98.5	-0.02	+0.07	+0.14	+0.18
		1	30	Pt/SS	Cell soln	0.0059	0.8×10^{-7}	B	0.5	99.5	0.00	+0.03	+0.14	+0.18
		7	30	Pt/SS	Cell soln	0.0017	0.2×10^{-7}	B	0.15	99.8	+0.03	+0.05	+0.18	+0.26
		0	90	Pt/SS	Cell soln	0.041	5.6×10^{-7}	B	3.6	96.7	+0.06	+0.15	+0.21	+0.21
		1	90	Pt/SS	Cell soln	0.0086	1.2×10^{-7}	B	0.76	99.4	+0.12	+0.13	+0.18	+0.19
		7	90	Pt/SS	Cell soln	0.0019	0.26×10^{-7}	B	0.17	99.8	+0.12	+0.20	+0.27	+0.28
1M N_2H_4	5M HNO_3	0	25	Pt/SS	Cell soln	0.00165	2.0×10^{-7}	A	1.32	98.7	+0.37	+0.43	+0.52	+0.54
		1	25	Pt/SS	H_2O	only half cell run					+0.36	+0.42	+0.50	+0.52
		6	25	Pt/SS	Cell soln	0.0061	7.4×10^{-7}	A	4.76	95.5	+0.31	+0.39	+0.50	+0.52
		11	25	Pt/SS	Cell soln	only half cell run					+0.34	+0.40	+0.47	+0.48
		0	90	Pt/SS	Cell soln	0.086	107×10^{-7}	A	62.7	59.8	+0.40	+0.41	+0.44	+0.45
		6	90	Pt/SS	Cell soln	0.356	440×10^{-7}	A	283	26	+0.34	+0.36	+0.42	+0.43
		11	90	Pt/SS	Cell soln	0.171	210×10^{-7}	A	135	42.5	+0.35	+0.36	+0.43	+0.45
1M MMH	5M HNO_3	0	90	Au/SS	Cell soln	0.070	86.4×10^{-7}	C	139	41.7	+0.49	+0.53	+0.57	+0.59
		4	90	Au/SS	Cell soln	0.0076	9.4×10^{-7}	C	15.1	86.8	+0.43	+0.49	+0.53	+0.65
1M UDMH	5M HNO_3	0	90	Au/SS	Cell soln	0.023	28.2×10^{-7}	D	72.7	58	+0.47	+0.58	+0.62	+0.63
		4	90	Au/SS	Cell soln	0.0046	5.65×10^{-7}	D	14.5	87.5	+0.35	+0.43	+0.51	+0.52
1M N_2H_4	5M H_3PO_4	0	30	Pt/SS	Cell soln	0.0004	0.5×10^{-7}	A	0.32	99.7	+0.11	+0.24	+0.39	+0.41
		7	30	Pt/SS	Cell soln	only half cell run		A			+0.07	+0.17	+0.33	+0.35
		0	90	Pt/SS	Cell soln	0.005	6.1×10^{-7}	A	4.0	96.2	+0.03	+0.11	+0.17	+0.20
		7	90	Pt/SS	Cell soln	only half cell run		A			+0.01	+0.11	+0.25	+0.27
1M MMH		0	90	Au/SS	Cell soln	0.012	14.7×10^{-7}	C		81	+0.28	+0.38	+0.48	+0.48
		8									+0.29	+0.49	+0.55	+0.56

*A - $H^+ + 3N_2H_5^+ \longrightarrow N_2 + 4NH_4^+$ (Ref. 13)

B - $N_2H_4 \longrightarrow N_2 + 2H_2$ (Ref. 12)

C - $4H^+ + 3CH_3NHNH_2 \longrightarrow N_2 + 3CH_3NH_3^+ + NH_4^+$

D - $4H^+ + 3(CH_3)NNH_2 \longrightarrow N_2 + 3(CH_3)NH_2^+ + NH_4^+$

**Open Circuit = O.C.

the effect on coulombic efficiency is significant. The reason for this is the large electron changes that are involved in the half cell reaction for complete utilization of the fuel, i.e., to N_2 and CO_2. For MMH, n = 10, and for UDMH, n = 16. Thus, as seen in Table 17, for 5M HNO_3, assuming electrode current of 100 ma/cm², and a 10 electron change, the coulombic efficiency of MMH is 42% initially, and after 4 days 87%. For UDMH, n = 16 and the efficiencies are 50% initially and 87% after 4 days. When a third attempt was made to find decomposition after 7 days, the electrode catalyzed the chemical reaction with HNO_3, and tests with HNO_3 were stopped. Only MMH was tried in 5M H_3PO_4 and its efficiency, initially 81%, was better than in 5M HNO_3.

b. Effect of Open-Circuit Storage on Electrochemical Activity

N_2H_4 in 1M KOH showed a degradation of the electrode upon length of time stored in the cell solution (Table 18). This directly compares to decreased open circuit decomposition. After 7 days, the potential at 100 ma/cm² became poorer by 0.26 volt compared to normal activity with Pt on SS electrodes. This occurred at both 30°C and 90°C.

In 5M H_3PO_4, after 7 days' storage, there was no significant change in electrode activity.

The activity change with time was also insignificant with MMH and UDMH in 5M H_3PO_4 and 5M HNO_3.

2. Closed-Circuit Stability Studies (Electrochemical)

a. Hydrazine

(1) Electroplated Catalysts

Previous contract work on hydrazine anodes in base showed grave half-cell potential deterioration under operating conditions within 24-hour periods (ref. 16). Electroplated catalysts in this work also deteriorate badly. Figure 2 shows results over a 24-hour period for Rh/SS and Pt/SS at 30°C and 90°C in 1M KOH. The rhodium catalyst performed 0.1 volt better than platinum at both temperatures. The difference between the 30°C and 90°C tests was 0.3 volt, with the 90°C test performing best. Even at 90°C with Rh/SS, the half-cell potential after 24 hours was +0.4 volt from reversible HE performance. This value is not good enough for a useful full cell. When polarization of the oxidant electrode and IR drop are included a full cell potential of 0.5 volt would probably be the best possible at 100 ma/cm².

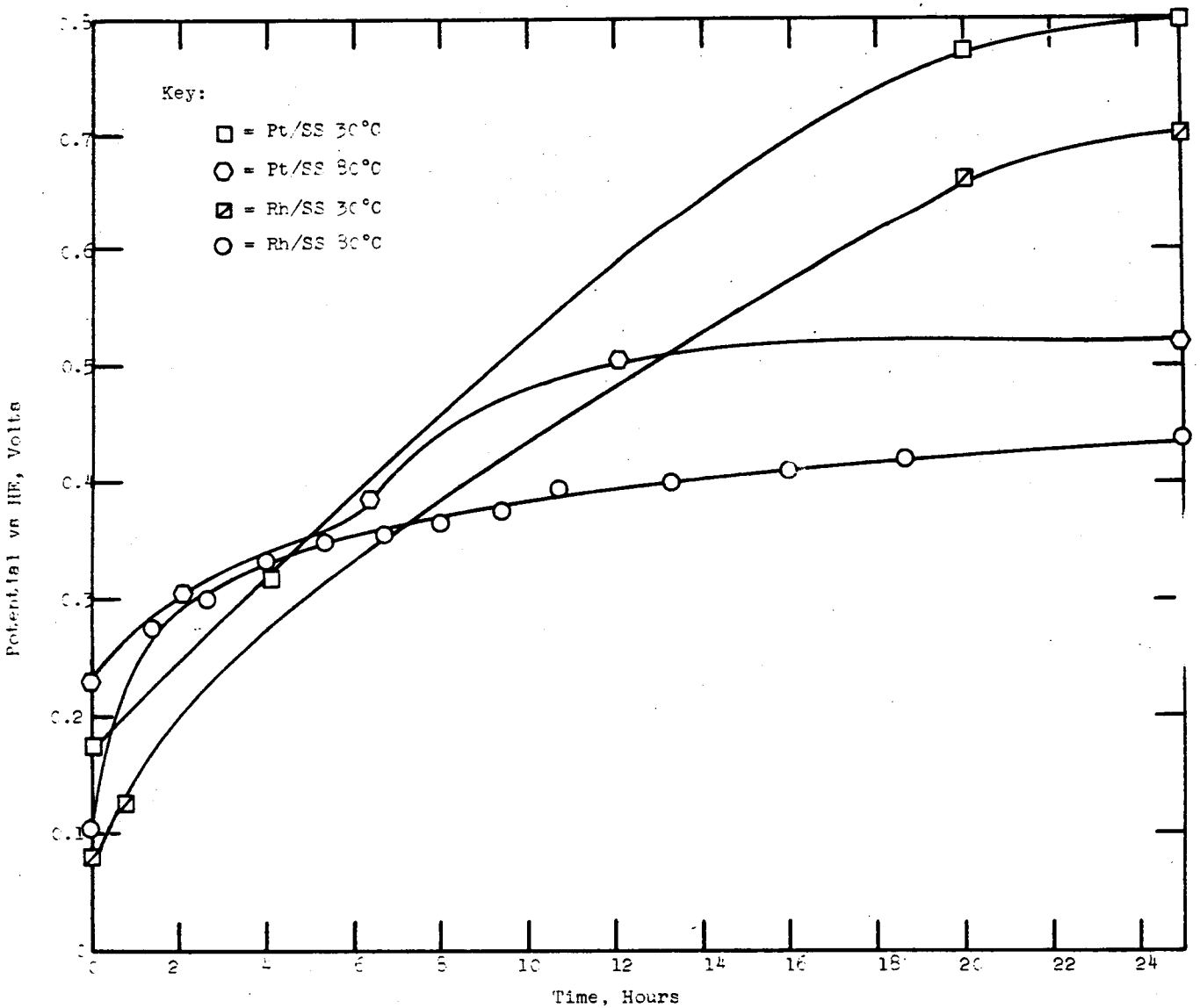

Figure 2. Chronopotentiometric Plot Half-Cell Potential for Electro-oxidation of 1M N_2H_4 in 1 M KOH using Electroplated Catalysts

Current Density = 100 ma/cm²

No previous long-term use of N_2H_4 in acidic solutions was found. Figure 3 shows long-term tests with Pt/SS electrodes in 5M H_3PO_4 at 90°C at 100 ma/cm^2. At 90°C the initial potential was +0.24 from HE, and over a period of 3 hours the potential deteriorated to +0.4 volt versus HE and then very slowly polarized until it reached +0.46 volt versus HE after 24 hours. Once again the potentials reached after 24 hours are not useful for full cell work.

(2) Precipitated Catalysts

The failure of electroplated catalysts led to the testing of the precipitated catalysts. Those catalysts that showed good half-cell short-term polarization tests were put on long-term test for further tests at 100 ma/cm^2.

Figure 4 shows tests made with 1M N_2H_4 in 1M KOH at 30°C with rhodium, ruthenium, and iridium (32%)-ruthenium (68%). At the end of 145 hours the rhodium and ruthenium were at potentials of +0.19 volt and +0.26 volt from HE respectively, which is a significant improvement over the electroplated catalysts. Shortly thereafter both electrodes deteriorated rapidly. However, even these were poor compared to the iridium-ruthenium mixture, which ran for 700 hours at which time its potential was only +0.17 volt versus HE. The reason for this spectacular long-term run is not known; it must be reproduced to be sure the catalyst itself was responsible.

Figure 5 shows tests made using 1M N_2H_4 in 1M KOH at 80°C. Catalysts of rhodium, ruthenium, platinum (80%)-ruthenium (20%) and iridium (32%)-ruthenium (68%) all showed a quick initial drop to +0.20 to +0.26 volt versus HE, where they leveled off somewhat and then rapidly deteriorated. The rhodium potential fell off after 96 hours, Pt-Ru and Ru after 150 hours, and Ir-Ru lasted 300 hours before +0.3 volt versus HE was reached. In one test ruthenium performed better than the other catalysts, but it was found that the KOH concentration had accidentally increased to 4M and N_2H_4 to 3M. These should be studied further.

Tests in 5M H_3PO_4 with N_2H_4 were only done at 80°C, because of poor potentials at 30°C and also because the resistivity of 5M H_3PO_4 was too high at 30°C (~5 ohm.-cm.) for practical use in a full cell. At 80°C the resistivity drops to ~3.0 ohm.-cm.

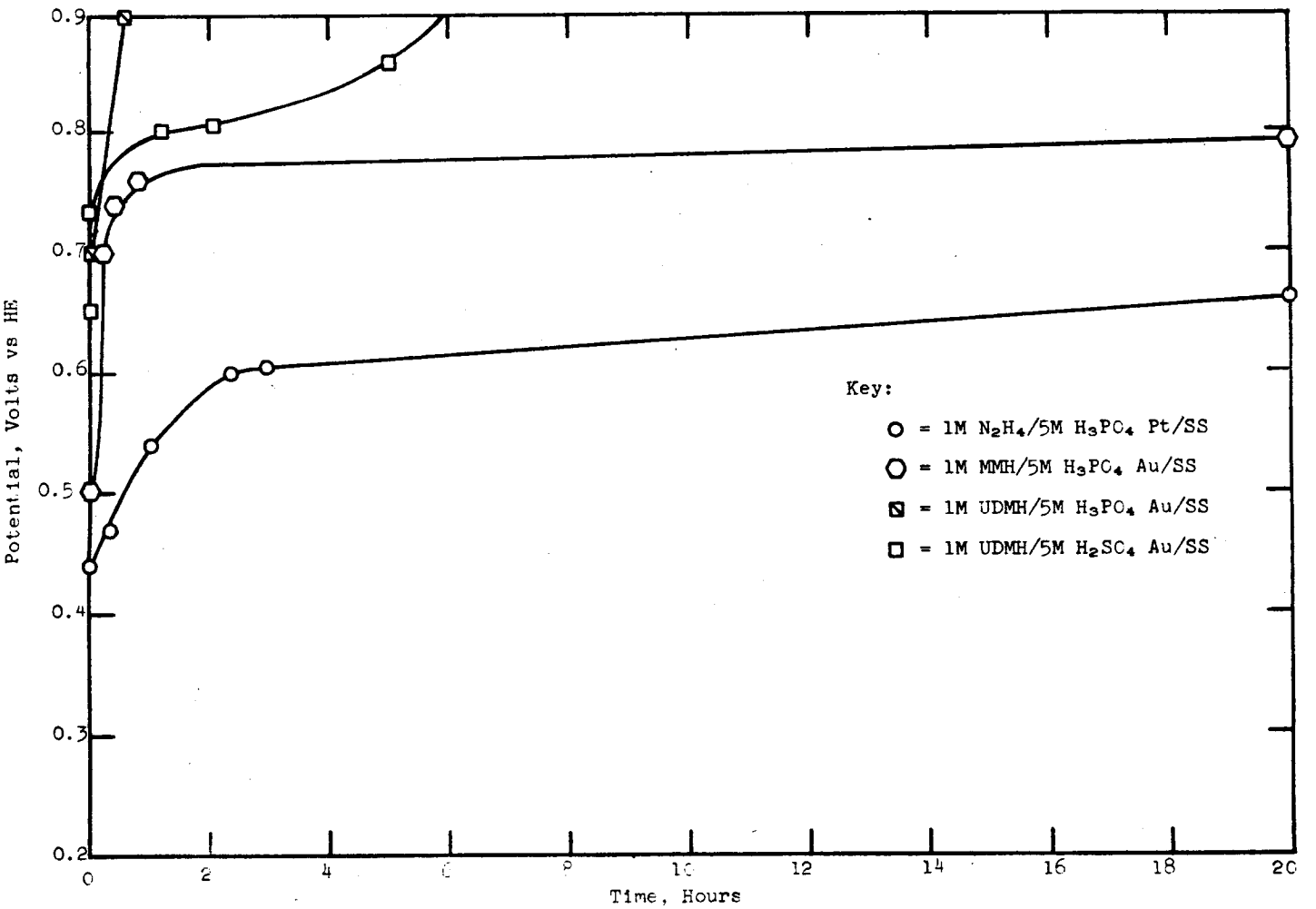

Figure 3. Chronopotentiometric Plot Electro-oxidation of Hydrazine-type Fuels at Electroplated Catalysts I = 100 ma/cm²

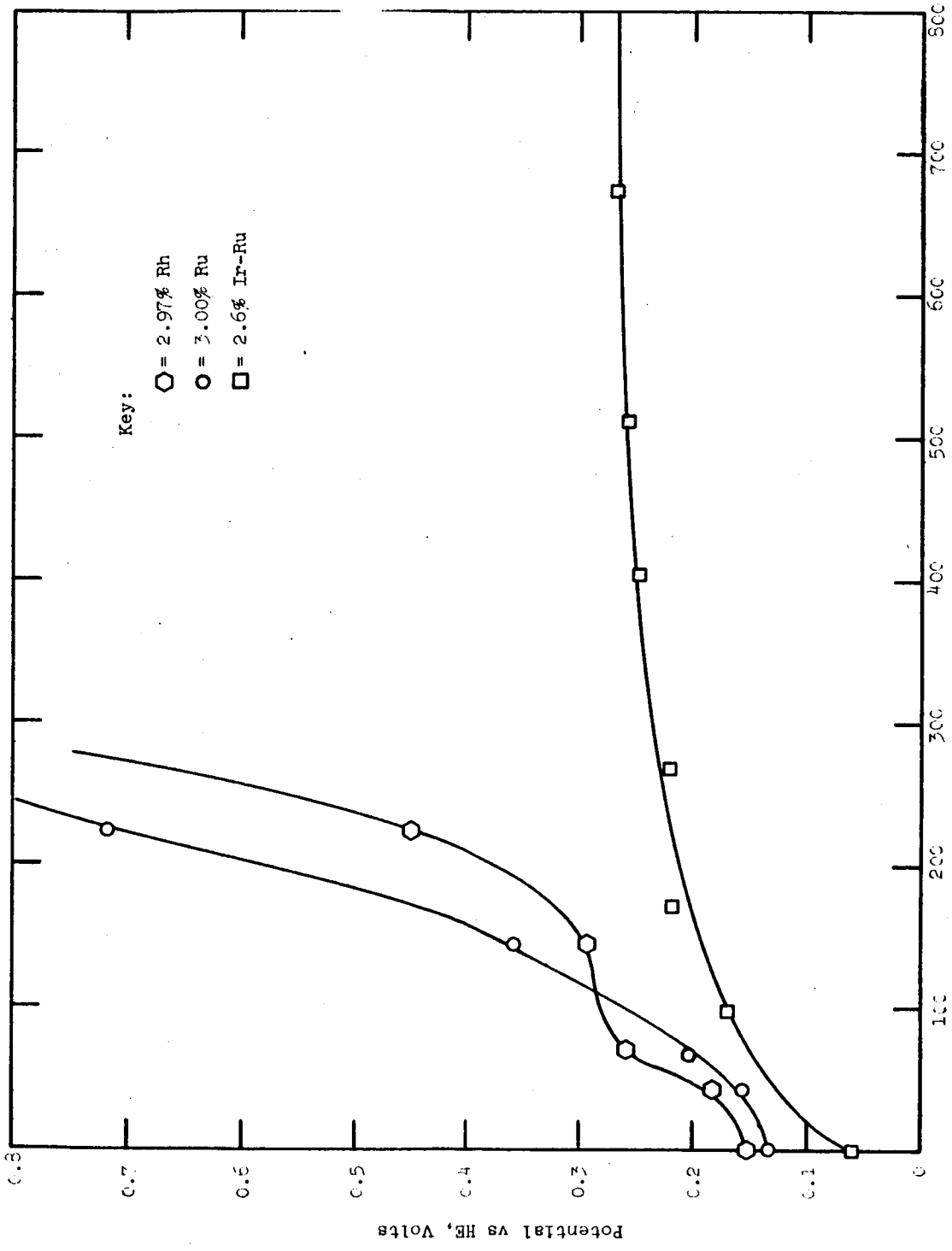

Figure 4. Chronopotentiometric Plot Electro-oxidation of 1 M N_2H_4 in 1 M KOH at 30°C using Precipitated Catalysts I = 100 ma/cm²

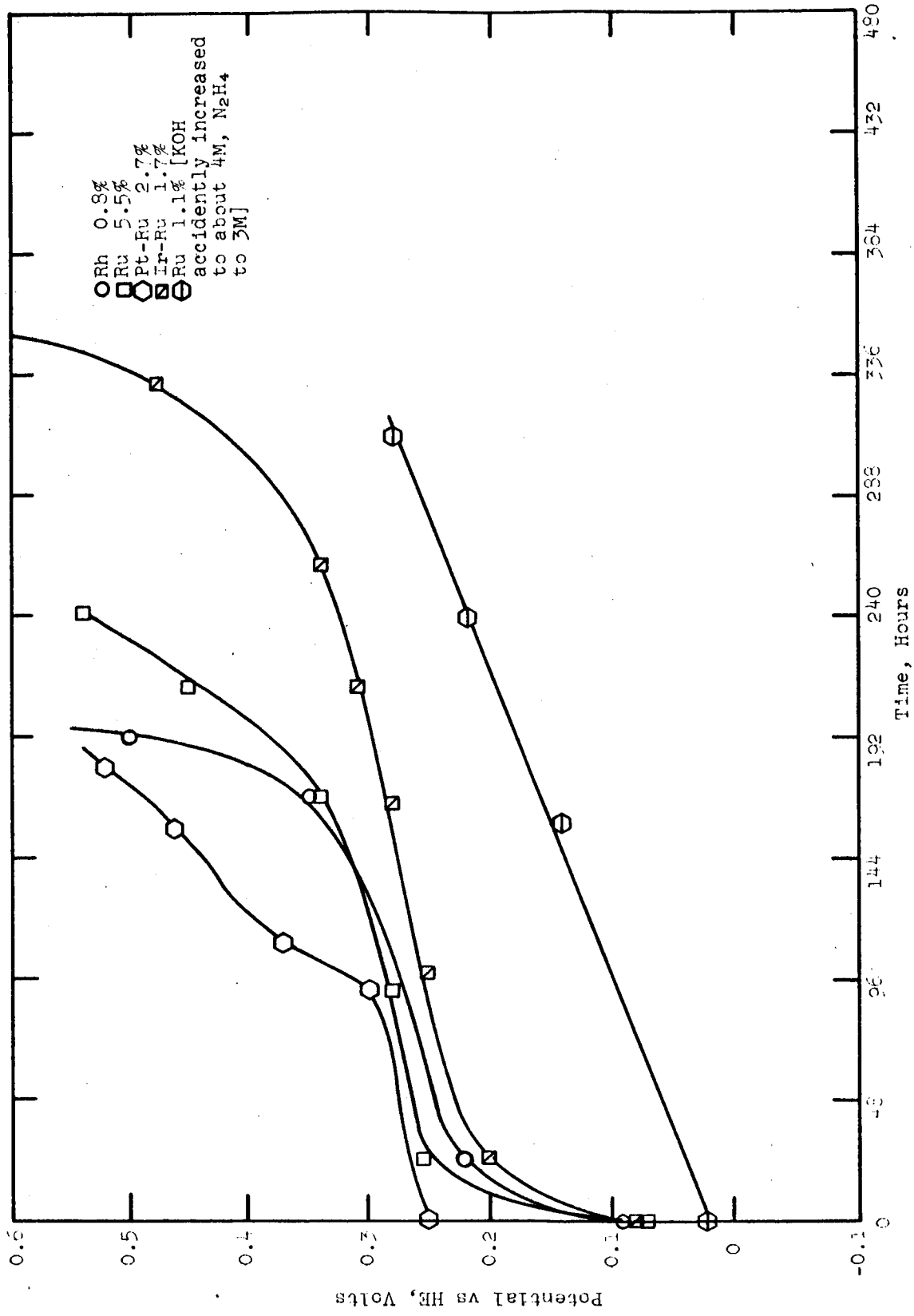

Figure 5. Chronopotentiometric Plot Anodic Oxidation of 1 M N_2H_4 in 1M KOH at 80°C using Precipitated Catalysts

I = 100 ma/cm²

Figure 6 shows data for 1M N_2H_4 in 5M H_3PO_4 at 80°C. All catalysts except ruthenium fell to +0.48 volt versus HE within 20 to 200 hours depending on specific catalysts. Ruthenium on the other hand levels off at 0.25 volt and after 600 hours only polarized by another +0.05 volts. However, this curve is not smooth, as shown in Figure 6. The actual behavior consisted of large voltage fluctuations shown in Figure 7. The sudden drop in voltage occurred when fuel was added to bring the solution back to 1M concentration. The values plotted on Figure 6 are taken 10 hours after addition of fuel. The fluctuation does not seem to be caused by the lowering of fuel concentration, which drops to only 0.8 M at the time of fuel addition. This does not seem to be an effect of stirring either, for the length of time required for the potential to deteriorate to the same value in successive fluctuations is about 50 hours. With catalysts other than ruthenium this fluctuation did not occur, as shown in Figure 7 for rhodium.

To find more information about this effect, another ruthenium electrode was tested using 2M N_2H_4. The results of this test are also shown in Figure 7. The fluctuations still occur, but with much smaller amplitudes. A plot of potentials 10 hours after fuel addition did not differ significantly from 1M N_2H_4 plots. The reason for this behavior is not known, but might have a fundamental relation to the long-term deterioration of all electrodes in N_2H_4 solutions. Contaminants apparently build up at the electrode in different amounts depending on the catalyst. With ruthenium, this build-up might be very slow; thus, stirring tended to transport it from the surface of the electrode. With 2M N_2H_4 even less build-up seemed to occur. Figure 8 shows tests with a number of catalysts using 2M N_2H_4. There was a significant improvement with rhodium, Ir-Ru, and Pt-Rh-Au using 2M N_2H_4.

b. Monomethylhydrazine

(1) Electroplated Catalysts

Figure 3 shows data for 1M MMH in 5M H_3PO_4 at 80°C using a Au/SS electrode. The potential rapidly deteriorated from the initial value of +0.30 volt versus HE to +0.60 volt versus HE where it leveled off and remained fairly constant until the end of 24 hours. The potential deteriorated rapidly after 45 hours.

(2) Precipitated Catalysts

Figure 9 shows tests made with 1M MMH in 5M H_3PO_4 at 80°C with precipitated catalysts. Rhodium and ruthenium catalysts deteriorated badly within 24 hours. Rh (80%) - Ni (20%)

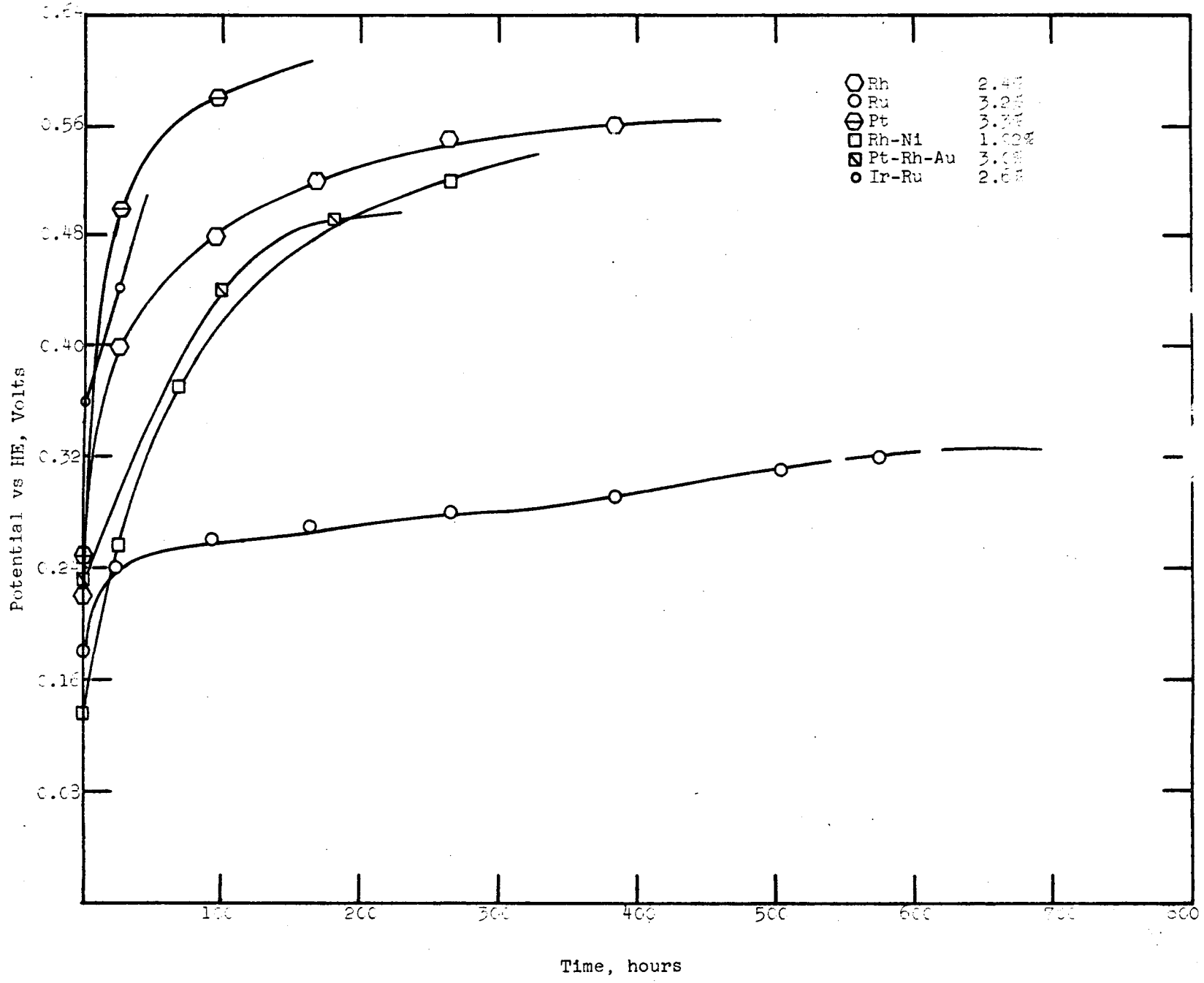

Figure 6. Chronopotentiometric Plot Anodic Oxidation of 1 M N_2H_4 in 5 M H_3PO_4 at 80°C using Precipitated Catalysts. I = 100 ma/cm²

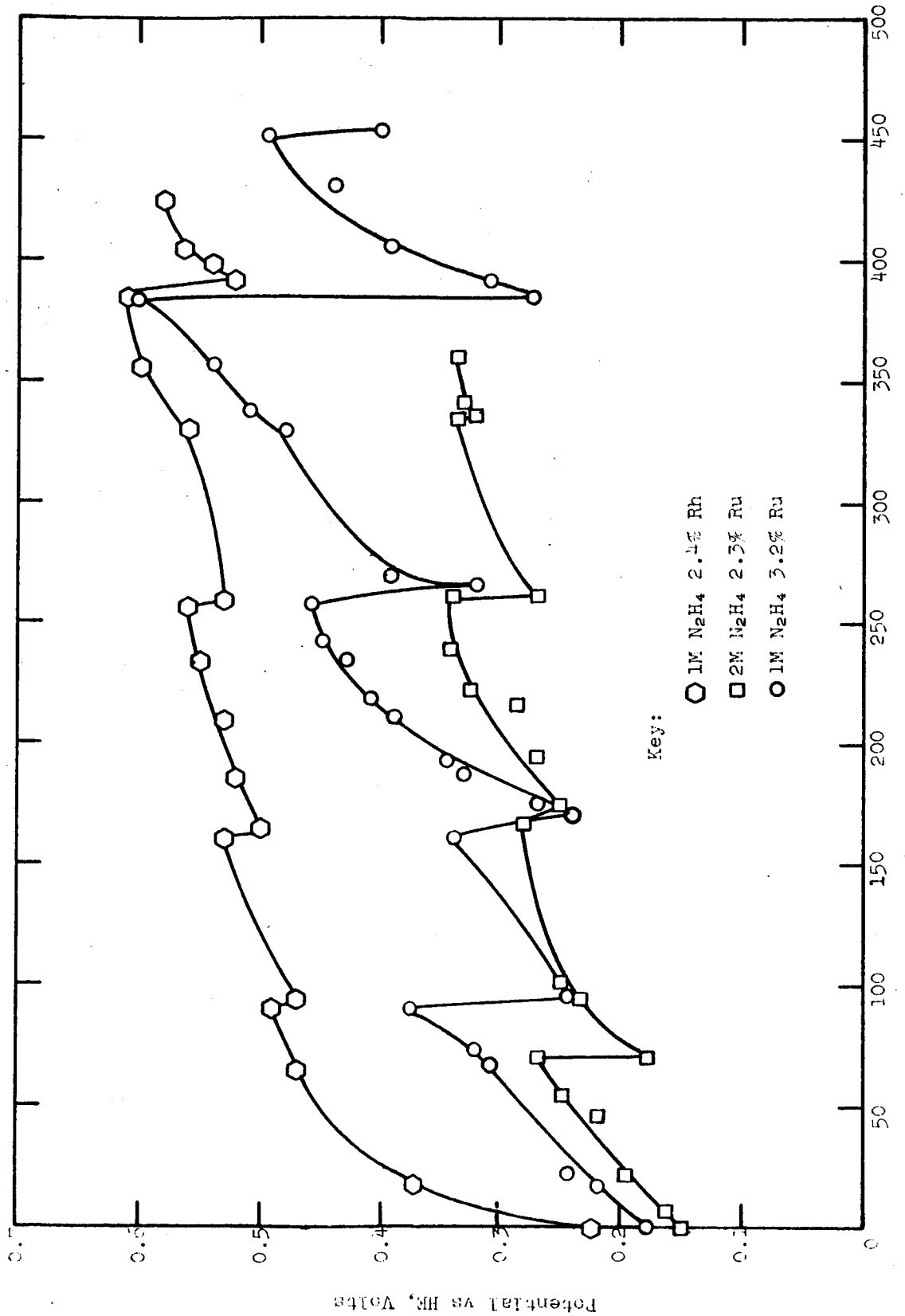

Figure 7. Comparison of Fluctuation of Long Term N_2H_4 Half Cells in 5 M H_3PO_4 using Precipitated Catalyst Electrodes. I = 100 ma/cm²

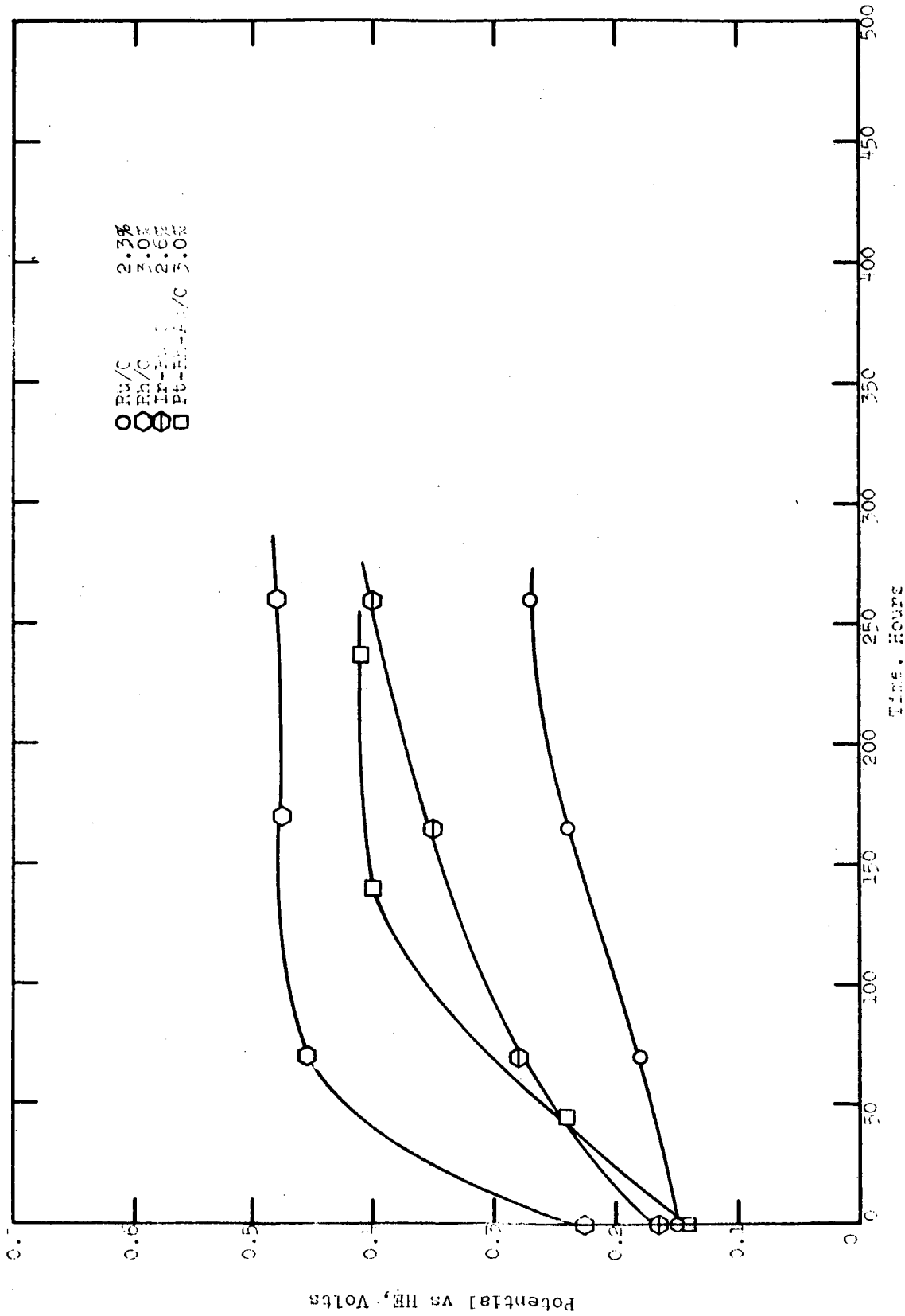

Figure 8. Chronopotentiometric Plot Anodic Oxidation of 2 M N_2H_4 in 5 M H_3PO_4 at 80°C using Precipitated Catalysts

I = 100 ma/cm²

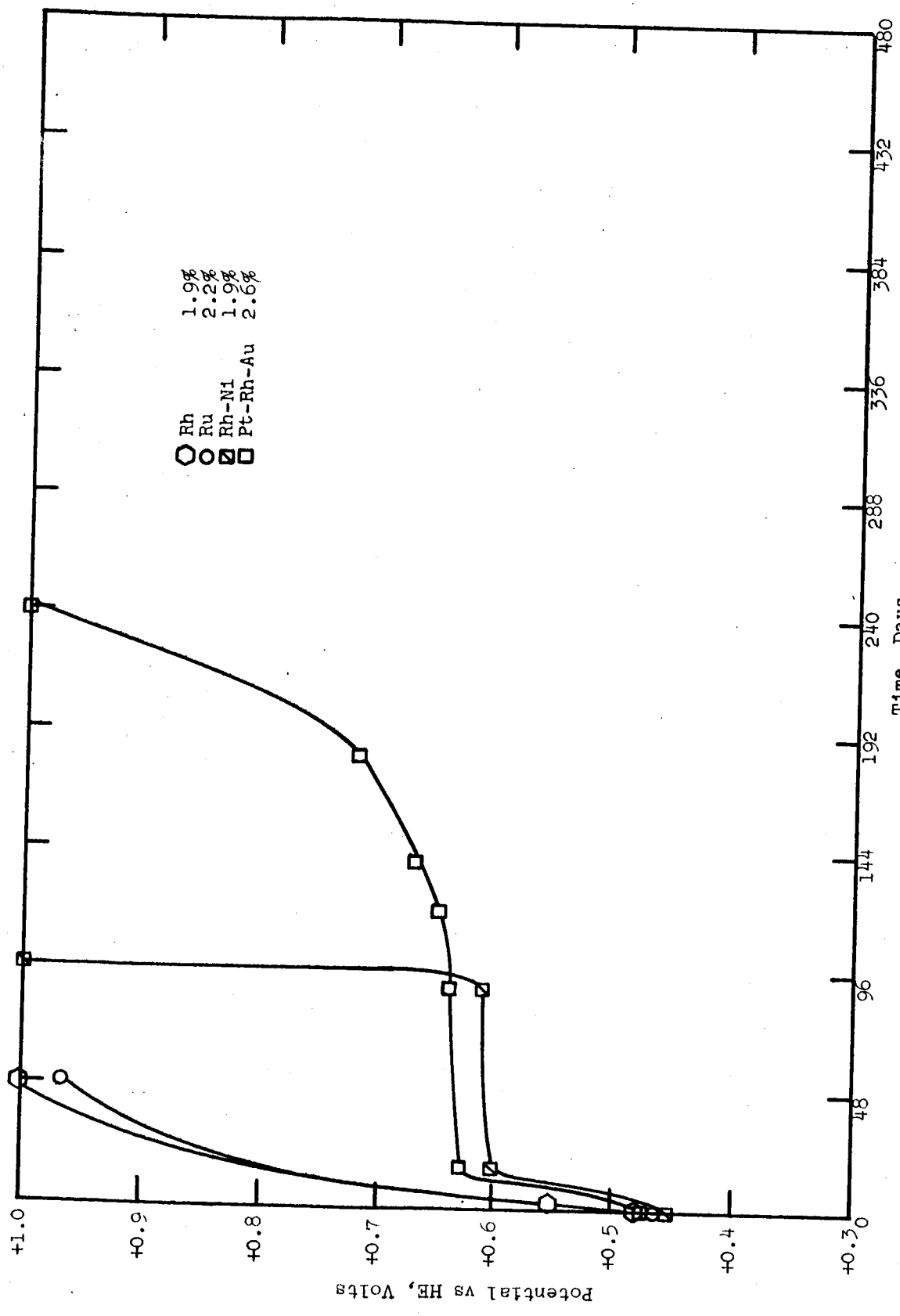

Figure 9. Chronopotentiometric Plot Anodic Oxidation of 1 M MMH in 5 M H_3PO_4 at 80°C using Precipitated Catalysts

I = 100 ma/cm2

maintained a potential of +0.60 volt versus HE for 90 hours and then rapidly deteriorated. The best catalyst was Pt (60%)-Ru (20%)-Au (20%) which maintained potentials between +0.60 to +0.70 versus HE for 180 hours. However, at a potential of +0.60 volt from HE there would not seem to be any practical use for MMH in a full cell.

c. Unsymmetrical Dimethylhydrazine

Figure 3 shows data for 1M UDMH in 5M H_3PO_4 and 5M H_2SO_4 at 80°C. The 5M H_2SO_4 electrolyte gave better long-term performance. However, the polarization was too severe for a useful anode.

d. Nitric Acid

Figure 10 shows long-term data for 5M HNO_3 oxidant solution using a Au/SS electrode at 30°C. There was almost no change in potential after 40 days' operation. The potential of +0.99 volt versus HE is very good, since, coupled with a fuel electrode at +0.15 versus HE, the full-cell voltage without IR drop would be +0.80 volt.

C. ANALYTICAL STUDIES - REACTION PRODUCTS

The experimental procedure and apparatus used for the analytical runs are outlined in Appendix A-3, Figures A-8 and A-9. Analytical data are summarized in Table 19.

1. Hydrazine

In general, the only electrochemical reaction expected of N_2H_4 is:

(1) $N_2H_4\ (aq) \longrightarrow N_2 + 4H^+ + 4e^-$ in base, and

(2) $N_2H_5^+ \longrightarrow N_2 + 5H^+ + 4e^-$ in acid.

For both these reactions, the volume of gas produced per ampere-hour is equal to

$$V_{liters} = \frac{NRT}{P}$$

where N = mole N_2H_4 used = $\frac{I\Delta t}{nF}$. Thus, $I\Delta t$ = 3600 coulombs per

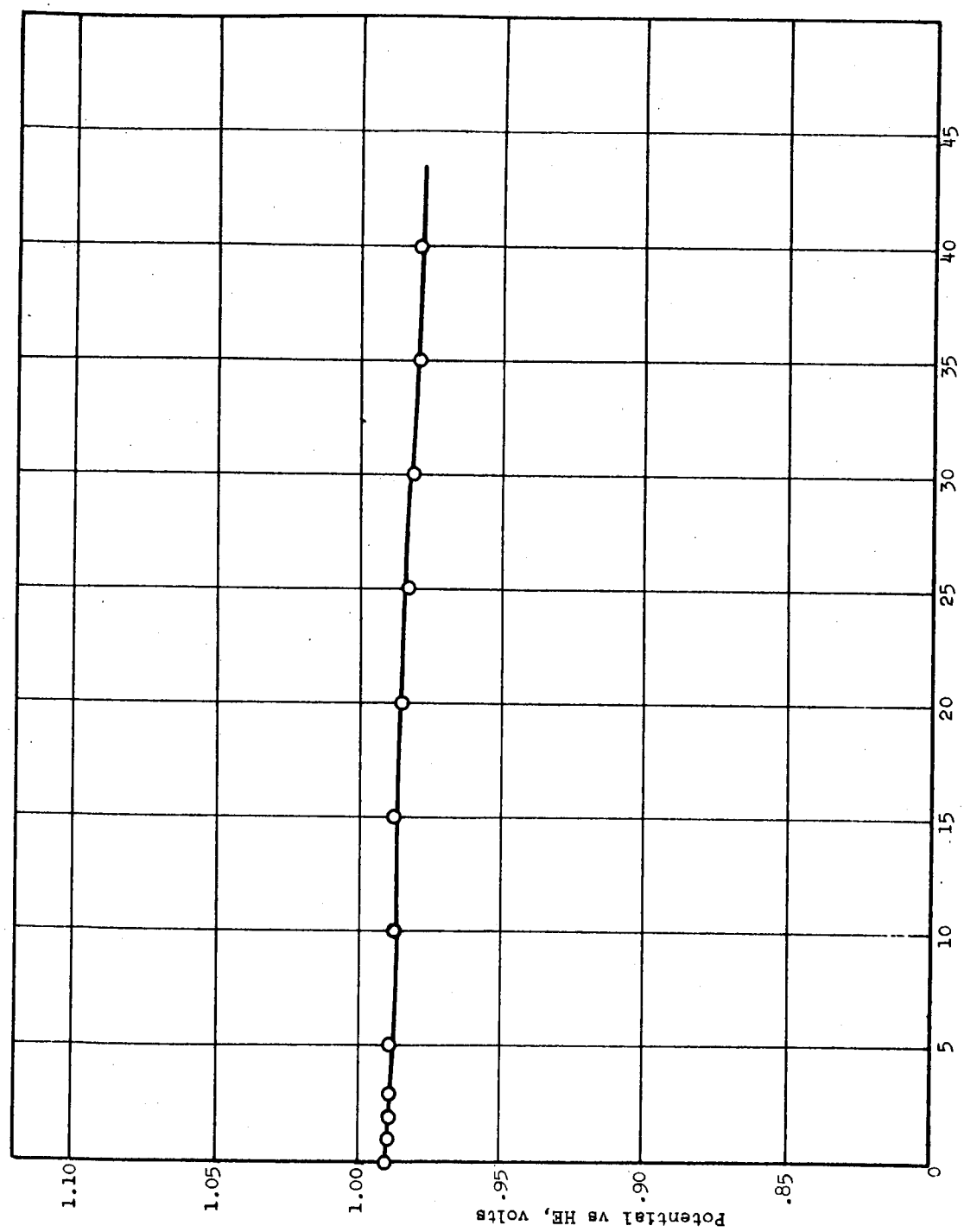

Figure 10. Chronopotentiometric Plot Electro-oxidation of 5 M HNO_3 with Au/SS Electrode

Current Density, 100 ma/cm²

Temperature, 30°C

Table 19

EXPERIMENTAL DATA OBTAINED IN MECHANISM STUDIES

Half Cell Operating Conditions					Gas Volume Measurements ml/amp-hr				Fuel or Oxidant Concentrations at End, moles/liter					Notes
Fuel or Oxidant	Electrolyte	Catalyst	Temp. °C	Current Density ma/cm²	Expt'l.	Theory	Reaction*	VPC Analysis	Expt'l.	Theory for Δe^-		Theory for Δe^-		
1M N_2H_4	1M KOH	Au/Ni	30	100	223	227	(1)	100% N_2						
1M N_2H_4	5M H_3PO_4	Pt/SS	60	100	222	227	(2)	100% N_2	0.23	0.25	4	0	3	
1M MMH	5M H_3PO_4	Au/SS	60	100	222	227	(3)	100% N_2	0.52	0.44	4	0.69M/L	6	Found 0.6M CH_3OH in solution, theory product 0.75M
1M UDMH	5M H_3PO_4	Au/C	60	50				100% N_2	0.62	0.64	4	0.48M/L	3	Would not perform long enough time for accurate gas measurement
1M UDMH	5M H_2SO_4	Au/C	90	50	None at first, slowly increased			100% N_2	0.35	0.46	3	0.51M/L	4	Yellow color formed, no gas evolution initially
5M HNO_3	-	Au/C	30	100	258	304	(16)	99% NO	2.48	3.00	4	2.30M/L	3	Faint bluish color in solution
4M HNO_3	-	Au/C	30	50	-	-		96% NO 4% N_2	2.37	2.68	4	1.95M/L	3	Faint bluish color in solution
5M HNO_3	-	Au/C	60	100	-	-		-	-	-		-	-	Brown gas N_2O_4 at first, changing to NO
1M HNO_3	5M H_2SO_4	Au/C	30	100	275	304	(16)	99% NO	-	-		-	-	

*Reaction listed in text

amp-hr, n = 4 eq/mole, and F = 96,500 coul/eq. At atmospheric pressure and 25°C (298°K), the volume expected is 227 ml/amp-hr. The only possibility of lowering the coulombic efficiency would be the electrode decomposition reaction of N_2H_4 or $N_2H_5^+$; the products of this decomposition would add to the calculated volume. The quantity and nature of the gas products from the oxidation of 1M N_2H_4 in 5M H_3PO_4 strongly indicated complete formation of N_2. The data in Table 19 substantiate this indication. The concentration found by titration with KIO_3 at the end of the test agrees within experimental accuracy with that expected from the number of coulombs passed. If a three-electron change had occurred, the cell would have used up all the N_2H_4 solution.

The gas volume and VPC* data for 1M N_2H_4 in 1M KOH also shows complete oxidation to N_2.

2. Monomethylhydrazine

The following electrode reactions are possible with MMH in acid electrolyte. At the right is listed the gas volume (ml) expected at 25°C per amp-hr.

		Gas Evolution ml/amp-hr. at 25°C and 1 atm
(3)	$H_2O + CH_3NHNH_2 \longrightarrow CH_3OH + N_2 + 4H^+ + 4e^-$	227
(4)	$H_2O + CH_3NHNH_2 \longrightarrow CH_2O + N_2 + 6H^+ + 6e^-$	151.5
(5)	$2H_2O + CH_3NHNH_2 \longrightarrow HCOOH + N_2 + 8H^+ + 8e^-$	113.5
(6)	$2H_2O + CH_3NHNH_2 \longrightarrow CO_2 + N_2 + 10H^+ + 10e^-$	182

The data from Table 19 indicate that reactions 3, 4, and 5 might be occurring, but 3 is predominant. Gas volumes measured are very close to those expected from reaction 3. However, solution analysis for MMH and the concentration of CH_3OH found by VPC indicate slightly better than a four-electron change. No CO_2 was found, thus eliminating reaction 6.

*Vapor Phase Chromatography (VPC)

3. Unsymmetrical Dimethylhydrazine

The most probable reactions of UDMH electrochemically are listed below:

		Gas Evolution in ml/amp-hr at 25°C
(7)	$2H_2O + (CH_3)_2NNH_2 \longrightarrow 2CH_3OH + N_2 + 4H^+ + 4e^-$	227
(8)	$2H_2O + (CH_3)_2NNH_2 \longrightarrow 2CH_2O + N_2 + 8H^+ + 8e^-$	113.5
(9)	$4H_2O + (CH_3)_2NNH_2 \longrightarrow 2HCOOH + N_2 + 12H^+ + 12e^-$	76
(10)	$4H_2O + (CH_3)_2NNH_2 \longrightarrow 2CO_2 + N_2 + 16H^+ + 16e^-$	171
(11)	$H_2O + (CH_3)_2NNH_2 \longrightarrow (CH_3)_2N\text{-}N{=}O + 4H^+ + 4e^-$	0
(12)	$(CH_3)_2NNH_2 \longrightarrow 1/2\ (CH_3)_2NN{=}NN(CH_3)_2 + 2H^+ + 2e^-$	0
(13)	$(CH_3)_2NNH_2 + H_2O \longrightarrow (CH_3)_2NHOH^+ + 2H^+ + \frac{1}{2} N_2 + 3e^-$	151

a. 5M H_3PO_4 Electrolyte

Analysis of product gas showed only N_2. Analysis for UDMH after test showed the concentration expected for a four-electron change.* The fuel would not run for a long enough time for accurate measurements of gas volumes, nor for enough CH_3OH, if produced, to be found by vapor phase chromatographic examination. Reaction 7 is most probable. The system showed insufficient promise to warrant testing further.

b. 5M H_2SO_4

UDMH supported better potentials in sulfuric acid than in phosphoric acid electrolyte. However, a number of different reactions seemed to occur as the potential changed with time. At the best potentials (when first started) no gas was evolved, but a yellow color was produced in the cell at the electrode. Then gas evolution slowly increased as the potential deteriorated.

---

*Table 19

Reactions 11 or 12 could account for the lack of a product gas. The product of reaction 11, yellow dimethylnitrosamine, can be formed by the reactions of a secondary amine with HNO_3 (ref. 17). The product of reaction 12 is a tetrazene. The titration of UDMH with KIO_3 results in a quantitative two-electron reaction (ref. 18). Also, the oxidation of unsymmetrical diphenylhydrazine with HgO results in the corresponding tetrazene (ref. 19). It is not known if the dimethyltetrazene product has a yellow color.

Analysis of the solution after the termination of the test indicated less than a three-electron change. Thus, the most likely pair of reactions would be 7 and 12. Reaction 7 would account for N_2 gas evolved as potential deteriorated.

4. Nitric Acid

The following are the most probable electrochemical reactions of HNO_3:

		Theoretical Gas Evolution ml/amp-hr
(14)	$H^+ + 1e^- + HNO_3 \longrightarrow NO_2 + H_2O$	Gas soluble
(15)	$2e^- + 2H^+ + HNO_3 \rightarrow HNO_2 + H_2O$	0
(16)	$3e^- + 3H^+ + HNO_3 \rightarrow NO + 2H_2O$	304
(17)	$4e^- + 4H^+ + HNO_3 \rightarrow 1/2\ N_2O + 5/2\ H_2O$	113.5
(18)	$5e^- + 5H^+ + HNO_3 \rightarrow 1/2\ N_2 + 3H_2O$	91

Unless reaction 18 predominates, gas volume measurements are not very accurate because of at least partial solubility of NO_2, NO, and N_2O. NO can be found along with N_2O and N_2 by VPC studies, if it is present in product gas. If a combination of reactions are occurring, NO_3^- analysis of the solution offers the most accurate information.

For HNO_3 as both oxidant and electrolyte, and with H_2SO_4 electrolytes, the predominant product seems to be NO. In 5M HNO_3, NO_3^- concentrations indicate about a 3.2-electron change. About 4% N_2 is found in product gas with 4M HNO_3, while NO_3^- tests show about 3.5-electron change. At high temperatures NO_2 is initially produced, but when saturated, the reaction shifts to NO (Table 19).

D. FULL-CELL STUDIES

1. Soluble N_2H_4-HNO_3 Cell

The work on complete cells was started by building a hydrazine/nitric acid cell and a hydrazine/dinitrogen tetroxide cell.

Figure 11 shows the hydrazine/nitric acid cell. The anolyte was an aqueous solution of 1M N_2H_4 and 5M H_3PO_4. The catholyte was 4M HNO_3. An anion ion-exchange membrane prevented gross mixing of the reactants.

A Au on stainless steel mesh cathode and a Pt on stainless steel mesh anode, both 1 cm^2 in geometrical area, were fabricated. The cell was made of Lucite and contained about 15 ml in each compartment. This simple arrangement showed feasibility from the standpoint of open-cell voltage and electrode polarization characteristics.

The open-circuit voltages for three different runs were 0.88 volt, 0.90 volt and 0.91 volt, in good agreement with the half cell results.

The total polarization, determined with a Kordesch-Marko (KM) bridge at 100 ma/cm^2, was 0.4 volt from open circuit, also in good agreement with the half cell data.

Next, a HNO_3-N_2H_4 system was tried using a porous carbon cathode against a cation exchange membrane. Against the other side of the cation exchange membrane was a Pt-on-SS mesh anode.

In Table 20 the data for the cell are shown. The individual electrode potentials were also measured (IR free) along with the full cell voltage with and without IR drop. The cell ran for two hours at currents from 20 ma to 90 ma. However, the cell potential fell off because of failure of the HNO_3 compartment, presumably because of filling of the carbon electrode with product gas. Full-cell potentials at 40 to 80 ma were very low because of poor cathode performance.

---

*Where IR-free measurements were desired, the cell was driven and potential measurements were made by a Kordesch-Marko bridge; otherwise cells were discharged through a variable resistance at constant current.

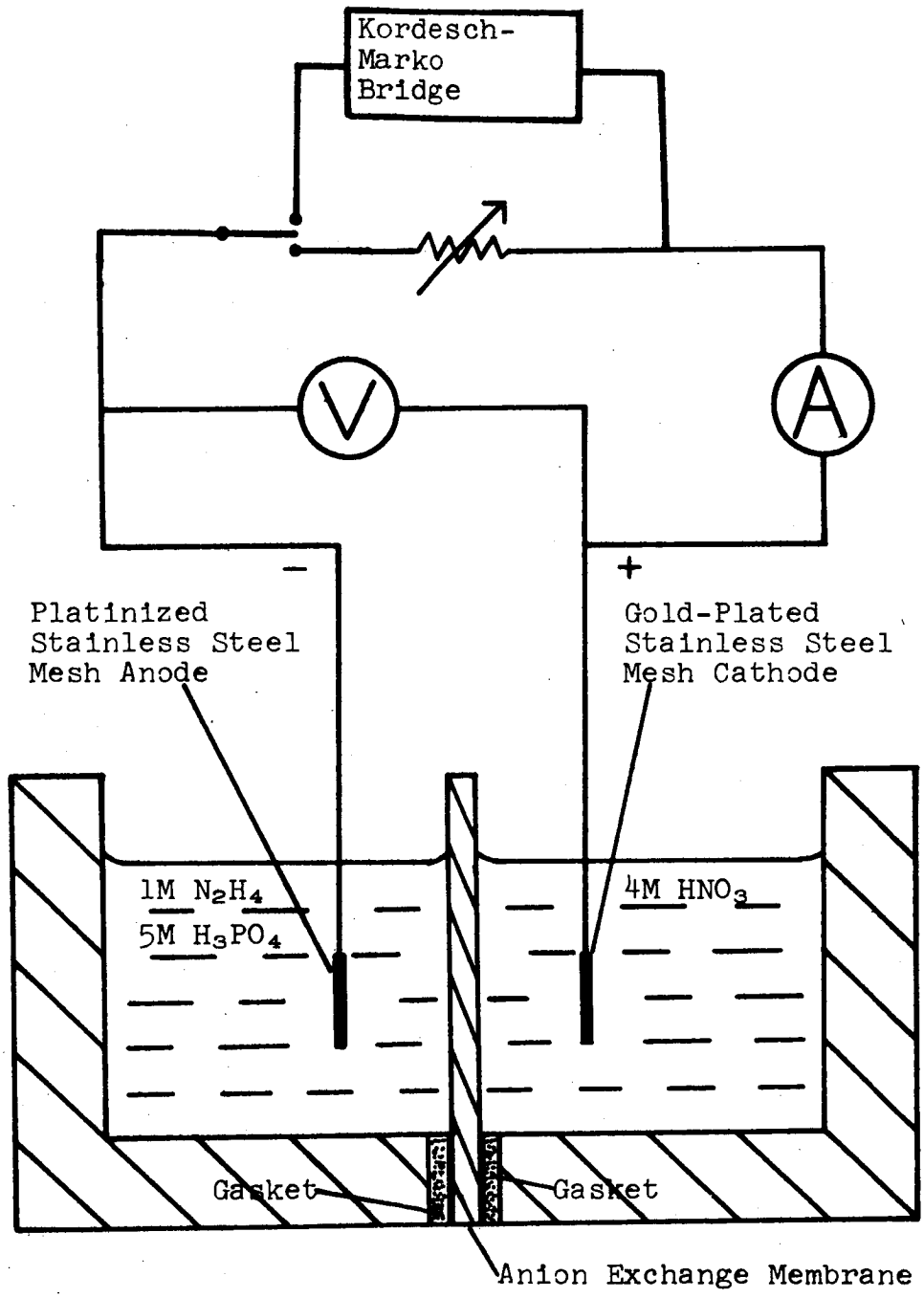

Figure 11. N_2H_4 - HNO_3 Fuel Cell, Soluble Reactants

Table 20

HNO_3 - N_2H_4 FULL CELL

Oxidant - 5M HNO_3; electrode, porous carbon FC-13, 2.5 cm^2 area
Fuel - 1M N_2H_4 in 5M H_3PO_4. Electrode, Pt/SS 100 mesh, 1.8 cm^2 area
Separator - Ionic's Cation exchange membrane - 61AZL-183
Temperature - 40°C.

Time, min.	Total Current, ma	Full cell voltage, volts With IR	Full cell voltage, volts Without IR*	Anode* vs HE, volts	Cathode* vs HE, volts
0	0.C.	+0.84	+0.84	+0.20	+1.04
12	20	+0.57	+0.64	+0.35	+0.97
34	40	+0.31	+0.45	+0.44	+0.89
50	80	0	+0.21	+0.46	+0.67
70	92	-0.29	+0.02	+0.48	+0.50
126	60	-0.08	+0.16	+0.50	+0.66

Discontinued because of poor cathode potential.

---

*IR Free, and anode and cathode potentials measured with Kordesch-Marko Bridge.

Cells were also run using a porous carbon flow-through electrode with 5M HNO_3. With this system, the HNO_3 electrode maintained a potential of +1.00 volt vs HE even at high current densities. The IR drop was higher because there was another compartment between the carbon electrode and the ion exchange membrane.

2. Soluble N_2H_4 - Vapor N_2O_4 Full Cell

Figure 12 shows the hydrazine-N_2O_4 cell. The cathode was a porous carbon disk (Pure Carbon FC-13) with a tantalum lead. The anode was a disk of 100-mesh stainless steel plated with platinum. Geometrical areas were 2.54 and 1.8 cm^2, respectively. The fuel was a 1M solution of N_2H_4 in 5M H_3PO_4. Separating the fuel and 5M H_3PO_4 electrolyte compartments was a cation exchange membrane (Ionics, Inc.). Viton rubber O-rings were used to seal the cell compartments.

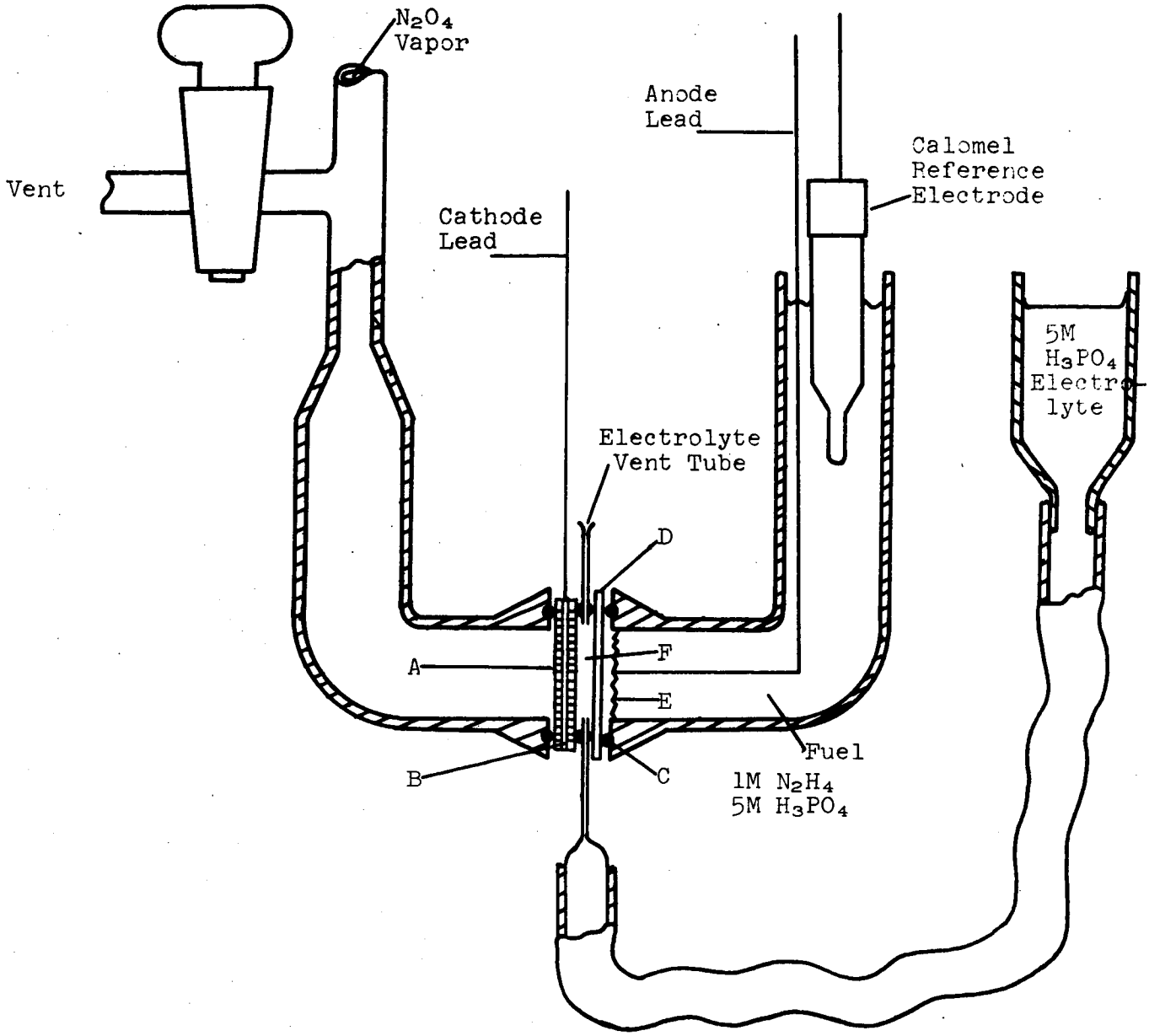

A Porous Carbon Cathode

B Tantalum Lead Ribbon

C Viton Rubber O-Ring

D Cation Exchange Membrane

E Platinized SS Mesh Anode

F Electrolyte Chamber

Figure 12. N_2H_4 - N_2O_4 Full Cell

Open-circuit voltages were 0.75 volt with this cell. At current densities of 30 ma/cm² (based on anode area), IR drop was about 0.25 volt when a small flow of electrolyte was maintained. With the electrolyte flow maintained, the cell was operated as described above for a period of 50 minutes without substantial change.

Results for a similar cell are shown in Table 21. Individual half-cell potentials were not measured. The open-circuit voltage is approximately that predicted from half-cell tests with acidic electrolytes. Values of full cell potential were measured with and without a Kordesch-Marko bridge, which eliminates IR drop. The difference between the two indicates the IR drop. The cell was run for 1/2 hour at 50 ma total current until potential collapsed. The full cell potential from the bridge dropped from +0.67 to +0.61 volt in that period, while the full cell potential including IR drop increased from +0.25 to +0.32 volt, indicating a decrease in cell resistance.

Table 21

N_2O_4 - N_2H_4 FULL CELL

Oxidant - N_2O_4 gas electrode, FC-13 porous carbon electrode, 2.5 cm²
Fuel - 1M N_2H_4 electrode, 1.5 cm² Pt/SS 100 mesh
Electrolyte - 5M H_3PO_4 for both fuel and oxidant
Separator - Ionic's Cation Exchange membrane
Temperature - 30°C

Time, min	Total Current, ma	Cell voltage, volts	
		With IR	IR Free
0	O.C.	+0.83	+0.83
2	2	+0.80	+0.80
4	10	+0.69	+0.76
6	20	+0.57	+0.72
8	50	+0.25	+0.67
20	50	+0.26	+0.59
50	50	+0.32	+0.61

Voltage deteriorated after 50 min.

A number of variations using N_2O_4 gas electrode without a large liquid compartment were tried. In once instance, the porous carbon was placed against the ion exchange membrane. Open-circuit voltages were about the same as with the cell described above, but the electrode polarized with very small currents, because of lack of a gas-electrolyte interface. In another variation, asbestos was put between the porous carbon electrode and the ion exchange membrane and was continually soaked with electrolyte. This performed better initially; however, gas products eventually built up and the cell polarized badly.

A N_2O_4-N_2H_4 cell was set up using 1M KOH electrolyte. Open-circuit voltage was +1.8 volts, which was expected from half-cell runs. The data are shown in Table 22. Because of gross leakages, pressure was not maintained on the cathode as in the half-cell runs, and the electrode did not perform in the same manner.

Table 22

N_2O_4 - N_2H_4 FULL CELL

Oxidant - N_2O_4 gas, porous carbon FC-14 electrode, 2.5 cm^2
Fuel - 1M N_2H_4, Pt/Ni porous electrode 2.5 cm^2 area
Electrolyte- 1M KOH for both fuel and oxidant with separator
Separator - Ionics, Inc. Cation exchange membrane
Temperature- 25°C

Time, min	Total Current, ma	Voltage, volts			
		Full Cell With IR	IR Free*	Anode* vs HE	Cathode* vs HE
0	O.C.	+1.86	+1.86	+0.02	+1.88
3	10	+1.78	+1.85	+0.03	+1.86
8	20	+1.65	+1.80	+0.03	+1.82
19	50	+1.36	+1.70	+0.04	+1.73
25	50	+1.11	+1.56	+0.04	+1.53
43	20	+1.43	+1.57	+0.04	+1.60
60	30	+0.68	+0.90	+0.06	+0.96

*Values measured with Kordesch-Marko Bridge.

This initial attempt at full cells drew attention to the main construction requirements that must simultaneously be satisfied:

(1) Provide and maintain three-phase contact with the catalyst surface.

(2) Provide a means of escape for the reaction products from the catalyst surface.

(3) Maintain sufficient but not excessive feed of reactants to the catalyzed electrode.

3. Porous Teflon Vapor Electrode Full Cells with Electrolyte

At this point a new concept in electrode construction offered, in theory, a solution to the problem areas outlined above. This electrode is termed the "porous Teflon vapor diffusion electrode." This electrode, schematically depicted in Figure 13 as it appeared in the initial full-cell trials, consisted of porous Teflon, one side impregnated with catalyst, pressed against a perforated stainless steel plate acting as current collector, physical support, and means of preventing the catalyst from being abraded. In theory the Teflon serves as a barrier to nonwetting liquids such as hydrazine hydrate and nitric acid. However, the reactants can diffuse through the pores to the electrode as vapor. Thus, gaseous products can diffuse away from the electrode without hindrance from bulk liquid.

These electrodes were made by spreading catalyst on a disk of porous Teflon and overlaying this with a perforated stainless steel sheet that had the same catalyst black plating. This sandwich was pressed at 1400 psi at room temperature. The 304 stainless steel sheet was 0.004 in. thick with 0.014 in. holes comprising 65% open area; it was manufactured by Perforated Products, Inc. The catalyst for the anode was 35 mg/cm^2 of rhodium or platinum black and for the anode was 35 mg/cm^2 of platinum black or powdered gold (0.1-10 microns). Initially, the porous Teflon was 9-micron pore, 1/16 in. thick, manufactured by Pall Corporation. Electrodes of this type were then used without any separator for both fuel and oxidant, with an electrolyte in between, consisting of either 5M H_2SO_4, 1M H_3PO_4, 1M KOH, or 1M Na_2SO_4, thus providing three different pH's. $N_2H_4 \cdot H_2O$ (85%) was used to feed fuel in the vapor state to the electrode, while 95% HNO_3 was used in the same manner for oxidant. N_2O_4 was fed as a gas to the back side of the oxidant Teflon electrode. H_2O_2 (30% aqueous solution) was also tested as feed for either H_2O_2 or O_2 gas.

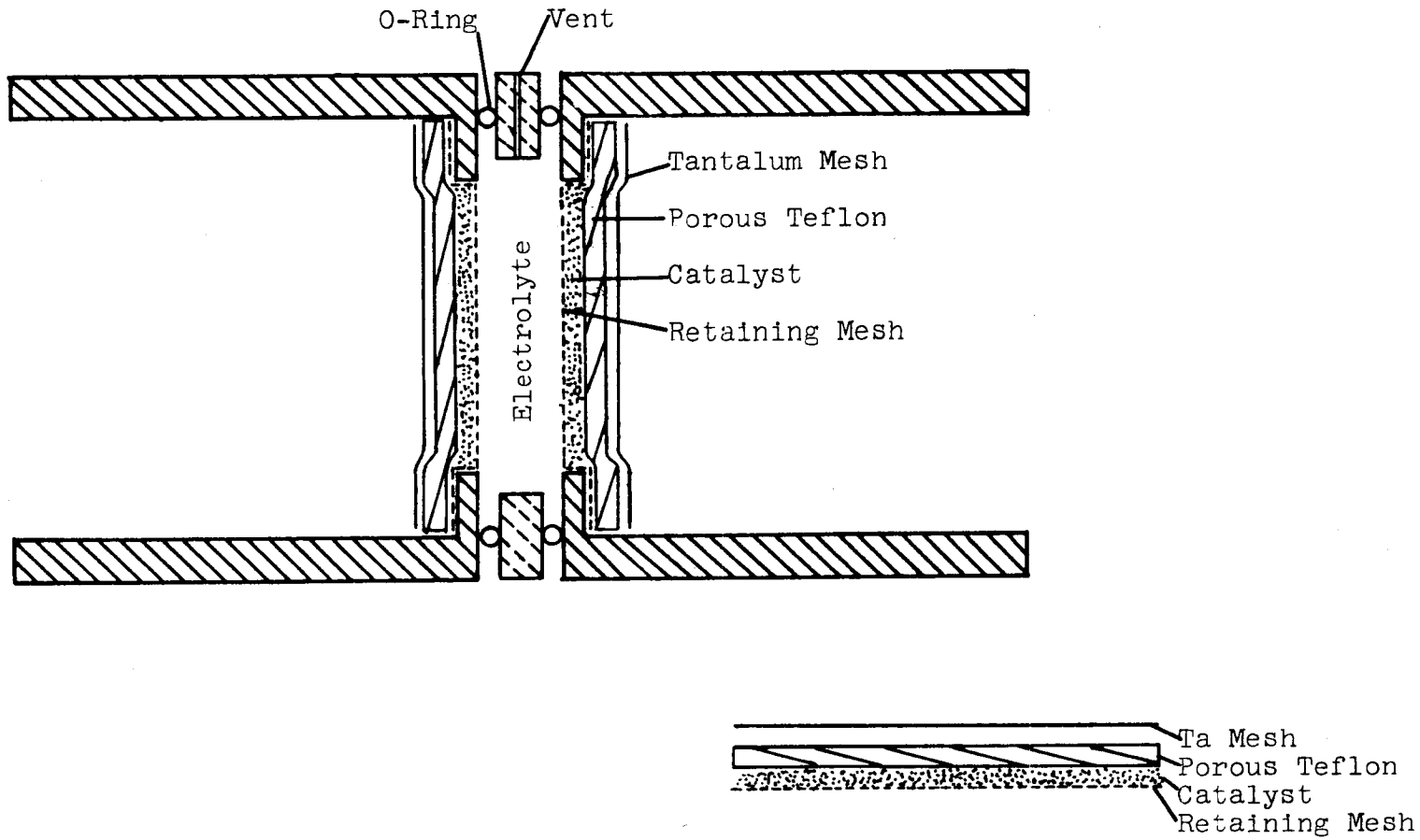

Figure 13. Porous Teflon Vapor Diffusion Electrode Fuel Cell

Many different cells comparing these variables were set up, with a Luggin capillary set into electrolyte solution so that half-cell and full-cell potentials could be measured. A Kordesch-Marko bridge gave IR-free measurements of these potentials.

The results obtained indicated that the mechanical parameters of the system were more important than the specific catalysts used for each half cell. That is, Pt, Rh, Ru blacks made little or no difference in the half cell characteristics.

Difficulty in controlling the vapor transport of both fuel and oxidant at a given temperature led to contamination of the electrolyte and eventually deteriorated one of the electrodes severely.

Table 23 gives open-circuit voltages and the best performance obtained with specific full-cell systems. The mechanical imperfections in the design of the electrodes led to a new procedure for making them, which is described in Appendix A-2.

4. Porous Teflon Vapor Electrode-N_2H_4-Soluble HNO_3 Full Cells with Cation Exchange Membrane

Previous experiments demonstrated that the porous Teflon electrode worked for both the anode and cathode. However, the problem of electrolyte deterioration remained. The diffusion of the reactants into the electrolyte also deteriorated electrode performance. Therefore, to investigate the performance of this type of electrode in the absence of the effects of diffusion, a cation exchange membrane in direct contact with the anode was used to separate the compartments. Thus, the only material transported to the Rh/SS mesh electrode pressed between the opposite sides of the Teflon and a cation exchange membrane consisted of N_2H_4 and H_2O vapor (Figure 14).

On the opposite side of the ion exchange membrane was the oxidant solution, consisting of either 5M HNO_3 or 1M HNO_3 and 5M H_2SO_4. A Luggin capillary with the oxidant solution as a bridge to a calomel reference electrode was situated next to the membrane.

A Kordesch-Marko bridge was used to measure IR-free potentials. The anode half cell, cathode half cell, and full-cell potentials without IR drop could also be measured. Furthermore, the approximate resistance of the membrane was found by measuring the anode potential including IR drop and subtracting the

Table 23

FULL CELL DATA FROM TEFLON POROUS VAPOR DIFFUSION ELECTRODES

Anode	Cathode	Current Density (ma/cm²)	Electrolyte	Anode Feed	Cathode Feed	Potential vs HE* at same PH and Temp: Anode	Cathode	Full Cell	Temp °C
Rh	Au	0	5M H_2SO_4	85% $N_2H_4.H_2O$	70% HNO_3	+0.27	+1.10	0.83	50
"	"	20	"	"	"	+0.45	+1.06	0.61	70
Pt	Au	0	"	"	"	+0.26	+1.17	0.91	70
"	"	20	"	"	"	+0.45	+1.05	0.60	
Pt	Au	0	1M H_3PO_4	"	"	+0.17	+1.00	0.83	
"	"	8	"	"	"	+0.21	+0.90	0.69	90
Pt/Ru/Au	Pt	0	5MKOH	"	30% H_2O_2	+0.22	+1.02	0.80	
"	"	4	"	"	"	+0.16	+0.90	0.74	
Pt/Ru/Au	Au	0	"	"	N_2O_4	+0.43	+1.47	1.03	46
"	"	8	"	"	"	+0.60	+1.59	+0.99	96

* IR Free

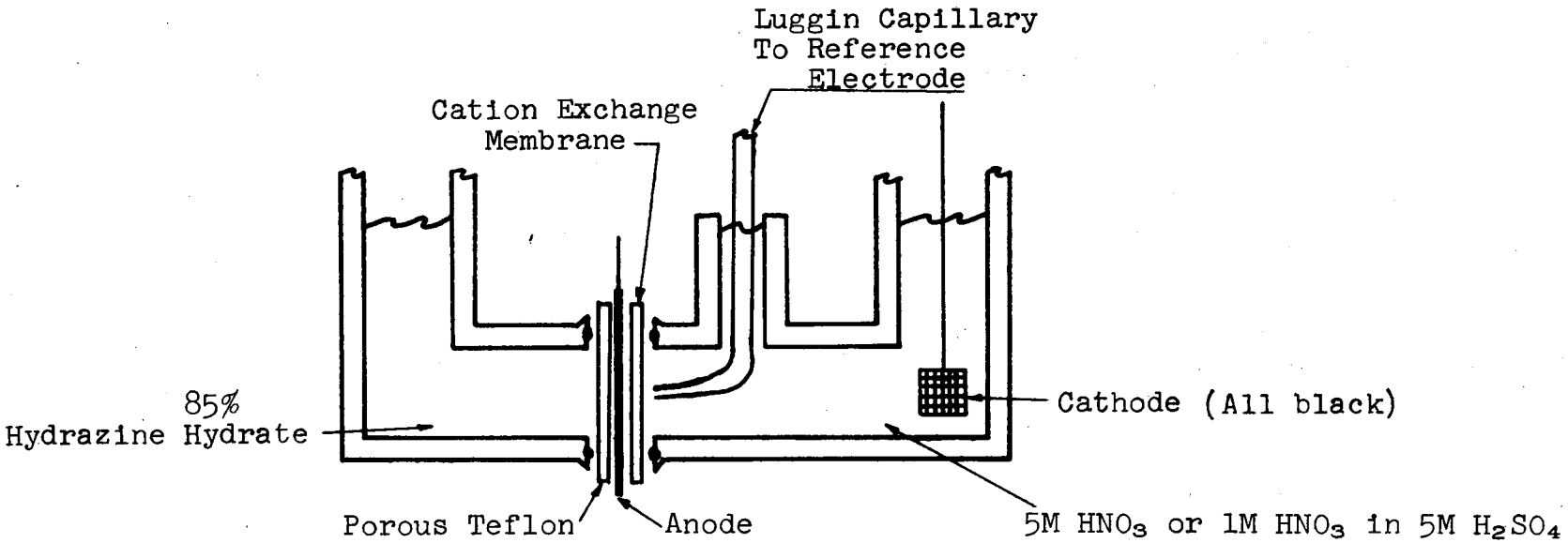

Figure 14. N_2H_4 Vapor Fuel Cell with Soluble HNO_3 as Oxidant

IR free anode potential. The $\Delta E/I$ was the approximate membrane resistance.

The cathode was set about 10 cm from the ion exchange membrane, and was a gold/stainless steel (Au/SS) mesh.

The advantages of these quasi-full cell arrangements were the following:

1. IR-free potentials for each electrode could be determined.

2. Values for membrane or separator resistance under full-cell conditions could be determined.

3. Problems of short circuiting of cell were eliminated so that basic investigations of full cell systems could be made.

4. Leakage problems were absent.

The full-cell open circuit potential at 60°C varied between 1.50 and 1.55 volts. The anode potential was -0.38 volt versus the standard hydrogen electrode (SHE) while the HNO_3 potential was +1.12 volts vs SHE. This high potential was probably due to the pH difference between the anode and cathode. Under these conditions the current was probably carried by $N_2H_5^+$. This results in loss of N_2H_4 by neutralization.

The performance of the cell was highly dependent on the temperature; an elevated temperature was needed to raise the vapor pressure of the hydrazine fuel. At 30°C the open-circuit potential was +1.42 volts and at 60°C the cell showed a polarization of less than 0.1 volt up to 50 ma/cm^2. For experimental reasons we could not increase the current further, although the IR-free voltages were still very good. At 30°C the full-cell potential dropped off at over 1 ma/cm^2, because of anode failure. This temperature dependence is an excellent indication that the N_2H_4 is being transferred as a vapor, and that it is also being used in that form, for the vapor pressure of N_2H_4 in H_2O increases exponentially with the temperature (see Figure 15).

Over a 48-hour period of discontinuous usage, which included two 4-hour periods of continuous drain at 20 ma/cm^2, the full-cell potential decreased by only 0.08 volt, all of which occurred at the anode (see Figure 16).

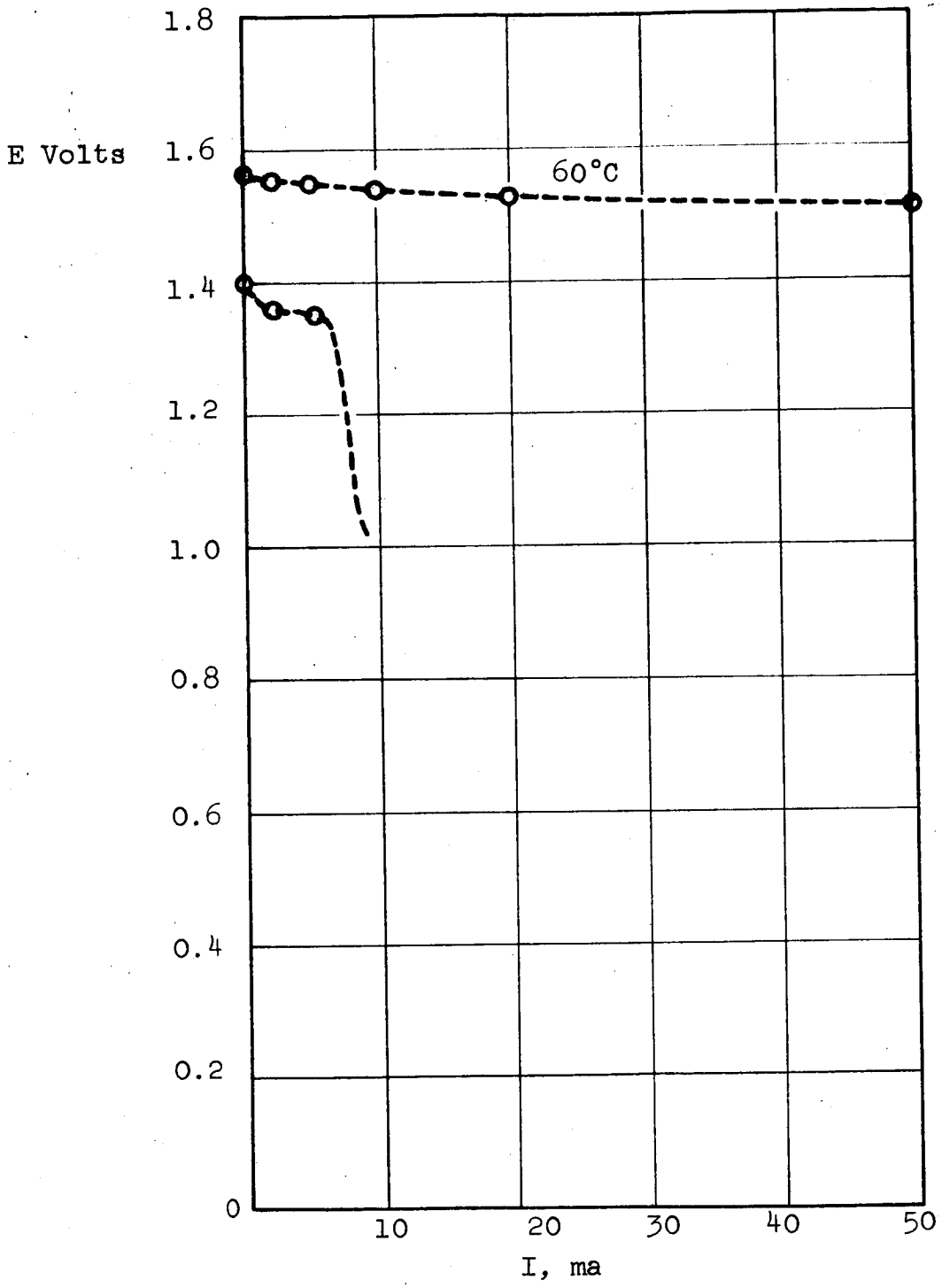

Figure 15. N_2H_4-HNO_3 Porous Teflon Cell. Variance with Temperature

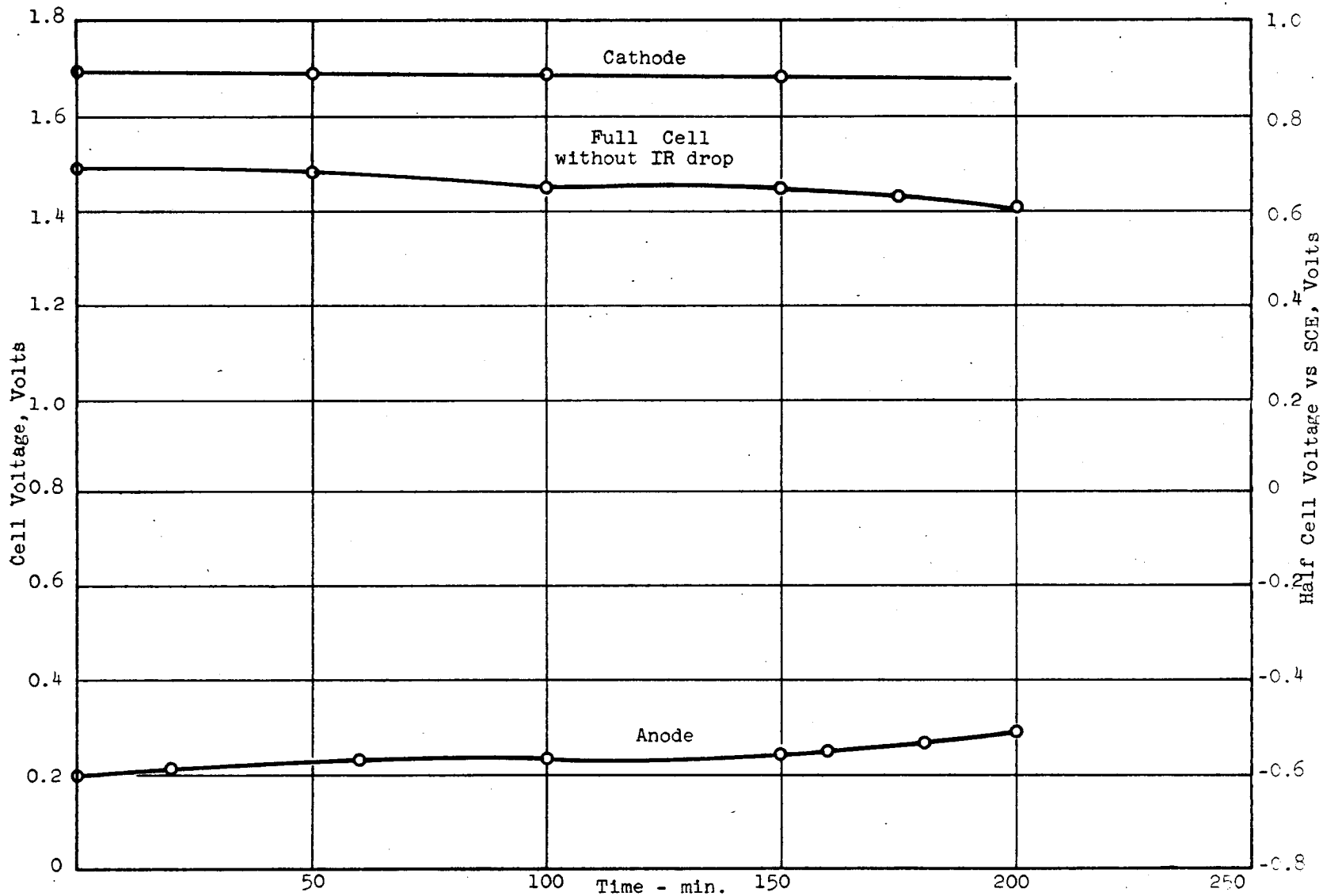

Figure 16. Chronopotentiometric Plot for Porous Teflon N_2H_4-HNO_3 Cell Current = 17.5 ma/cm^2
T = 80°C

5. Porous Teflon Vapor Electrode Full Cell with Ion Exchange Membrane

The next step was to eliminate liquid electrolyte in a full cell by placing the electrodes against the opposite sides of a cation exchange membrane. Figure 17 illustrates the type of construction used in full cells employing an ion exchange membrane as separator. The perforated steel sheet (retaining mesh) provided good continuous contact with the cation exchange membrane type 61-AZ1-183 (sulfonated polystyrene on a Dynel® backing) manufactured by Ionics, Inc. Further contact between the catalyst and ion exchange membrane was provided by a liquid film (H_2O + N_2H_4) which diffused to the anode and condensed, while H_2O was formed as a consequence of the electrochemical reaction at the cathode. This insured three phase contact.

The electrode backing was a Teflon-impregnated cloth 0.006 in. thick with 15-micron pores (type TV-20A-40, manufactured by Pallflex Products, Division of Pall Corporation). The active electrode area was 2.85 cm^2.

Three sequences of experiments were run to establish the advantages and limitations of the porous Teflon electrodes in combination with an ion exchange membrane. Refinements were sacrificed to cover ground and establish feasible areas for future investigations.

a. Porous Teflon with Cation Exchange Membrane (Sequence I, Table 24)

In sequence I, 9-micron, 1/16 in. thick porous Teflon was used in the construction of the electrodes. In the full cell the cation exchange membrane was used and the cell was operated at 90°C. This sequence established:

1. Porous Teflon electrodes can be used for the anode and cathode in a full cell operating on 85% hydrazine hydrate and concentrated nitric acid employing a cation exchange membrane as electrolyte and separator.

2. Using this electrode construction with the ion exchange membrane, negligible spontaneous decomposition of the hydrazine occurred compared with the direct immersion of the active electrode surface in liquid hydrazine hydrate.

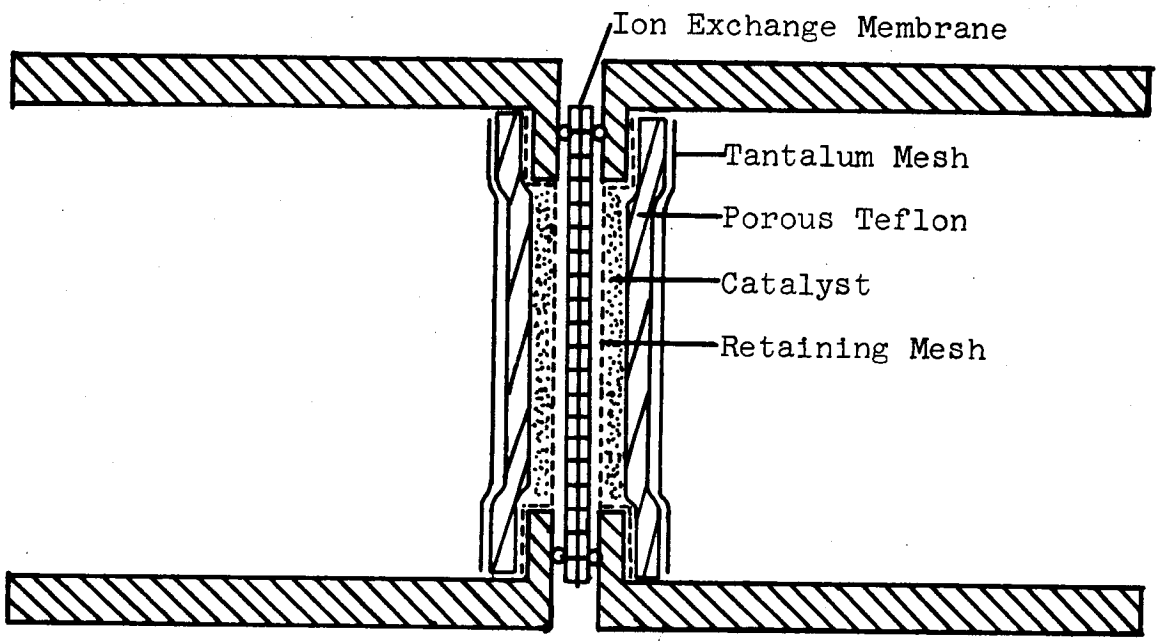

Figure 17. Fuel Cell Construction: Porous Teflon Diffusion Electrodes with Ion Exchange Membrane

Table 24

FULL CELL SEQUENCE I - ION EXCHANGE ELECTROLYTE FULL CELL FEASIBILITY TESTS

Membrane - Ionics cation exchange
Anode - Rh catalyst
Cathode - Au catalyst
Porous Teflon: 9μ porosity, 1/16 in. thick

Run	Fuel	Oxidant	Electrochemical Performance				Temp. °C	Notes
			OCV volts	Current density ma/cm²	K-M Voltage volts	Voltage + IR volts		
I	85% $N_2H_4.H_2O$	70% HNO_3	1.03				30	Full cell ran
			1.30				65	overnight at 30°C
			1.37	7	1.28	1.26	95	
				17.5	0.94	0.86	95	
				24.5	0.50	0.42	95	New electrodes and cation membrane
II	85% N_2H_4 H_2O	N_2O_4	1.35	would not carry any current			90	Took N_2O_4 test 7 hours for stabilization
	98% MMH	70% HNO_3	1.38	10.5	1.28	1.22	90	
III	85% $N_2H_4.H_2O$	70% HNO_3	0.92	could not carry any current			85	Asbestos separator saturated with 5M H_2SO_4. Asbestos became stiff with hydrazine sulfate ppt.

3. Monomethylhydrazine could be used directly at the same anode used for hydrazine with the cation exchange membrane.

4. Dinitrogen tetroxide did not replace nitric acid; this evidently shows the need for a water film at the interface.* However, this result does not exclude dinitrogen tetroxide if other modifications are allowed (e.g., H_2SO_4 electrolyte).

5. An asbestos mat saturated with 5N H_2SO_4, used as separator, was much inferior to the cation exchange membrane; the open-circuit voltage was 0.5 volt less, the cell would support virtually no current, and the mat permitted gross diffusion of the hydrazine.

b. Teflon-Impregnated Cloth (Sequence II, Table 25)

In sequence II, run at 30°C, Teflon-impregnated cloth was used in the electrode construction. This offered much less resistance to the diffusion of the reactant vapors than the porous Teflon employed in Sequence I. The same set of electrodes was used throughout the three runs over an eight-day period. The cation exchange membranes were replaced as needed. To obtain half-cell performance, asbestos saturated with 1N H_2SO_4 was sandwiched between two cation exchange membranes. A hypodermic needle attached to a syringe containing 1N H_2SO_4 was inserted into the asbestos and a reference electrode was set in the syringe, (Figure 18). Figure 19 shows the short-term performance of this cell. In general, the half cells added up to the full cell, while the absolute half-cell potentials shifted with time and the direction from which a given current was approached. This sequence established that:

1. Resistance to diffusion of the reactant vapors greatly influences electrode performance. This cell performed better at 30°C in terms of full-cell voltage and polarization than the Sequence I cell did at 90°C using the thicker and less porous Teflon.

2. With good separation in terms of interdiffusion of reactants, no spontaneous decomposition of reactants was evident. If the separator failed and allowed diffusion between anode and cathode, the voltage dropped and spontaneous gassing occurred.

3. The voltage rose rapidly after addition of reactants (Figure 20).

---

*See Table 24

Table 25

FULL CELL SEQUENCE II - ION EXCHANGE ELECTROLYTE FULL CELL. PALL TEFLON-IMPREGNATED GLASS ELECTRODES

Used Two Cation Exchange Membranes with 1M H_2SO_4 Saturated Asbestos Between the two Membranes.

Rh Catalyst - Anode
Au Catalyst - Cathode

Run	Fuel	Oxidant	Electrochemical Performance: O.C.V. volts	Current density ma/cm²	K-M voltage volts	Voltage + IR volts	Temp. °C	Notes
I	85% $N_2H_4.H_2O$	70% HNO_3	1.63	35	1.57	1.26	30	No visible gassing at electrodes
				53		cathode failed		ran over weekend at 35 ma/cm², failed at undetermined time due to cathode mechanical failure.
II	85% $N_2H_4.H_2O$	70% HNO_3					30	See Figure 19 and 20 for polarization curve, short term, and O.C.V. voltage rise after reactant addition.
				17.5	1.29	1.43	30	ran overnight.
III	85% $N_2H_4.H_2O$	70% HNO_3	1.66	17.5			30	Same cell as above, fresh reactants. Ran for 32 hours, see Figure 21

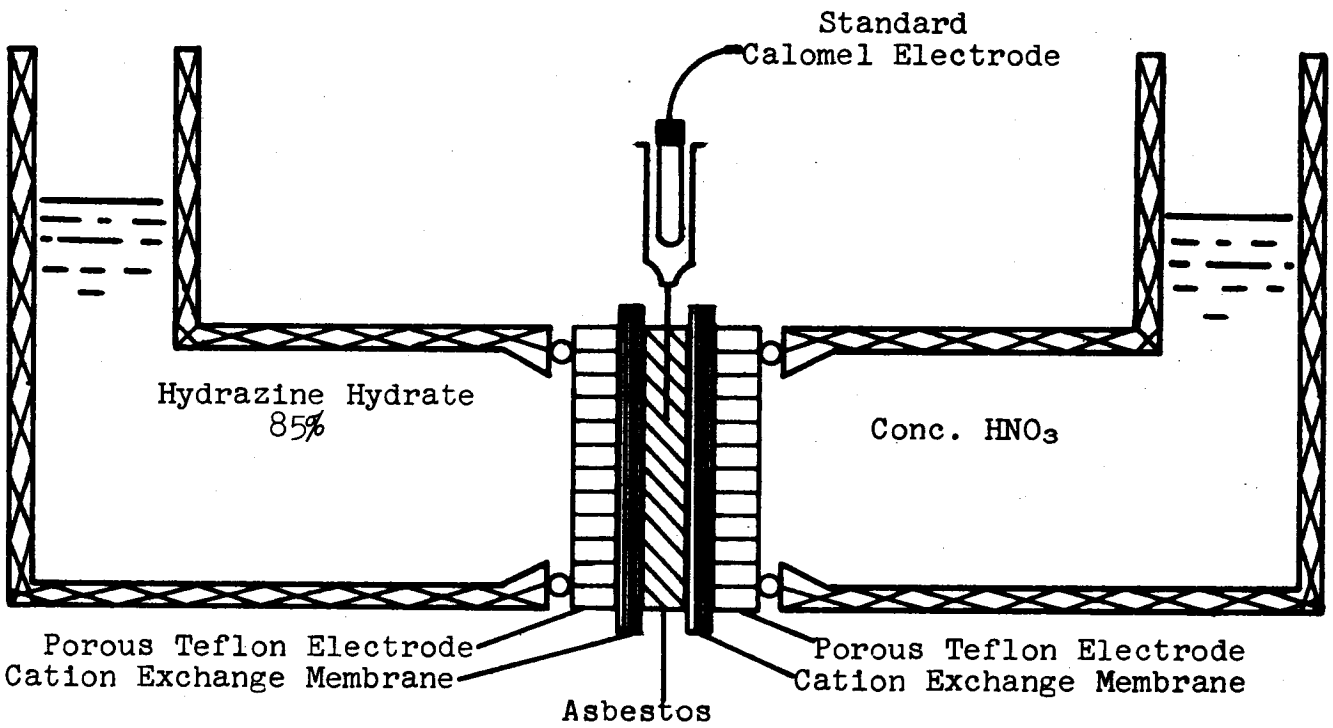

Figure 18. Full Cell Construction, Employing Porous Teflon Vapor Diffusion Electrodes and Ion Exchange Membrane, Used for Half-Cell Measurements

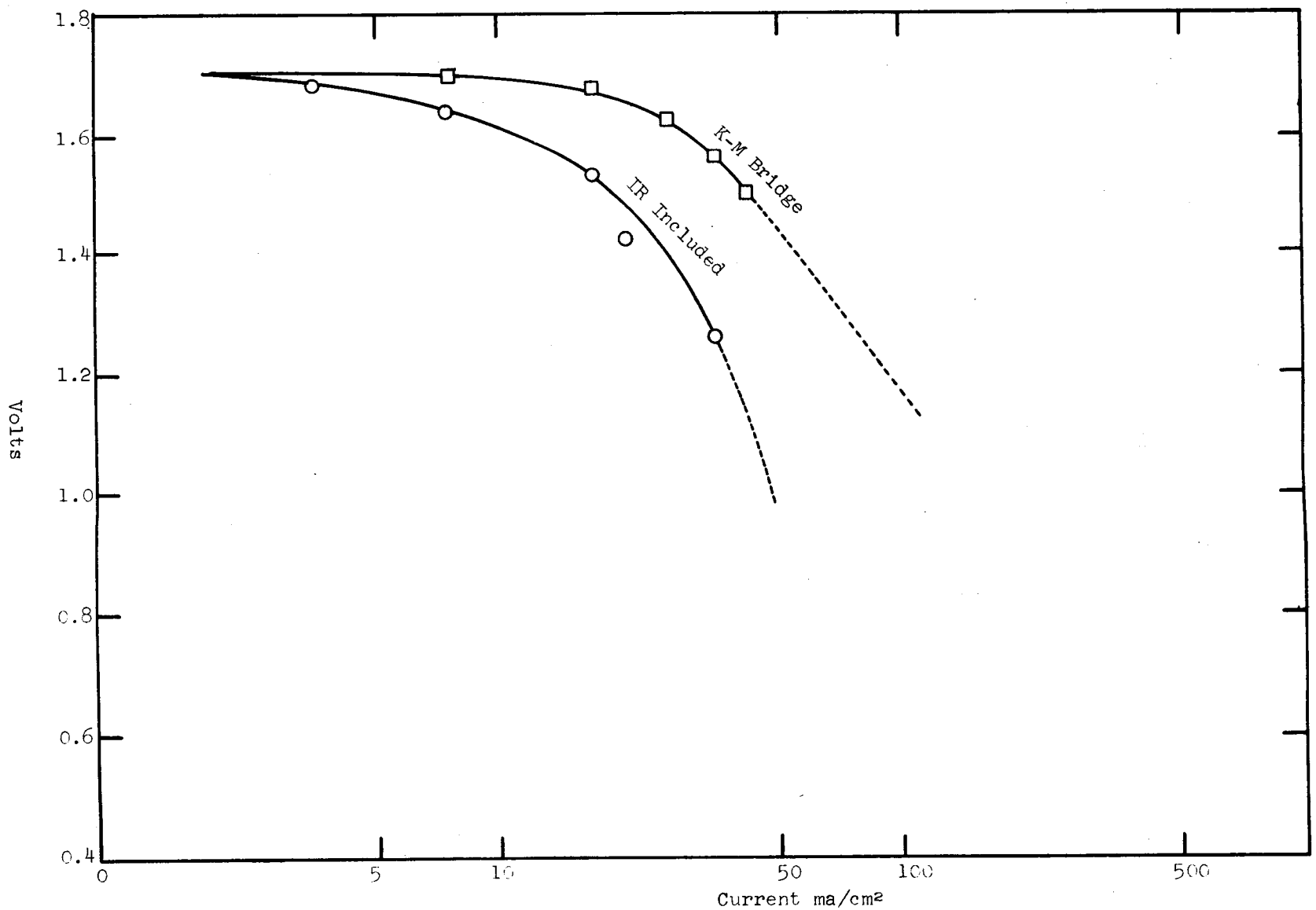

Figure 19. Short Term Performance of Full Cell Using Porous Teflon Electrodes and Cation Exchange Membrane with Asbestos Separators at 30°C

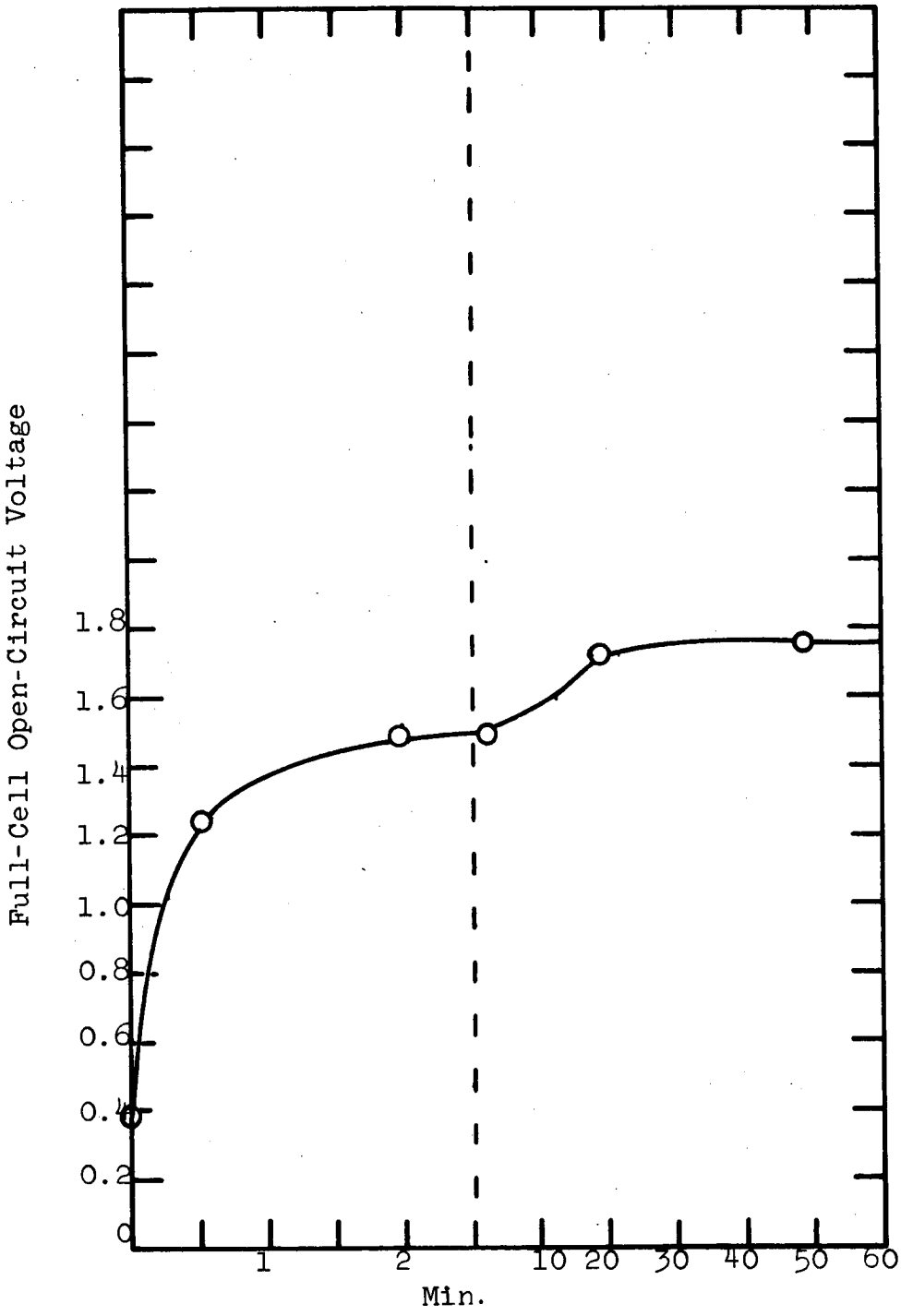

Figure 20. Voltage Rise After Addition of Reactants

4. The electrodes after 8 days' use retained their performance at 17.5 ma/cm^2.

5. All of the polarization at 17.5 ma/cm^2 took place in 6 hours (Figure 21). For the remainder of the 30-hour run the voltages stayed constant.

c. Teflon Electrode with Dual Ion Exchange Membrane (Sequence III, Table 26)

In Sequence III a set of electrodes identical to those of Sequence II was used: This series of runs established that an anion exchange membrane could be used in place of the cation exchange membrane or in combination with the cation membrane and still yield similar open-circuit voltages. However, polarization as a function of current was greater than with just the cation exchange membrane. Monomethylhydrazine was run with nitric acid and an anion exchange membrane at 30°C.

These experiments indicated that the porous Teflon electrode was stable and versatile. However, the open-circuit voltages of 1.7 volts were unexpected and at first were believed due to a pH difference across the separator. Analysis showed that if H^+ or OH^- was the current-carrying ion, the pH difference would not contribute to the full-cell potential. However, if more than one ion carried the current or if cations and anions other than H^+ or OH^- carried the current, then the pH difference contributed to the full-cell potential. With the cation exchange membrane, it was suspected that current was being carried by the $N_2H_5^+$ ion, thus accounting for the high voltage. To check the disappearance of reactants by diffusion and decomposition, a full cell was set up with the porous Teflon electrodes and one cation exchange membrane. This cell was filled with electrolyte and examined at no load. To prevent leakage, the junction of the electrodes and cation membrane was sealed with paraffin. Samples of the reactants were withdrawn and titrated. Figure 22 shows the disappearance of reactants. For hydrazine this rate was 0.00121 moles per hour per square centimeter, which if used electrochemically could provide:

$$0.00121 \frac{\text{mole}}{\text{hr}} \times 4 \frac{\text{equivalents}}{\text{mole}} \times 96{,}500 \frac{\text{coulombs}}{\text{equivalent}} \times \frac{1}{3600} \frac{\text{hr}}{\text{sec}} = 130 \frac{\text{ma}}{\text{cm}^2}$$

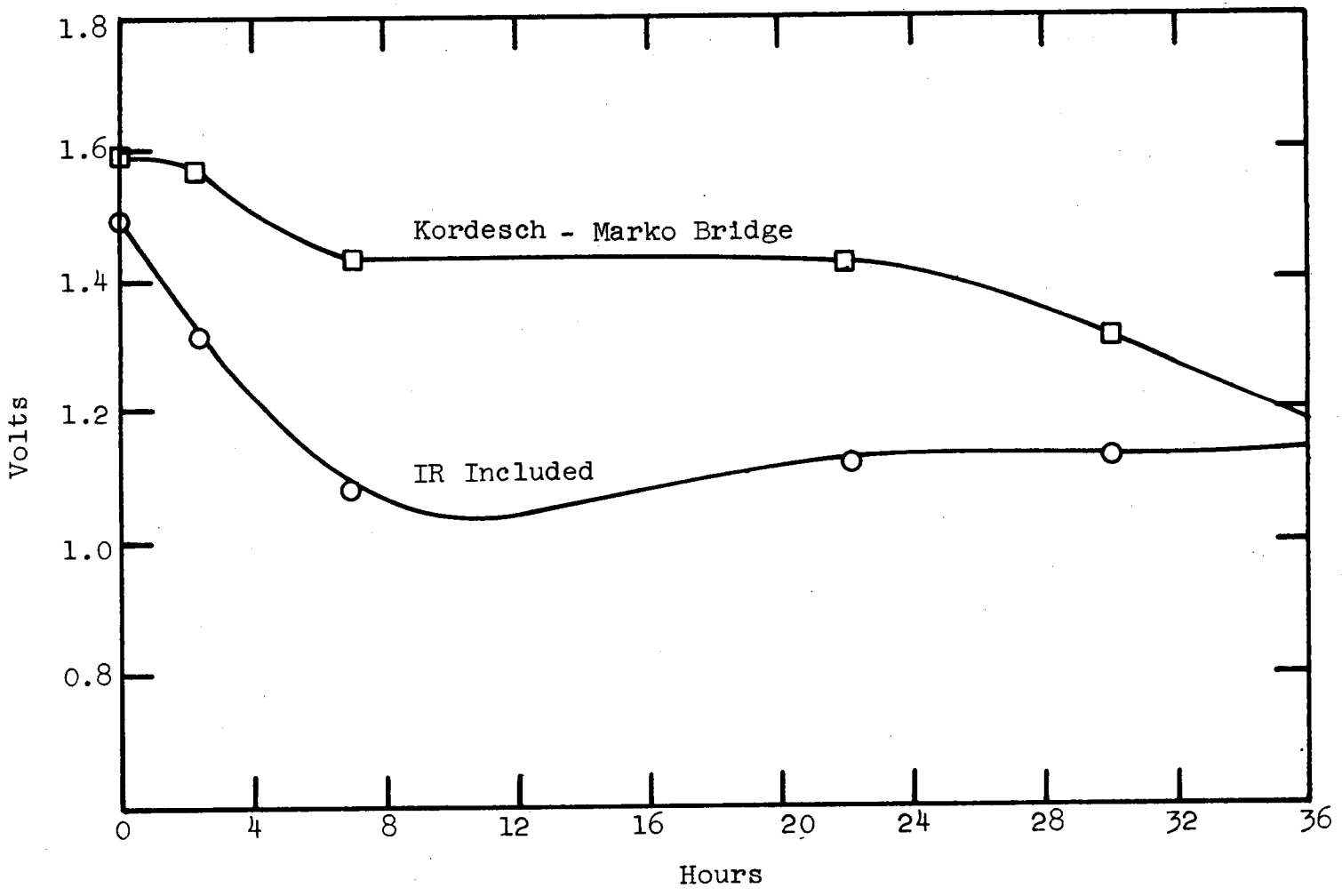

Figure 21. Full Cell Polarization Versus Time

C. D. = 17.5 ma/cm^2

Table 26

FULL CELL SEQUENCE III - ION EXCHANGE ELECTROLYTE FULL CELLS WITH CATION AND/OR ANION MEMBRANES

All Other Conditions the same as for Sequence II

Run	Fuel	Oxidant	Electrochemical Performance				Temp. °C	Ion* exchange membrane sequence	Notes
			O.C.V. volts	Current density ma/cm^2	K-M voltage volts	Voltage + IR volts			
I	85% $N_2H_4.H_2O$	70% HNO_3	1.50	17.5	1.40	1.18	30	AS/A	Asbestos saturated with 1M KOH. N_2O_4 produced at cathode.
II	85% $N_2H_4.H_2O$	70% HNO_3	1.70	17.5	1.25	1.05	30	Anode/Ca/AS/A/ Cathode	Distilled H_2O in asbestos N_2O_4 produced at cathode.
III	85% $N_2H_4.H_2O$	70% HNO_3	1.68	17.5	1.11	0.25	30	Anode/A/AS/Ca/ Cathode	Gassing at cathode, no N_2O_4.
IV	98% MMH	70% HNO_3	1.83	10.5	1.00	0.37	30	A/AS/A	KOH in asbestos

*A - Anion Membrane - Ionics
AS- Asbestos
Ca- Cation Membrane - Ionics

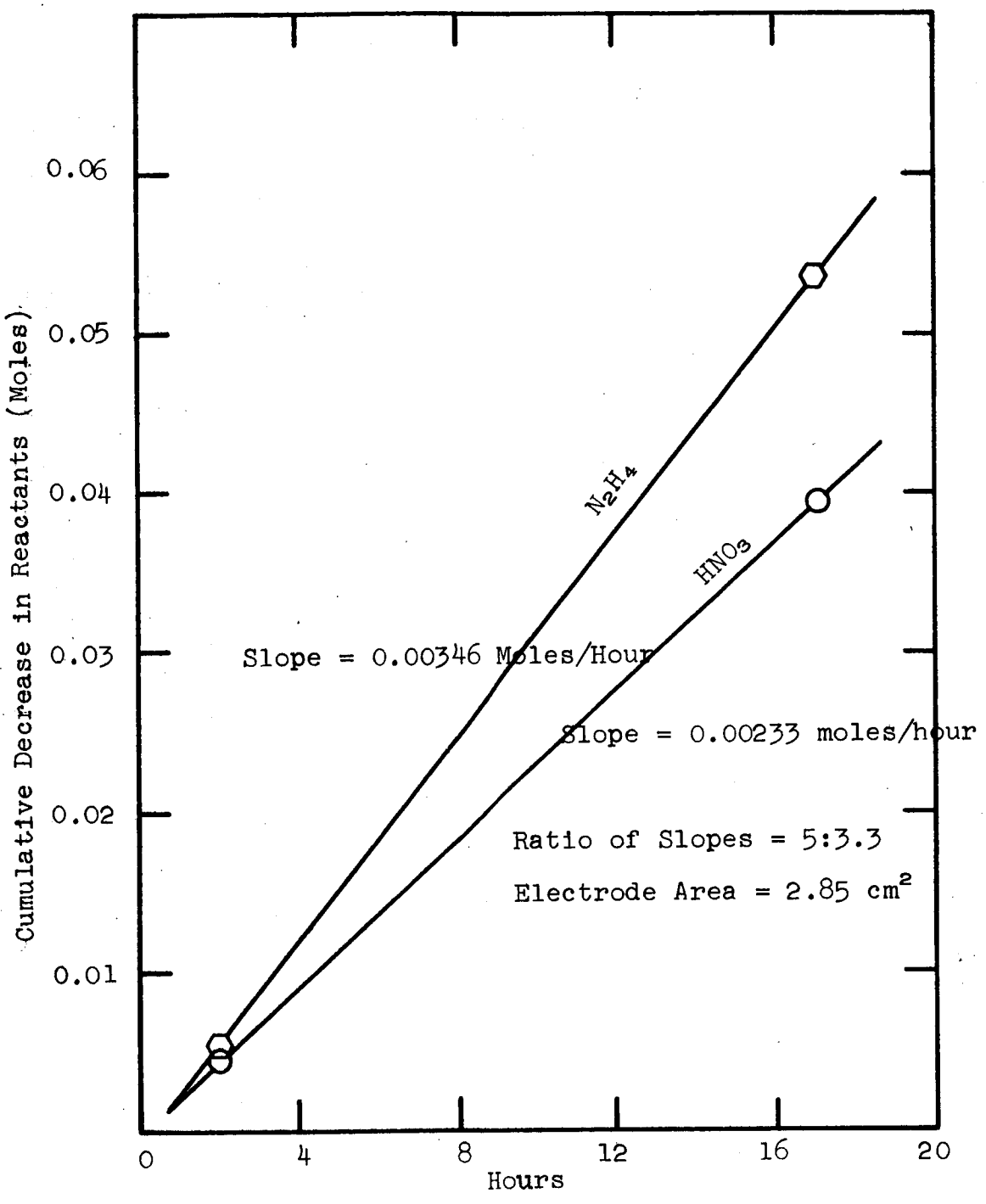

Figure 22. Disappearance of Reactants at Open Circuit

For nitric acid the rate of disappearance was 0.00082 moles/hr/cm^2. Because the electron change was not known this figure could not be used to check the hydrazine disappearance or to establish the amount decomposed versus the amount diffused. We assumed most of the reactants disappeared because hydrazine diffused to the cathode compartment to react directly with the nitric acid.

At this point it became necessary to use the new electrode construction described in the Appendix A-3. Previously the catalyst was prepared by reducing soluble salts of rhodium and gold with hydrazine. Using catalyst prepared this way no problem of separation of the Teflon-impregnated cloth and perforated steel was encountered, yielding a simple and easily constructed electrode. Use of the commercial rhodium black and powdered gold saved preparation labor but separation of the cloth and steel occurred after a few minutes' operation in a full cell because of the formation of gas pockets. The new electrode prevented this separation.

Figure 23 shows the short-term polarization of a full cell using the new electrode construction and a cation exchange membrane. Figure 24 shows the rate of disappearance of reactants for the above cell at 17.5 ma/cm^2. The rate of disappearance of reactants was greater than for the cell standing at no load, so it appears that in this case $N_2H_5^+$ was the current carrying species. This would contribute to the full-cell voltage as explained in the theoretical discussion.* This fact would result in excessive use of reactants, which is the main disadvantage of this system. However, the following other advantages of the porous Teflon vapor diffusion electrode in combination with an ion exchange membrane separator still remain:

1. Storage of the concentrated reactants adjacent to the Teflon is possible without excessive spontaneous decomposition occurring, eliminating many problems associated with the pumping and feeding of reactants to electrodes.

2. If hydrogen peroxide can be used in combination with an anion exchange membrane, it is probable that OH^- from the electrochemical reduction of H_2O_2 would be the sole current carrying ion, thus eliminating waste of reactants due to diffusion of ions other than those formed electrochemically. The same argument applies to the direct use of hydrogen at the anode in combination with a cation exchange membrane.

---

*See Section IV-E

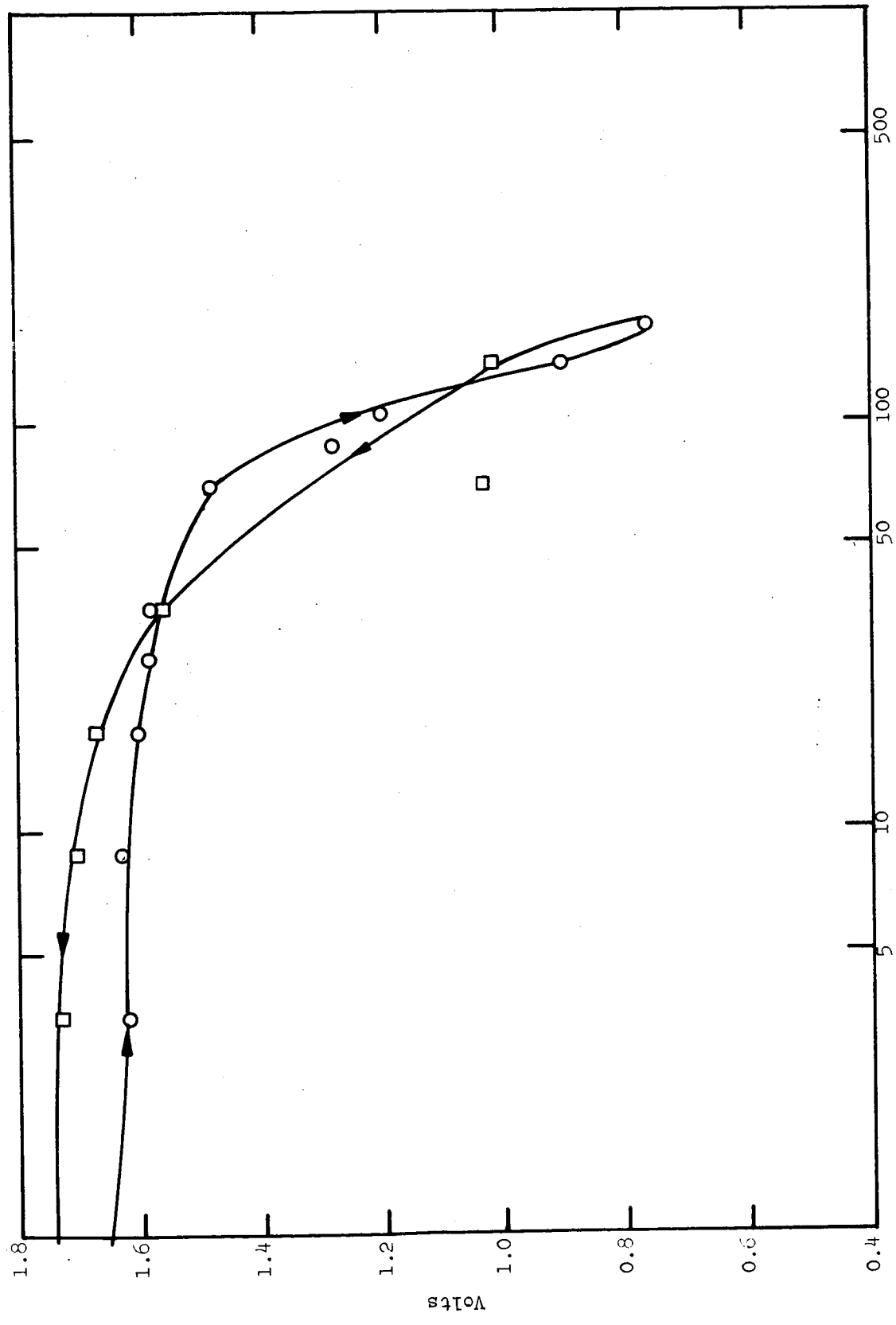

Figure 23. Short Term Polarization of N_2H_4-HNO_3 Full Cell Utilizing Porous Telflon Electrodes & Cation Exchange Membrane

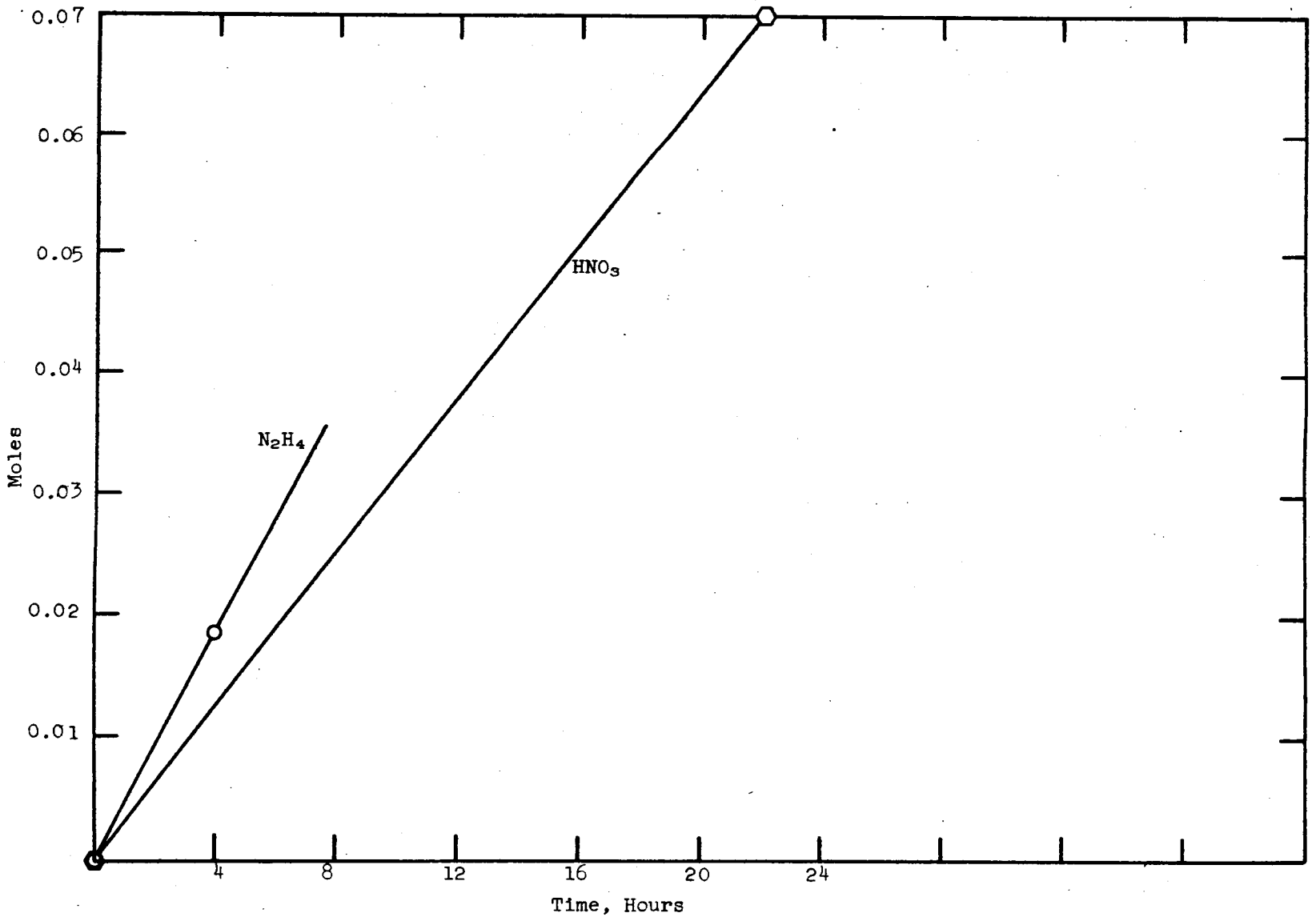

Figure 24. N_2H_4-HNO_3 Full Cell. Disappearance of Reactants under 17.5 ma/cm² Load at 30°C.

VI. FUEL CELL ELECTRODES IN NONAQUEOUS ELECTROLYTES

The purpose of this investigation was to determine the feasibility of using nonaqueous electrolytes in fuel cells. Although water has many advantages for use as a fuel-cell solvent for electrolyte (its excellent ionizing ability and economy, for example) special applications of fuel cells may warrant the use of solvents other than water. For instance, water solutions will freeze or become viscous at arctic temperatures or will boil above 100°C. The reactivity of water with many active metals excludes their use in aqueous systems. Some potent oxidizers react with water and therefore cannot be used as cathodic materials in aqueous systems. The use of nonaqueous electrolytes may broaden the temperature limitations of fuel cells as well as permit use of some powerful oxidizers or reducing materials that decompose water.

Two nonaqueous solvent systems were investigated:

(1) anhydrous hydrogen fluoride (AHF) and fluoride salts, and
(2) anhydrous organic solvents.

A. ANHYDROUS HYDROGEN FLUORIDE SYSTEMS

Although little electrochemical work has been done on solutions in hydrogen fluoride, it is a likely candidate for such studies. Because of its high dielectric constant (66), hydrogen fluoride would be expected to dissolve some salts to form conducting solutions. A striking analogy exists between (1) hydrogen fluoride and metal fluorides, and (2) water and metal oxides or hydroxides. Because of the considerable advances in fluorine chemistry and the improvement of materials of construction, the use of fluorine electrochemical systems should be considered, particularly for specialized application.

The most potent oxidizers known, elemental fluorine and chlorine trifluoride, are rocket fuel candidates and may conceivably be used as electrochemical oxidants for the production of electrical power in the rocket being propelled. Since fluorine is the most active oxidant, only completely fluorinated materials such as hydrogen fluoride or fluoride salts can be considered as solvents or electrolytes for fluorine or chlorine trifluoride oxidants. Since such fuels as hydrogen and hydrazine are compatible with hydrogen fluoride, it is possible that a fuel cell can be devised that uses fluorine or chlorine trifluoride as the oxidant and hydrogen or hydrazine as the reductant.

Chlorine trifluoride (CTF) and anhydrous hydrazine were selected as reactants for this exploratory investigation. Their reactions in a fuel cell were postulated to be:

$$\begin{array}{ll} \text{(Anode)} & N_2H_4\ (l) \rightarrow N_2 + 4H^+ + 4e^- \\ \text{(Cathode)} & ClF_3\ (g) \rightarrow Cl^{\ominus} + 3F^- - 4e^- \end{array}$$

$$\text{(Cell)} \qquad ClF_3\ (g) + N_2H_4\ (l) \rightarrow N_2 + HCl + 3HF$$

$$\Delta F^\circ = -223 \text{ Kcal}$$
$$E^\circ = 2.42 \text{ volts}$$

Energy Density = 950 watt-hours/lb.

The unusually high maximum voltage of this combination is one of the interesting aspects of using CTF as a cathodic material.

The initial phase of this investigation was concerned with the cathodic reduction of CTF and the anodic oxidation of hydrazine in AHF and in fused KF-AHF melts.

1. Anodic Oxidation of Hydrazine in Anhydrous Hydrogen Fluoride

The anodic polarization of catalyzed electrodes in contact with a 1M solution of hydrazine dihydrogen fluoride (HDHF) that was 0.5M in sodium fluoride was measured with the apparatus shown in Figure 25.

The Teflon cell, designed for half-cell measurements of polarized electrodes, contained the test electrode of platinum or carbon, a reference electrode, and a platinum or carbon polarizing electrode.

A mercury thermometer in the half cell was protected by a thermowell of Kel-F tubing. A slow stream of dry nitrogen passed through the cell to suppress atmospheric contamination. The test electrode was a platinum rectangle of 1 cm^2 total area spot welded to a platinum lead and plated with the catalyst metal under investigation.* The catalyzed electrodes were mounted in Teflon holders that could be inserted, one at a time, in the solution of HDHF in AHF-NaF contained in the Teflon half cell (Figure 25).

---

*Details of electrode and reference electrode preparation are given in the Appendix.

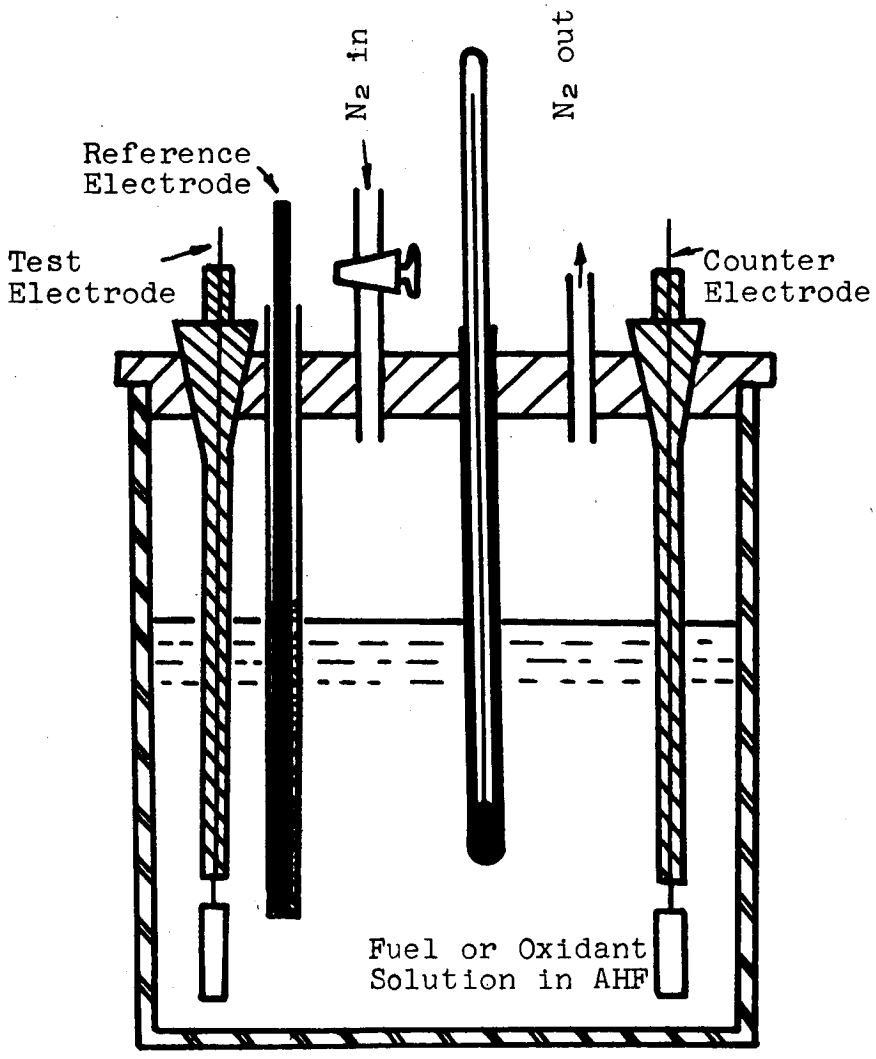

Figure 25. Anhydrous Hydrogen Fluoride Cell

The following test electrodes were used: carbon, platinum, and platinum plated with platinum black, gold, palladium, ruthenium, and iridium. The data are shown in Figure 26. The best electrodes (those showing least polarization for a given current density) were carbon and platinized platinum. The uncatalyzed platinum, iridized platinum, and ruthenized platinum electrodes polarized severely under the test conditions.

Since hydrazine dihydrogen fluoride itself is an electrolyte,

$$N_2H_4 \cdot 2HF \quad = \quad N_2H_5^+ \quad + \quad HF_2^-$$

one series was run in which HDHF served the dual role of fuel and electrolyte. Anodic polarization results are plotted in Figure 27. Results were somewhat better than those in which sodium fluoride electrolyte was added (Figure 26). Carbon and platinized platinum electrodes showed the least polarization. These electrodes withstood current densities of 20 ma/cm^2 with 0.5 volt polarization. Unplatinized platinum and iridium were most severely polarized at a given current density.

2. Cathodic Reduction of Dinitrogen Tetroxide in Anhydrous Hydrogen Fluoride

Cathodic polarization experiments were conducted in solutions of dinitrogen tetroxide (N_2O_4) in anhydrous hydrogen fluoride (AHF).

Solutions were made 0.5M in sodium fluoride to improve the electrolytic conductance. Cathodic polarization curves for various electrode materials in contact with the N_2O_4 solutions in AHF are shown in Figure 28. The best cathodes (least polarization) were the ruthenized and platinized platinum and carbon electrodes. Cathode current densities as high as 100 ma/cm^2 were obtained with a polarization of 0.5 volt from the open-circuit potential. The polarized potentials, however, were too low to be of interest for a practical fuel cell. Also, the production of water as a result of N_2O_4 reduction,

$$N_2O_4 \quad + \quad 4HF \quad + \quad 4e^- \quad = \quad 2NO \quad + \quad 2H_2O \quad + \quad 4F^-$$

would contaminate the initial anhydrous system. No further work is planned on the use of N_2O_4 as an oxidizer in AHF solutions.

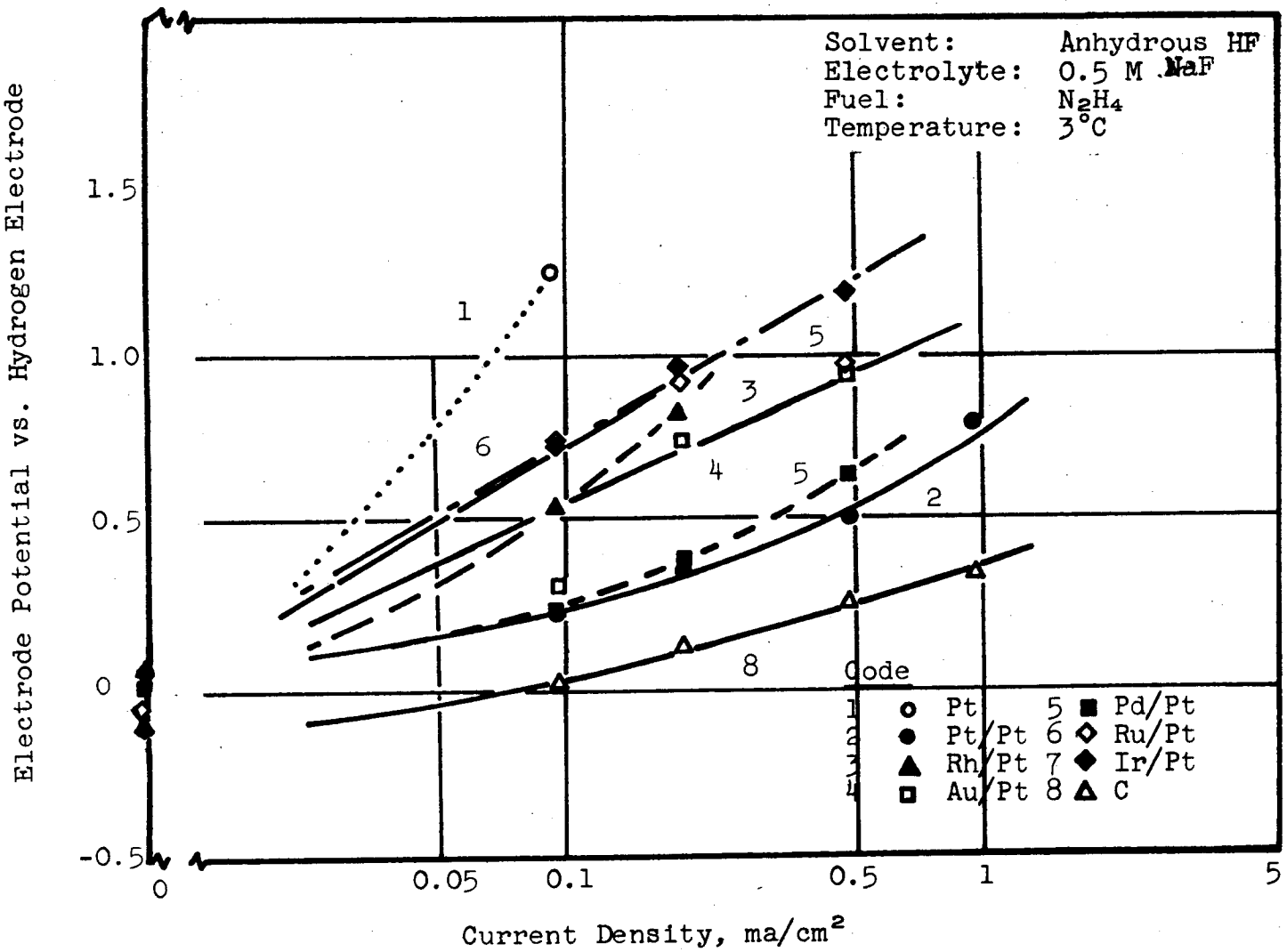

Figure 26. Anodic Oxidation of 1 M Hydrazine in Anhydrous Hydrogen Fluoride

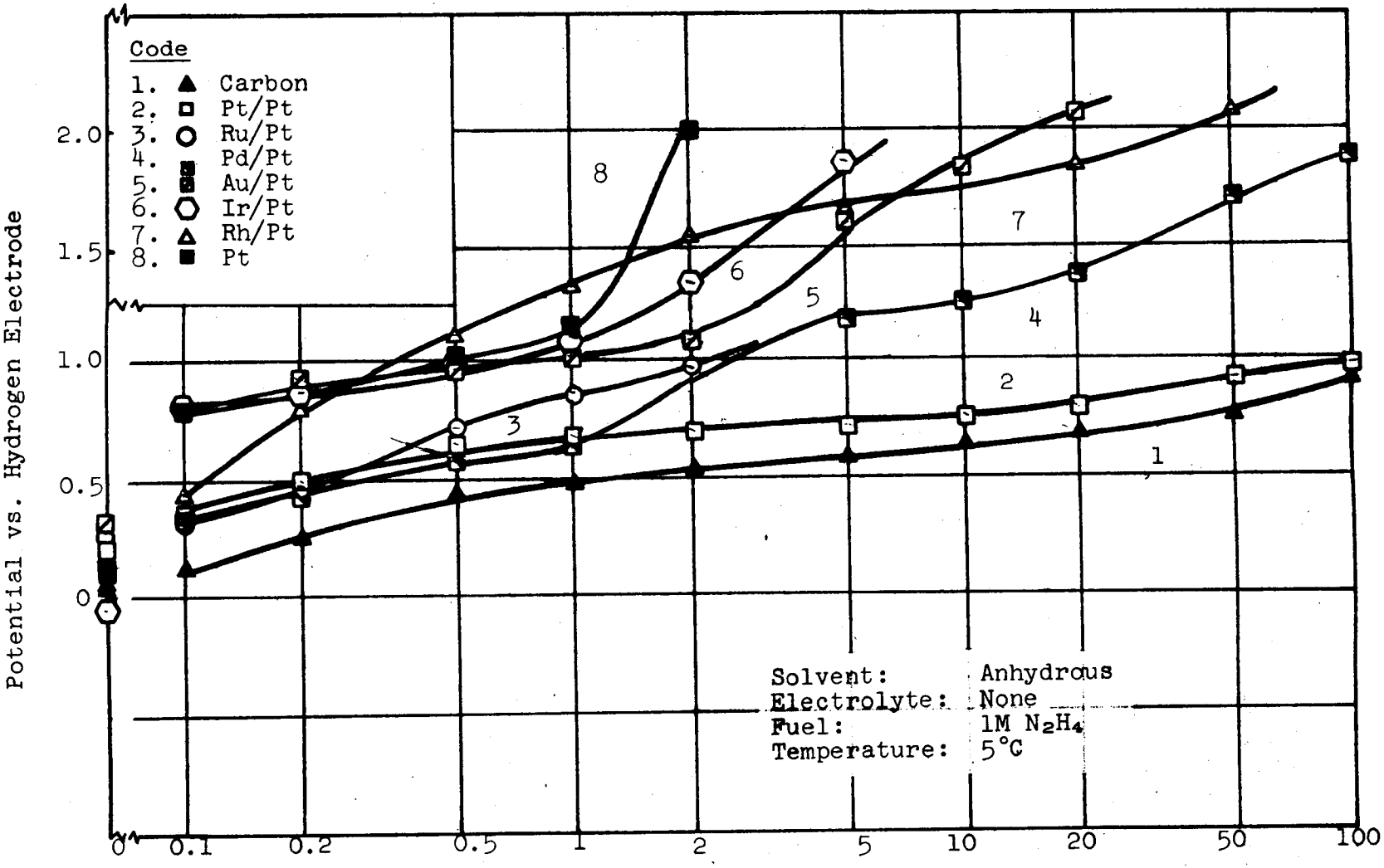

Figure 27. Anodic Oxidation of Hydrazine in Anhydrous Hydrogen Fluoride

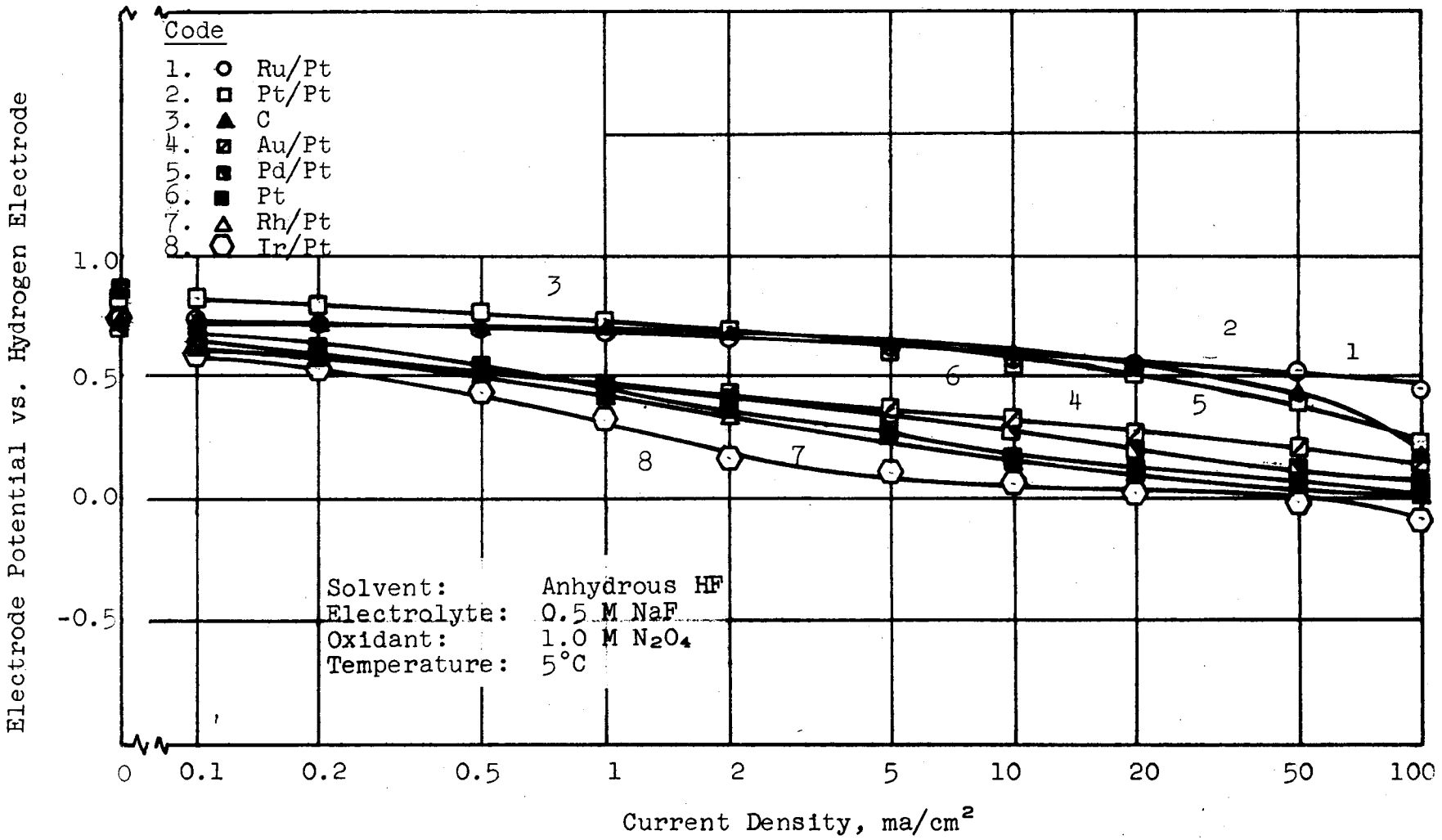

Figure 28. Cathodic Reduction of Dinitrogen Tetroxide in Anhydrous Hydrogen Fluoride

3. Cathodic Reduction of Chlorine Trifluoride in Anhydrous Hydrogen Fluoride

The apparatus used for studying the cathodic polarization of electrodes in chlorine trifluoride (CTF) solution was similar to that used with N_2O_4 studies except that a Dry Ice-carbon tetrachloride cooling bath was used instead of an ice bath because of the violent reactivity of CTF with water. AHF solutions were made 0.5M in sodium fluoride to improve the conductance of CTF-AHF solutions. (See Table 27).

Polarization studies at the platinized platinum and gold-plated platinum electrodes are shown in Figure 29. Both electrodes carried a current density of 100 ma/cm^2 with 0.5 volt polarization at 5°C. The potential of the platinized electrode was better than that of the gold-plated electrode. Both electrode potentials were much better than those obtained using N_2O_4 as the oxidant (Figure 28).

The plated gold on the platinum cathode as well as the platinum and carbon counter electrodes were noticeably attacked in the CTF solution. Further work is required to find materials that will withstand the oxidizing action of CTF and fluorine in AHF solution.

4. Anodic Oxidation of Hydrazine in Molten Mixtures of Anhydrous Hydrogen Fluoride and Potassium Fluoride

Molten mixtures of anhydrous hydrogen fluoride (AHF) and potassium fluoride were used as electrolytes for the anodic oxidation of hydrazine dihydrogen fluoride (HDHF). The boiling temperature of AHF can be increased from 19°C to 66°C by dissolving one mole of potassium fluoride in three moles of AHF. Potassium fluoride and AHF form a series of compounds with melting points within the range of 78 $\pm$ 5°C over the composition range from 37% to 60% KF (ref. 20). Such compositions are electrolyte candidates for hydrazine oxidation as well as for fluorine and CTF reduction at temperatures in the vicinity of 85°C. The advantages of using salt mixtures at 85°C instead of AHF at 5°C as an electrolyte for cathodic CTF reduction include the lower solubility of CTF at the higher temperature (73°C above its boiling temperature) and the greater reactivity associated with the higher temperature.

Table 27

CONDUCTANCE OF CHLORINE TRIFLUORIDE IN ANHYDROUS HYDROGEN FLUORIDE

Concentration moles HF/liter at 25°C	Specific Conductance mhos/cm x 10^8		Equivalent Conductance at 25°C, mhos/cm x 10^4
	-78°C	25°C	
0	0.65	0.49	0
1.00	4.5	2.96	0.25
1.35	9.5	5.49	0.45
2.57	82.5	43.7	1.68
4.67	460	350	7.5

Data of Rogers, Speirs, and Panish (ref. 24).

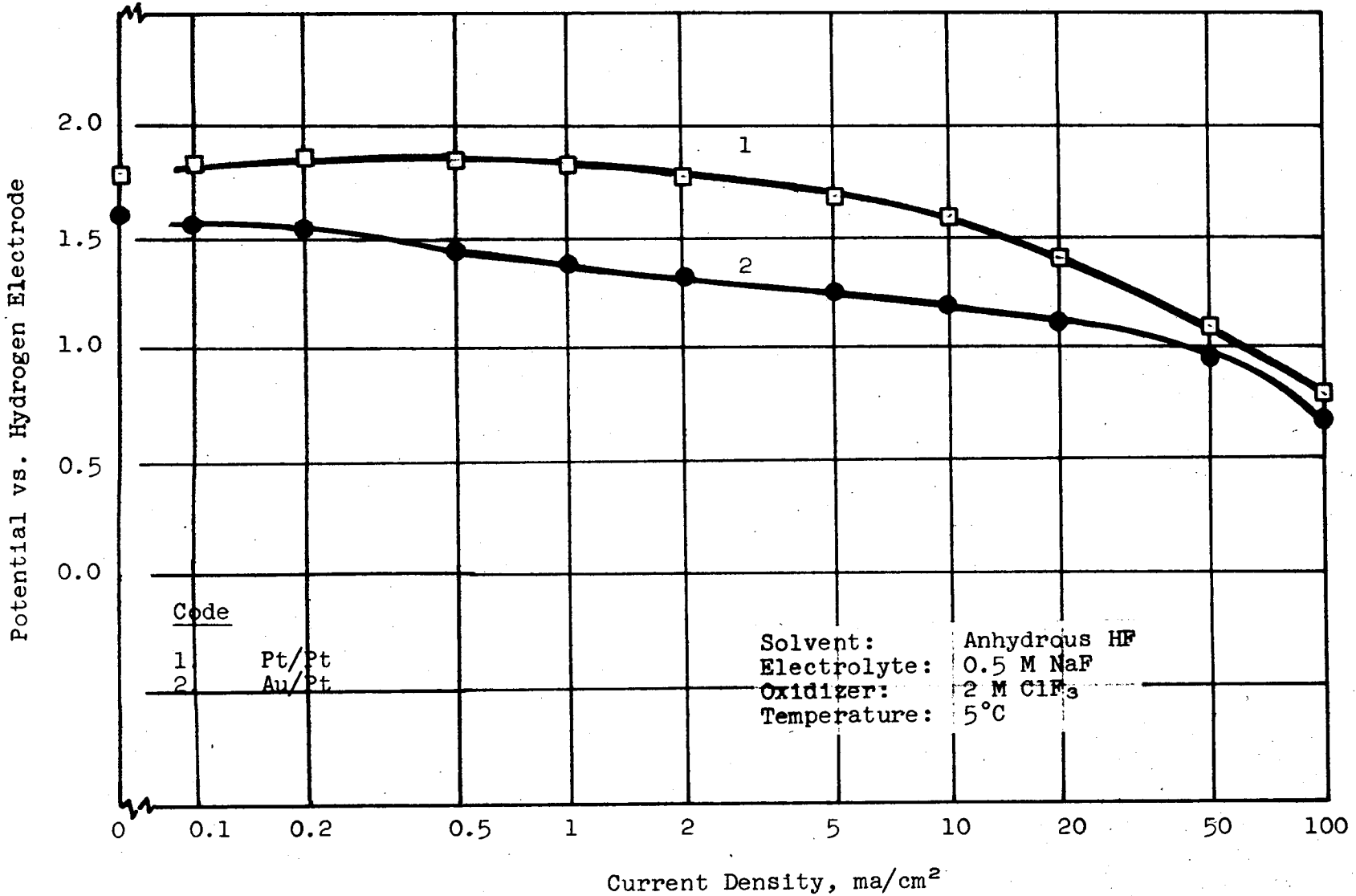

Figure 29. Cathodic Reduction of Chlorine Trifluoride in Anhydrous Hydrogen Fluoride

The composition KF·3HF was prepared by slowly stirring small increments of potassium bifluoride into liquid AHF in a tared Teflon flask. Polarization measurements were made in apparatus similar to that shown in Figure 25 except that a stainless steel beaker was used as a container instead of Teflon because of the better thermal conduction of the metal. Sufficient HDHF was weighed into the molten salt to make it 1M in hydrazine. The assembly was immersed in a fluidized sand thermostat for temperature regulation at 85°C. The cell was purged with dry nitrogen to exclude air and moisture.

Rhodium and ruthenium-plated platinum were the best anodes for oxidation of hydrazine in AHF (Figure 30). Both materials sustained current densities up to 100 ma/cm^2 at a polarization of 0.5 volt at 85°C. Carbon, plain platinum, and gold-plated platinum polarized badly at very low current densities.

5. Cathodic Reduction of Chlorine Trifluoride in Molten Mixtures of Anhydrous Hydrogen Fluoride and Potassium Fluoride

The apparatus used for studying the cathodic reduction of CTF in AHF-KF melts was identical to that used for polarization studies of hydrazine in these melts at 85°C.

Since the melting point of KF·3HF (66°C) is higher than the boiling temperature of CTF, the oxidant was fed to the cell as a gas when operating at 85°C. The CTF gas was slowly bubbled into the molten KF·3HF melt directly below the solid catalyzed platinum electrode. The void space above the melt was continuously purged with dry nitrogen to exclude air and moisture.

The most effective cathode material for CTF reduction in molten KF·3HF at 85°C was carbon (Figure 31). The current-voltage curve was flat up to a current density of 2 ma/cm^2 but fell sharply at higher currents. Solid platinum electrodes electroplated with rhodium, iridium, gold, and platinum black had somewhat lower potentials and polarized at the same current density of 2 ma/cm^2. Potentials of all these cathodes up to current densities of 2 ma/cm^2 were higher than those of CTF in AHF at 5°C (see Figure 29).

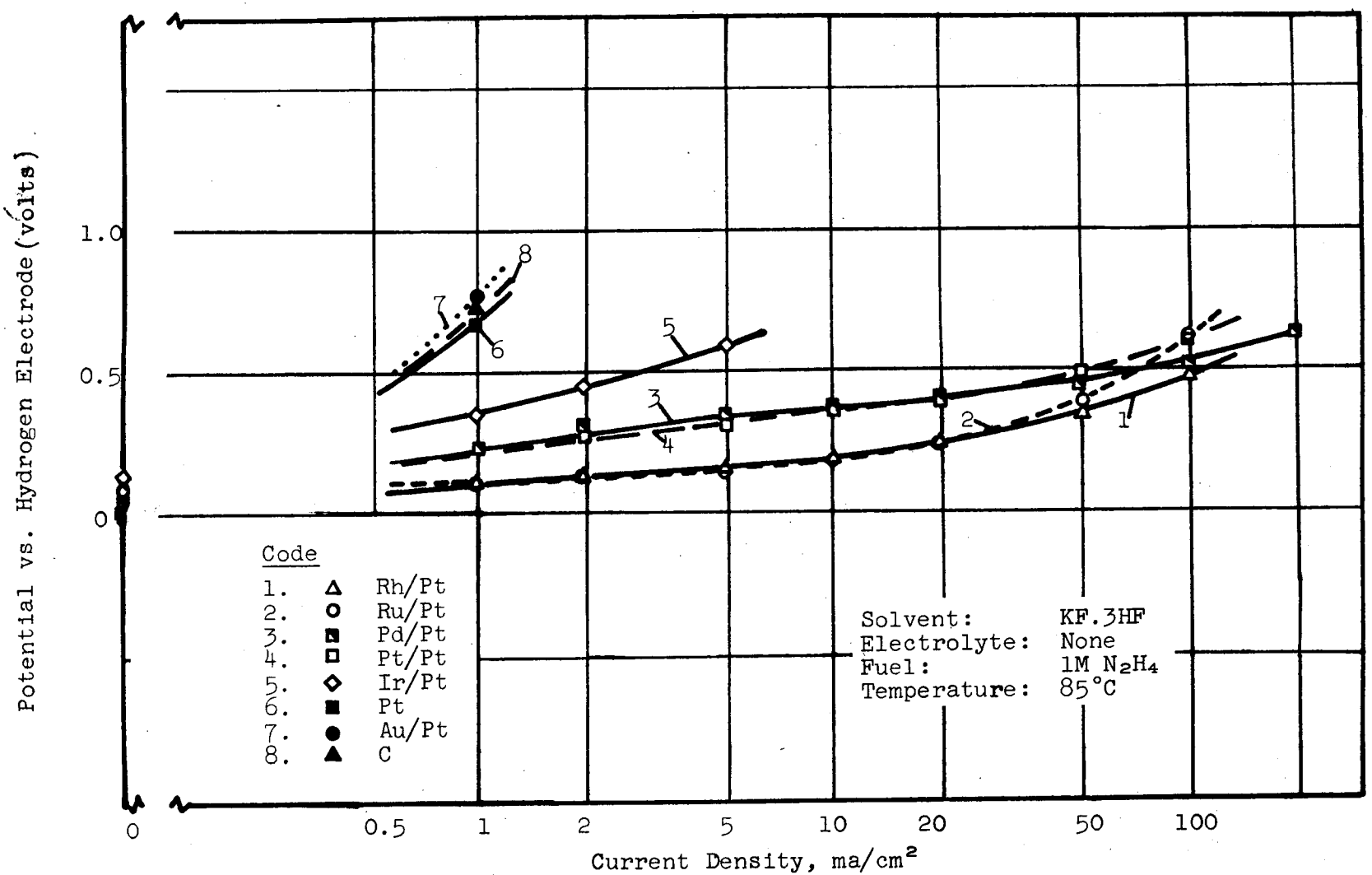

Figure 30. Anodic Oxidation of 1M Hydrazine in KF.3HF

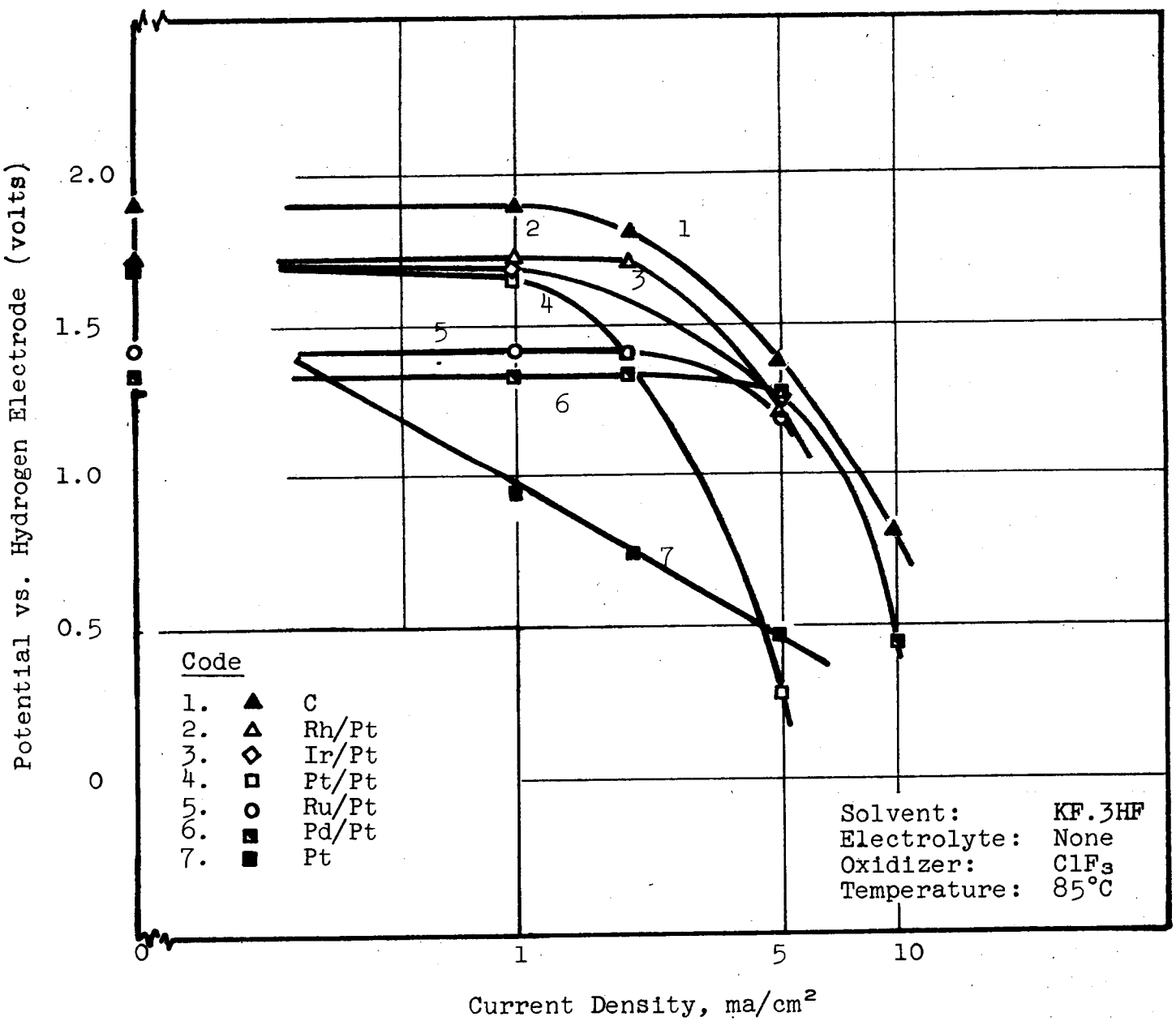

Figure 31. Cathodic Reduction of Chlorine Trifluoride in KF.3HF

6. Chlorine Trifluoride Compatibility with Hydrazine in Anhydrous Hydrogen Fluoride

Since chlorine trifluoride (CTF) and anhydrous hydrazine mixtures are hypergolic (ref. 20-A), some concentration limits of compatibility were determined in liquid anhydrous hydrogen fluoride (AHF) solution. Compatibiility between these materials is particularly important in full cells where anolyte and catholyte mixing may occur by diffusion through the separator. CTF solutions in AHF at -23°C were mixed with hydrazine dihydrogen fluoride (HDHF) solutions in AHF at several concentrations in an open Kel-F test tube. Starting at 3M CTF with 2M HDHF, all mixtures reacted explosively when one solution was added dropwise to the other at -23°C, except those of 1M concentrations. In the latter case, a mild crackling noise was heard on addition of the first few drops of CTF tothe HDHF solution. Otherwise, no vigorous reaction or gas liberation was observed, even on warming the mixture to approximately 20°C. The CTF-HDHF solution became yellow (CTF in AHF is faintly yellow) and gave a positive test for oxidizer with moistened starch-potassium iodide paper. Low-concentration catholyte-anolyte mixing may be tolerable. Some of the vigorous reaction that occurs on mixing these materials may be caused by the reaction of CTF with traces of water in the HDHF solution. Commercial hydrogen fluoride was used for all runs.

B. NONAQUEOUS ORGANIC SYSTEMS

1. Conductance Measurements

The organic solvents chosen for study were acetonitrile, N,N-dimethyl-formamide (DMF), propylene carbonate, and pyridine. The solvents employed were all of good, commercially available quality and were used without further purification. These solvents are known to furnish conducting solutions with many inorganic salts. The inorganic salts were dried at elevated temperatures for three days. Specific conductance measurements were carried out using a Model 250-DA Electromeasurements, Inc., impedance bridge with a General Radio Precision Condenser 0.1100 μμf, and an Esi Model 855-Al oscillator-amplifier. The cell constant of a dip-type conductance cell was determined employing 0.1 demal KCl at 25°C.* The specific conductance in ohm^{-1} cm^{-1} of various solvent-salt electrolytes are listed in Table 28. The conductances of electrolytes and N_2O_4 in nonaqueous solvents are given in Table 29.

Considering conductivity alone, acetonitrile and DMF are superior to propylene carbonate and pyridine as solvents, and KSCN and $Mg(ClO_4)_2$ are superior to $C_6H_5SO_3Na$ as salts. The Ag/AgCl electrode was selected as the reference electrode for half cell studies because of

*0.1 D = 7.4789 gram KCl/1000 gm H_2O.

Table 28

ELECTRICAL CONDUCTANCE OF SALTS DISSOLVED IN NONAQUEOUS ORGANIC MEDIA

Salt	Weight, (g) Per 100 cc Solvent	Specific Conductivity at 25°C ohm^{-1} cm^{-1}	Comments
		Solvent - Acetonitrile	
None	-	6.4×10^{-7}	saturated solution
KSCN	10	2.8×10^{-2}	dissolved
$Mg(ClO_4)_2$	5	1.9×10^{-2}	dissolved
	10	2.8×10^{-2}	saturated solution
KCl	2	6.0×10^{-5}	saturated solution
NH_4Cl	1	2.7×10^{-5}	saturated solution
$(CH_3)_4NCl$	1	5.6×10^{-4}	saturated solution
$C_6H_5SO_3Na$	5	1.6×10^{-4}	
		Solvent - N,N-Dimethylformamide	
None	-	3.8×10^{-6}	
KSCN	10	2.6×10^{-2}	dissolved
$Mg(ClO_4)_2$	5	1.2×10^{-2}	dissolved
	10	1.9×10^{-2}	dissolved
KCl	2	1.5×10^{-4}	saturated solution
NH_4Cl	1	1.8×10^{-4}	saturated solution
$(CH_3)_4NCl$	1	1.5×10^{-3}	saturated solution
$C_6H_5SO_3Na$	5	4.8×10^{-3}	dissolved
		Solvent - Propylene Carbonate	
None	-	6.4×10^{-7}	dissolved
KSCN	10	7.8×10^{-3}	dissolved
$Mg(ClO_4)_2$	5	4.3×10^{-3}	saturated solution
	10	5.9×10^{-3}	saturated solution
KCl	2	2.4×10^{-5}	saturated solution
NH_4Cl	1	3.1×10^{-5}	saturated solution
$(CH_3)_4NCl$	1	4.9×10^{-4}	saturated solution
$C_6H_5SO_3Na$	5	8.2×10^{-5}	saturated solution
		Solvent - Pyridine	
None	-	2.2×10^{-7}	saturated solution
KSCN	5	1.5×10^{-3}	saturated solution
$Mg(ClO_4)_2$	5	5.0×10^{-3}	saturated solution
KCl	2	1.9×10^{-6}	saturated solution
NH_4Cl	1	8.8×10^{-7}	saturated solution
$(CH_3)_4NCl$	1	6.0×10^{-6}	saturated solution
$C_6H_5SO_3Na$	5	8.2×10^{-5}	saturated solution

Table 29

SPECIFIC CONDUCTANCE OF ELECTROLYTES AND N_2O_4-ELECTROLYTE SOLUTIONS

Solution	Experimental (this work) Specific Conductivity* $ohm^{-1}\ cm^{-1}$	Temp. °C	Literature Specific Conductivity	Temp. °C	Ref. No.
Acetonitrile (distilled from P_2O_5)	$1.6 \pm 0.8 \times 10^{-6}$	25	5×10^{-6} to 9×10^{-6}	24,25	Several
10% $Mg(ClO_4)_2$ in acetonitrile	2.95×10^{-2} 2.47×10^{-2}	26 0	2.38×10^{-2}	24	17
1M N_2O_4 in 10% $Mg(ClO_4)_2$-acetonitrile	2.18×10^{-2}	0	-	-	-
2M N_2O_4 in 10% $Mg(ClO_4)_2$-acetonitrile	2.07×10^{-2}	0	-	-	-
N,N-Dimethylformamide (distilled)	$\sim 0.4 \times 10^{-6}$	25	3×10^{-8} 2×10^{-6}	25 24	18 17
10% $Mg(ClO_4)_2$ in dimethylformamide	1.88×10^{-2}	25	1.59×10^{-2}	24	17
Dimethylforamide saturated with $Mg(ClO_4)_2$	1.39×10^{-2}	0	-	-	-
2M N_2O_4 in dimethylformamide saturated with $Mg(ClO_4)_2$	1.01×10^{-2}	0	-	-	-

*Measured in calibrated 1 cm cell with an Industrial Instruments Bridge, Model 1682.

its wide applicability in many nonaqueous solvent systems (ref. 21). This electrode requires the presence of chloride ion in solution. Of the three chlorides tested, $(CH_3)_4NCl$ gave higher conductivities than either KCl or NH_4Cl. The addition of KCl to KSCN solutions did not influence the specific conductivity.

2. Compatibility of Solvents with Propellants

Qualitative tests were performed to determine the compatibility of N_2H_4 and N_2O_4 with the candidate nonaqueous media. Ten ml of 1N solutions of N_2H_4 and N_2O_4 were prepared to note visible signs of reaction such as gas formation, heat release, color change, or insoluble product formation. Results are summarized in Table 30.

With N_2H_4, clear, water-white solutions resulted for all four solvents. A strong ammoniacal odor was observed after one day with dimethylformamide, and some indication of NH_3 formation was also observed in acetonitrile. However, the rates of these reactions may not be sufficiently fast to detract from the fuel-cell performance.

Acetonitrile and propylene carbonate appear to be compatible with freshly distilled N_2O_4. Addition of N,N-dimethylformamide to liquid N_2O_4 resulted in fuming, but the resulting solution appeared to be relatively stable. Pyridine reacted violently with N_2O_4 yielding a dark, solid residue. The three stable solutions are all bright green.

3. Anodic Oxidation of Hydrazine in Nonaqueous Organic Solvents

Preliminary half cell studies of the anodic oxidation of 1M N_2H_4 solutions were carried out employing a platinized catalyst anode on a steel substrate and a platinum cathode. Half-cell potentials were measured with reference to an Ag/AgCl electrode via a Luggin capillary. Voltages were recorded at open circuit and at increasing current loads up to the point at which the potential increase became very rapid.

The electrolytes studied are listed in Table 31. The polarization of the catalyst anode is illustrated in Figures 32 and 33 where half-cell potential versus the Ag/AgCl reference electrode is plotted versus the current density in ma/cm^2.

The best anodic polarization curve occurred in the case of DMF with tetramethylammonium chloride as the conducting salt. A current density of 10 ma/cm^2 at a polarization of 0.5 volt was obtained. Less favorable potentials at all current densities were obtained for the other nonaqueous organic systems.

Table 30

COMPATIBILITY OF SOME FUELS AND OXIDANTS
WITH ELECTROLYTE COMPONENTS

Key: N = no apparent reaction, some exhibit heat or cooling on mixing

C = complex formed

R = reaction

Fuel or Oxidant Reagent	H_2O_2*	N_2O_4	N_2H_4*
CH_3CN	N	N(C)	N
CH_3CN + KCNS	R	N	
CH_3CN + $Mg(ClO_4)_2$	N	N	
CH_3CN + $(CH_3)_4NCl$	N	N	
CH_3CN + AgCl			R
DMF	N	(C)	
DMF + $Mg(ClO_4)_2$	N	N	
DMF + KCNS		R	
DMF + AgCl			R
KCNS			N
$Mg(ClO_4)_2$			R
DMF + $CdCl_2$			N
Propylene Carbonate		N	N
Pyridine		R	N

*H_2O_2 and N_2H_4 gassed in all electrolytes in presence of Pt/Pt. Gassing was less than in aqueous media and less for N_2H_4 than for H_2O_2.

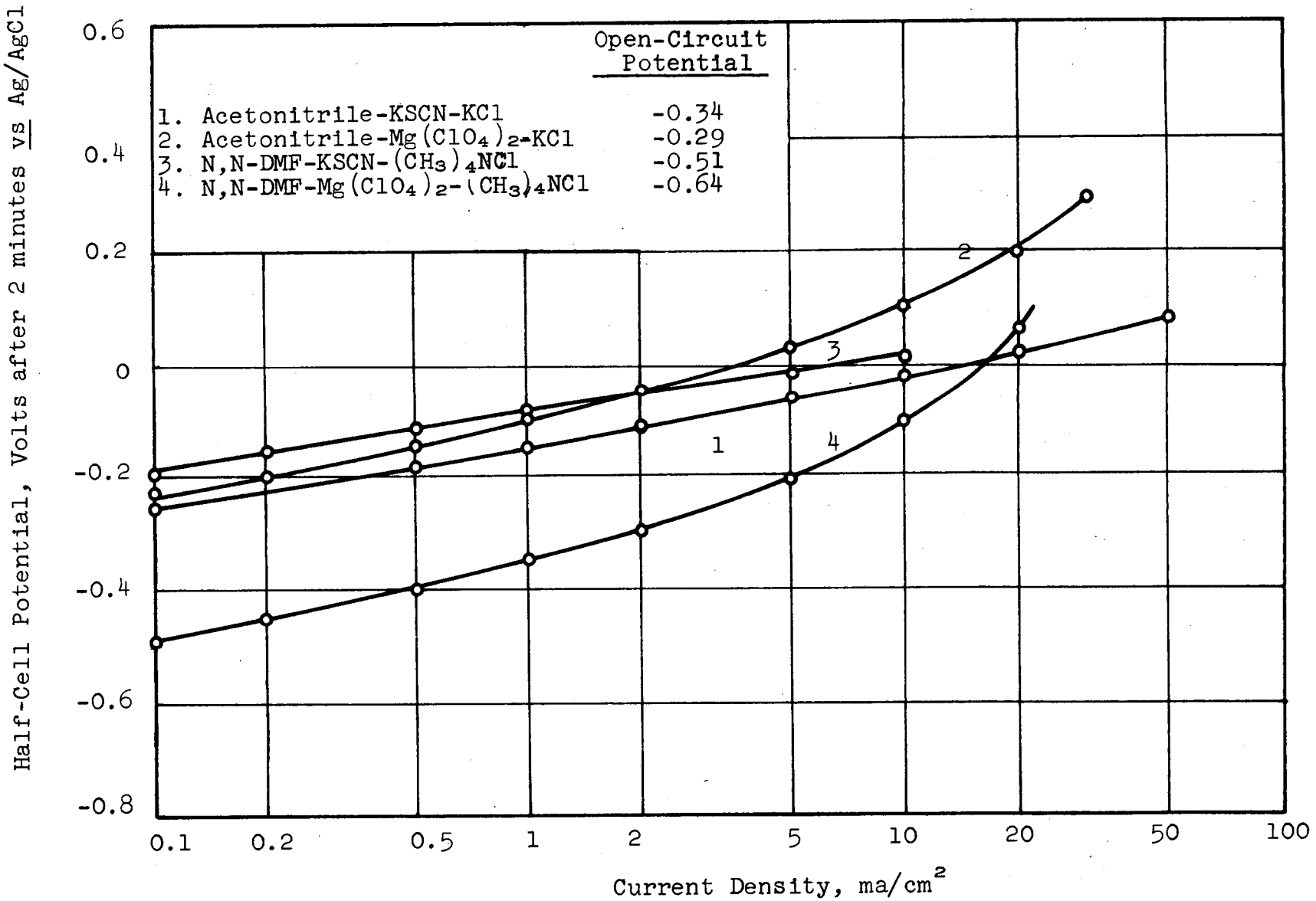

Figure 32. Anodic Oxidation of Hydrazine in Acetonitrile and Dimethylformamide

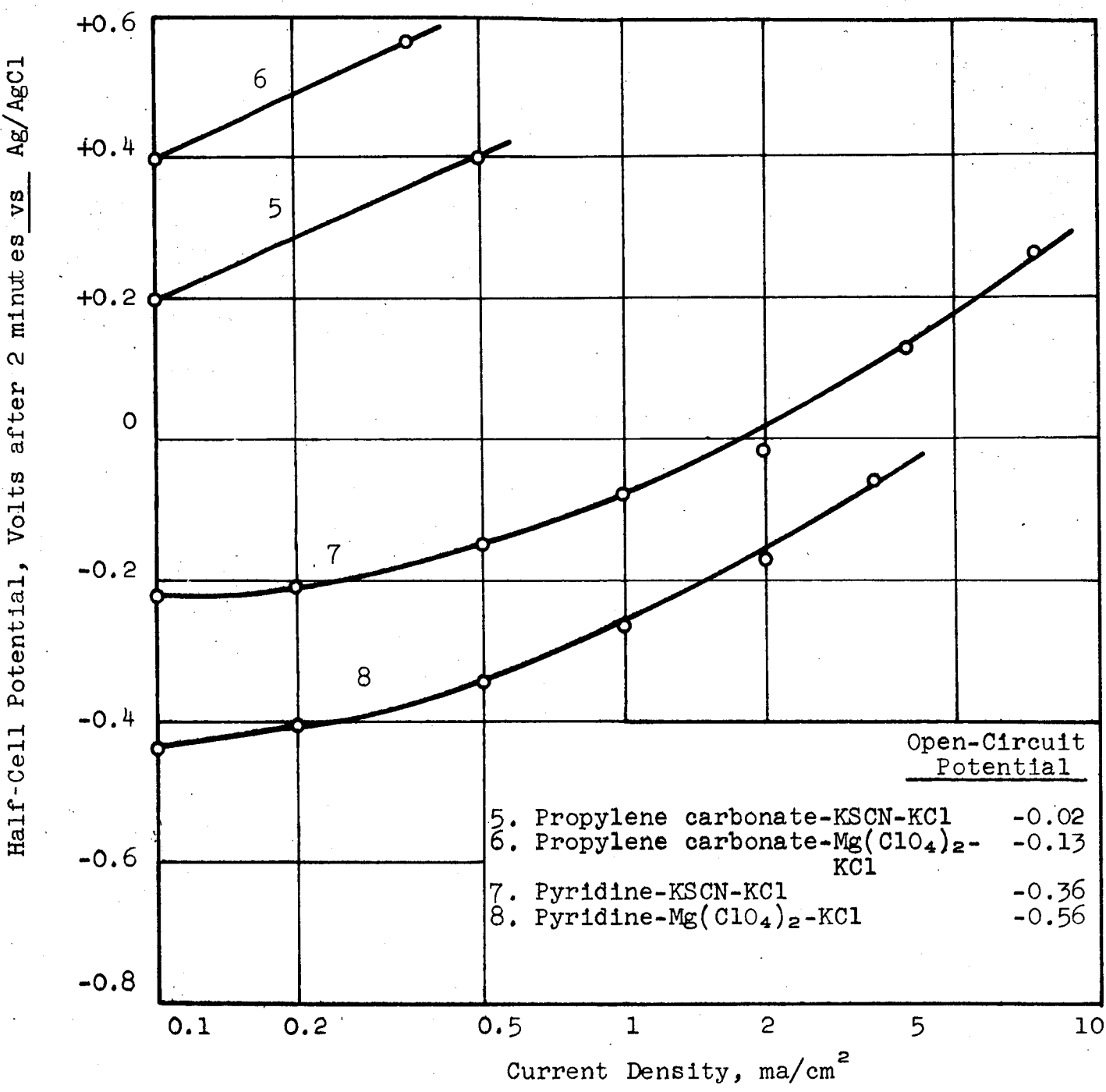

Figure 33. Anodic Oxidation of Hydrazine in Propylene Carbonate and Pyridine

Table 31

HALF-CELL STUDIES WITH 1M HYDRAZINE

Run No.	Solvent	Salt (wt g/250 ml)	Comments
1	Acetonitrile	KSCN (12.5)-KCl (1)	dissolved
2	Acetonitrile	$Mg(ClO_4)_2$ (12.5)-KCl (1)	dissolved
3	N,N-Dimethylformamide	KSCN (12.5) - $(CH_3)_4NCl$ (.5)	dissolved
4	N,N-Dimethylformamide	$Mg(ClO_4)_2$ (12.5)-$(CH_3)_4NCl$ (.5)	ppt on N_2H_4 addn. (suspension)
5	Propylene Carbonate	KSCN (12.5)-KCl (1)	dissolved
6	Propylene Carbonate	$Mg(ClO_4)_2$ (12.5)-KCl (1)	dissolved
7	Pyridine	KSCN (12.5)-KCl (1)	Saturated solution
8	Pyridine	$Mg(ClO_4)_2$ (12.5)-KCl (1)	saturated solution (suspension)

4. Cathodic Reduction of Dinitrogen Tetroxide in Nonaqueous Organic Solvents

The cathodic reduction of N_2O_4 was studied in an H-type cell with a fine glass frit separating the anode and cathode compartments. The working electrode was a 1 cm^2 area of platinized platinum on stainless steel; the dummy electrode was platinum. The anode compartment contained only electrolyte (e.g., 25 g $Mg(ClO_4)_2$ per 500 ml solvent). Half-cell potentials were measured with reference to a Ag/AgCl electrode via a Luggin capillary. The Ag/AgCl electrode was prepared by anodizing a silver wire in 0.1N HCl for 30 minutes at 0.4 ma. The electrode was immersed into the Luggin assembly containing a saturated solution of $(CH_3)_4NCl$ and AgCl in the solvent.

Voltages were recorded at open circuit and at increasing current loads up to the point where the potential decrease became very rapid. The cathodic reduction of 1M N_2O_4 in acetonitrile (AN) and N,N-dimethylformamide (N,N-DMF) containing $Mg(ClO_4)_2$ was studied in this fashion.

The voltage-current relationships (Table 32) measured for 1 and 2M N_2O_4 in 10% $Mg(ClO_4)_2$-acetonitrile at 0°C were identical, indicating polarization was probably mostly activation polarization. Tests of 2M N_2O_4 in saturated $Mg(ClO_4)_2$-DMF at 0°C and in 10% $Mg(ClO_4)_2$-DMF at 20°C are almost identical but show slightly higher polarization than 2M N_2O_4 in acetonitrile electrolyte. The perchlorate salted out at 0°C in DMF and the solution was bright blue, probably caused by a complex of N_2O_4 with DMF. Complexes of acetonitrile with N_2O_4 at low temperatures are known (ref. 16). Although no reference to the N_2O_4-DMF complex has been found in the literature, the changes in appearance of DMF on addition of N_2O_4, first, a complete discoloration of N_2O_4, second, a bright blue color, and third, the normal dark green color, indicate complex formation. The complex is probably present in greater concentration at 0°C than at 20°C. Since the discharge characteristics of the system are the same at 0 and 20°C, the presence of the complex probably does not affect activation polarization.

Electrolyte (10% $Mg(ClO_4)_2$-acetonitrile) containing no fuel or oxidant did not maintain 1 ma.

Current-voltage relationships for the reduction of N_2O_4 in anhydrous AN and DMF are presented in Figure 34 along with measurements conducted after the addition of successive increments of water.

It is apparent that electrodes do not polarize as rapidly in the AN - $Mg(ClO_4)_2$ electrolyte as in the N,N-DMF electrolyte, and that the AN is less affected by added water. Each increment of water added increased the molarity of the solution with respect to water by 1.1, so that the final run (6 vol-% H_2O) corresponded to about a 3M H_2O solution. This solution, when AN was used as solvent, decreased by about 10% in potential, while there was very little change in polarization. N,N-DMF, however, was more adversely affected by water.

Since N_2O_4 reacted rapidly with KSCN in either solvent, the choice of electrolyte for the N_2H_4 half cell is narrowed to $Mg(ClO_4)_2$. Some difficulty was recently encountered in the anodic oxidation of 1M N_2H_4 solution in either AN- or DMF-containing $Mg(ClO_4)_2$. Although the potentials of the half cells are as determined earlier, the current carrying capacities in recent experiments have been very low.

Table 32

CATHODIC POLARIZATION OF N_2O_4 ELECTRODES IN ORGANIC ELECTROLYTES

Current Density ma/cm²	Cathode Potential vs Ag/AgCl, $(CH_3)_4NCl$, AN or DMF, Volts			
	1M N_2O_4 in AN-10% $Mg(ClO_4)_2$ at 0°C	2M N_2O_4 in AN-10% $Mg(ClO_4)_2$ at 0°C	2M N_2O_4 in DMF-sat. $Mg(ClO_4)_2$ at 0°C	2M N_2O_4 in DMF-10% $Mg(ClO_4)_2$ at 20°C
0	1.16, 1.07	1.12, 1.02	1.24, 1.08	1.22, 1.07
1	1.09, 1.03	1.09, 0.94	1.22, 1.05	1.18, 1.07
3	1.07, 1.00	1.05, 0.90	1.17, 1.01	1.12, -
5	1.02, 0.97	1.02, 0.87	1.12, 0.96	1.07, 0.97
10	0.94, 0.90	0.93, -	1.00, 0.82	0.92, 0.80
20	0.79, 0.70	0.77, 0.64	- -	0.63, 0.53
25	- -	- -	0.54, 0.59	- -
50	0.48, 0.41	0.32, 0.24	-0.10,-0.11	-0.48,-0.56
75	- -	-0.01,-0.07	- -	- -0.81
100	- -0.29	- -1.68	-1.33,-1.57	-1.32,-1.32
200	-1.44 -1.58		- -	- -

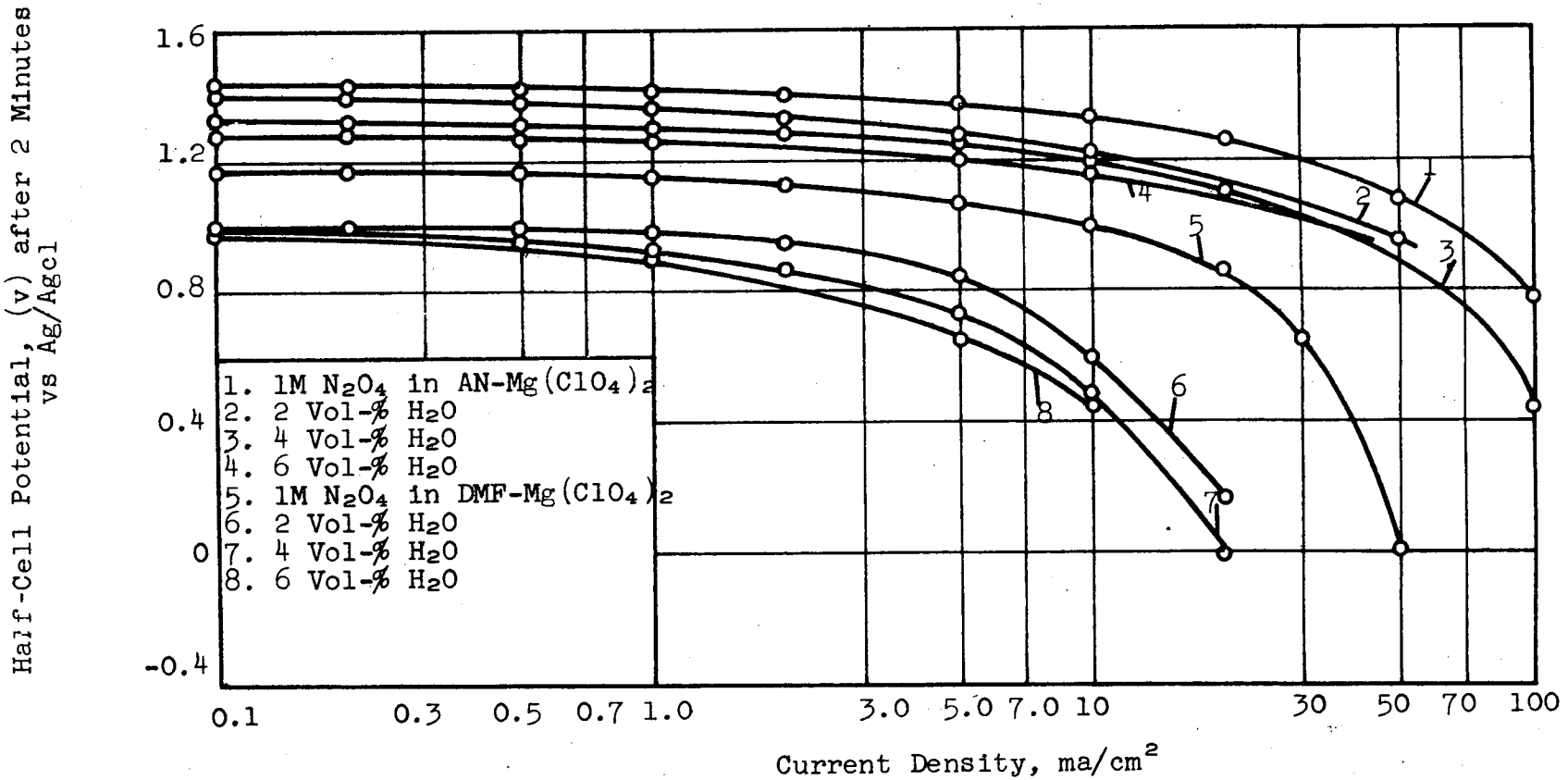

Figure 34. Cathodic Polarization of N_2O_4 Electrodes

VII. REFERENCES

1. Latimer, Wendell,M., Oxidation Potentials, 2nd Edition.

2. Lang, Norbert Adolph, Handbook of Chemistry, 8th Edition.

3. Scott, D.W., Oliver, G.D., Gross, M.E., Hubbard, W.N., and Huffman, H.M., J. Am. Chem. Soc., 71, 2293-97 (1949).

4. Hughes, A.M., Corruccini, R.J., and Gilbert, E.C., J. Am. Chem. Soc., 61, 2639-42.

5. Aston, J.G., Fink, H.L., Janz, G.L., and Russell, K.E., J. Am. Chem. Soc., 73, 1939-43 (1951).

6. Aston, J.G., Wood, J.L., and Zolki, T.P., J. Am. Chem. Soc., 75, 6202-04 (1953).

7. Donovan, T.M., Shomate, C.H., and McBride, W.R., J. Phys. Chem., 64, 281-2 (1960).

8. JANAF Thermochemical Data complied by Dow Chemical Co., Thermal Lab.

9. Hisatune, I.C, J. Phys. Chem., 65, 2249 (1961).

10. Kobe, K.P., Crawford, H.R., Pet. Ref. 37, 125 (1958).

11. Spencer, H.M., IandEC 40, 2154, (1948).

12. Perry, J.H., Chemical Engineers Handbook, 3rd Edition, McGraw-Hill (1950).

12a. Glasstone, S., "Electrochemistry" D. Van Nostrand (1942) 209.

13. Englehard Industries, Inc., "Fuel Cell Catalysts," Third Quarterly Jan-March 1963, Contract No. DA 36-039-SC-90691, U.S. Army Electronics R and D Lab.

14. Yost, D.M., and Russell, H., Jr., "Systematic Inorganic Chemistry," Prentice-Hall, Inc., New York (1944) 16.

15. Latimer, W. and Hildebrand, J.H., "Reference Book of Inorganic Chemistry," 3rd Edition, The Macmillian Co., New York (1951) 207.

16. Monsanto Research Corporation, "Compact Power Fuel Cell," Technical Document Report No. ASD-TDR-62-42, Jan. 1962, Flight Accessories Laboratory Contract No. AF 33(616)-7735.

REFERENCES (cont'd)

17. Quarterly Report No. 1, "Study of Fuel Cells Using Storable Rocket Propellants," 28 June to 28 September 1963, Contract NAS3-2791.

18. Sidwick, N.V., "Organic Chemistry of Nitrogen," Oxford Press, 1942, 451.

19. McBride, W.R., Henry, R.A, and Skolnik, S., Analytical Chemist 25, 1043 (1953).

20. Cady, G.H., J. Am. Chem. Soc., 56, 1431-1434 (1934).

20a. Jet Propulsion Laboratory, Technical Report No. 32-305, California Inst. of Tech., Pasadena, California, 15 May 1963.

21. Ives, D.J.G., and Janz, G.J., "Reference Electrodes," Academic Press (1961).

22. Addison, C.C., and Sheldon, J.C., J. Chem. Soc., 1956, 1941.

23. Kordesch, K. and Marko, A., J. Elect. Soc., 107, 480-483 (1960).

24. Rogers, M.T., Speirs, J.L. and Panish M.B., J. Phys. Chem., 61, 366 (1957).

25. Fredenhagen, K., and Candenbach, G., Z. physik chem. Abt A, 146, 245-80 (1930).

26. Jacke, A.W., Dissertation, Doctor of Philosophy, University of Washington (1952).

27. Koerber, G.G., and Devries, T., J. Am. Chem. Soc., 74, 5008-5011 (1952).

28. Smith, D.P., "Hydrogen in Metals," University of Chicago Press (1948)

29. Hoare, J.P., and Schuldiner, J., J. Phys. Chem., 61, 399 (1957).

30. Oswin, H.G., and Codosh, S.M., Preprint, Vol. 7, No. 4, Symposium on Fuel Cells, American Chemical Society, September 8-13 (1963).

31. Flanagan, B., and Lewis, F.A., Trans. Faraday Soc,, 55, 1400 (1959).

32. Ives, D.J.G., and Janz, G.L., Reference Electrodes, Academic Press (1961).

33. Robinson, C. S., and Gilliland, E. R., "Elements of Fractional Distillation", 56-59, McGraw-Hill (1950).

VIII. APPENDIXES

A. AQUEOUS SYSTEMS

1. Thermodynamic Sample Calculations

a. Free Energy of Formation of Liquid Hydrazine

$\Delta F^\circ_{f\ liq} = \Delta F^\circ_{f}$ gas at 14.35 mm i.e., vapor pressure of hydrazine at 298°K = 14.35 mm

$$\Delta F^\circ_{f\ gas\ 1\ atm} - \Delta F^\circ_{f\ gas\ 14.35\ mm} = \Delta H \Big|_{14.35\ mm}^{760\ mm} - T\Delta S \Big|_{14.35}^{760}$$

$$\Delta H = T\Delta S + \int_{14.35}^{760} V dp$$

$$\text{so, } \Delta F_{14.35}^{760} = \int_{14.35}^{760} V dp = RT \ln \frac{760}{14.35} = 2.35 \text{ Kcal/mole}$$

$\Delta F^\circ_{f\ gas\ 1\ atm} = 37.89$, so $\Delta F^\circ_{f\ liq} = \Delta F^\circ_{f\ gas\ 14.35\ mm} =$

$37.89 - 2.35 = 35.54$ Kcal/mole

b. Heat of Formation from Heat of Combustion

Monomethylhydrazine

$CH_3NHNH_2 + 5/2\ O_2 \longrightarrow N_2 + 3H_2O + CO_2$ $\Delta H_R = -311.711$ Kcal

$3H_2O \longrightarrow 3H_2 + 3/2\ O_2$ $\Delta H_R = 204.948$ Kcal

$CO_2 \longrightarrow C + O_2$ $\Delta H_R = 94.060$ Kcal

Overall

$N_2 + 3H_2 + C = CH_3NHNH_2$ $\Delta H_{f\ liq} = 12.703$ K cal/mole

$\Delta H^\circ_{f\ gas} = \Delta H^\circ_{f\ liq} + \text{latent heat} = 12.703 + 9.648 = 21.351$ K cal

c. Free Energy of Formation of Gaseous Monomethylhydrazine at 1 atm and 298°K

$\Delta F_f^\circ = \Delta H_f^\circ - T\Delta S$

$C + 3H_2 + N_2 \longrightarrow CH_3NHNH_2$

Entropy change = $\Delta S = 66.61 - 1.36 - 93.62 - 45.76 = -74.13$ cal/deg mole

$$\Delta F_{f\ gas}^\circ = \Delta H_f^\circ - T\Delta S = 21.351 - \frac{(298)(-74.13)}{1000} = 43.441 \text{ Kcal/mole}$$

d. Full-Cell Voltage

$2N_2H_4 \longrightarrow 2N_2 + 8H^+ + 8e^-$

$N_2O_4 + 8H^+ + 8e^- \longrightarrow N_2 + 4H_2O$

Overall reaction involves $8e^-$

$2N_2H_4 + N_2O_4 \longrightarrow 3N_2 + 4H_2O$

Mol wt = 2(32) + 92 = 156 grams

Reaction ΔF: $2(35.54) + 23.491 = 3(0) + 4(-56.69) - \Delta F$ cell

ΔF cell $= -226.76 - 23.49 - 71.08 = -321.33$ Kcal $= -1{,}334{,}766$ joules

$-1{,}334{,}766$ joules $= -nFE$, n = 8, so $E = \frac{1{,}334{,}766}{8 \times 96{,}500} = 1.74$ volts

$$\Delta F_{per\ gram} = 321.33 / 156 = 2.06 \frac{\text{Kcal}}{\text{g}} = 1086.5 \frac{\text{watt-hr}}{\text{lb}}$$

e. ΔH_{f363}, S_{363}, ΔF_{f363} of Dinitrogen Tetroxide

Specific Heat of Dinitrogen Tetroxide

C_p, cal/deg/mole	T°, K
15.72	300
16.60	350
17.39	400

These data are assumed fitted by $C_p = a + bT + cT^2$

so,

$$15.72 = a + 300b + 9 \times 10^4 c$$

$$16.60 = a + 350b + 12.25 \times 10^4 c$$

$$17.39 = a + 400b + 16 \times 10^4 c$$

Solving for a, b, and c gives:

$$C_p = 8.55 + 2.93 \times 10^{-2}T - 0.18 \times 10^{-4}T^2$$

$$(H_{363}-H_{298})_{N_2O_4} = \int_{298}^{363} C_p dT = 8.55T + \frac{2.93}{2} \times 10^{-2} T^2 - \frac{0.18}{3} \times 10^{-4} T^3 \Big|_{298}^{363}$$

$$= 1{,}054 \text{ cal/mole} = 1.054 \text{ Kcal/mole}$$

$$2 \times (H_{363}-H_{298})_{O_2} = 0.921 \text{ Kcal}$$

$$(H_{363}-H_{298})_{N_2} = 0.453 \text{ Kcal}$$

Therefore,

$$\Delta H_f)_{363} - \Delta H_f)_{298} = \Sigma n(H_{363}-H_{298}) = -0.321 \text{ Kcal}$$

so,

$$\Delta H_{f_{363}} = 2.309 - 0.321 = 1.988 \text{ Kcal/mol}$$

$$S_T = S_{298} + \int_{298}^{363} \frac{C_p dT}{T} = 72.73 + \left[8.55 \ln T + 2.93 \times 10^{-2}T - \frac{0.18}{2} \times 10^{-4}T^2 \right]_{298}^{T}$$

$$= 16.0877 + 8.55 \ln T + 2.93 \times 10^{-2}T - 0.09 \times 10^{-4}T^2$$

$$S_{363} = 75.9348$$

$$F_{363}-F_{298} = -\int_{298}^{363} SdT = -\left[16.0877T + 8.55\{T\ln T - T\} + 1.465 \times 10^{-2}T^2 - 0.3 \times 10^{4}T^3\right]_{298}^{363} = -4.830 \text{ Kcal}$$

$$\Delta F_f)_{363} = \Delta F_f)_{298} + (F_{363}-F_{298})_{N_2O_4} - (F_{363}-F_{298})_{N_2+2O_2} = 28.146$$

f. Internal Consistency: Sample Calculation for H_2O at 90°C

(1) Between Products and Reactants

$$\Delta F_f = \Delta H_f - T\Delta S_f \quad \text{or} \quad T\Delta S = \Delta H_f - \Delta F_f$$

$$\Delta S_f = S_{H_2O \text{ gas}} - 1/2S_{O_2} - S_{H_2} = -11.005 \text{ cal/deg/mole}$$

since 90°C = 363.16°K $T\Delta S = \frac{-11.005 \times 363.16}{1000} = -3.996$ kcal/mole

$\Delta H_f = -57.929$

$-\Delta F_f = 53.933$

so $\Delta H_f - \Delta F_f = -3.996$ check of $T\Delta S$

(2) Between Gas and Liquid Phase

$F_{liq}-F_{gas} = \Delta F_{f\ liq} - \Delta F_{f\ gas}$ $\Delta F = -.263$ Kcal/mole

likewise

$T\Delta S = \Delta H - \Delta F = -9.552$

$\Delta S = -26.296$ cal/deg/mole

$T\Delta S = \frac{-26.296 \times 363.16}{1000} = -9.550$ Kcal/mole

g. Calculation of Free Energy Loss Due to Solution of N_2H_4 in H_2O

(1) Calculation of Activity Coefficients

Assumption: vapor phases behave ideally

Equations:

$$p_a = \gamma_a x_a P_a \qquad (1)$$

$$\ln\gamma_a = \frac{C_a}{\left[1 + \frac{C_a x_a}{C_a x_b}\right]^z}, \quad \ln\gamma_b = \frac{C_b}{\left[1 + \frac{C_a x_b}{C_a x_a}\right]^z} \qquad (2)$$

These are the Van Laar equations. (ref. 33)

$$T\ln\gamma = \text{constant} \qquad (3)$$

This is the Gilliland equation (ref. 33)

Symbols:

p = partial pressure
P = vapor pressure of the pure liquid
γ = activity coefficient
x = mole fraction in the liquid
T = absolute temperature
C = constant
a = N_2H_4
b = H_2O

The activity coefficients are easily obtained from azeotropic data. Knowledge of these coefficients then permits calculation of the constants in the Van Laar equations.

Calculation:

At 560 mm and 111°C the azeotrope is $x_{N_2H_4} = x_a = 0.55$

$P_a = 720$ mm

$P_b = 111$ mm

$$\gamma_a = \frac{0.55 \times 560}{0.55 \times 720} = 0.78$$

$$\gamma_b = \frac{560}{1111} = 0.505$$

Substituting in the Van Laar equation

$$\ln 0.78 = \frac{C_a}{[1 + 1.22\ C_a/C_b]^2}$$

$$\ln 0.505 = \frac{C_a}{[1 + 0.85\ C_b/C_a]^2}$$

Solving the equation: $C_a = -2.94$

$C_b = -1.36$

85 wt-% hydrazine hydrate is 54.5 wt-% N_2H_4

$$\frac{x_{N_2H_4}}{x_{H_2O}} = \frac{x_a}{x_b} = \frac{54.5}{32} \times \frac{18}{44.5} = 0.69$$

$$\therefore \ln\gamma_a = \frac{-2.94}{[1 + (2)(0.69)]^2} \qquad \gamma_a = 0.595 \text{ at } x_a = 0.69 \text{ at } 111°C$$

$$\ln\gamma_b = \frac{-1.36}{[1 + (0.5)(1.45)]^2} \qquad \gamma_b = 0.633 \text{ at } x_b = 0.45 \text{ at } 111°C$$

at 90°C = 363°K = T

$$\ln\gamma_{90°} = \frac{384}{363}\ \ln\gamma_{111°C} \qquad \text{[see equation (3)]}$$

So, at 90°C: $\gamma_a = 0.577$

$\gamma_b = 0.617$

$P_a = 330$ mm

$P_b = 526$ mm

$$p_a = 0.577 \left(\frac{0.69}{1.69}\right) \quad 330 = 78 \text{ mm}$$

$$p_b = 0.617 \left(\frac{1.45}{2.45}\right) \quad 526 = 192 \text{ mm}$$

(2) Calculation of Free Energy Loss

This information can now be used to calculate the free energy difference between pure hydrazine liquid at 90°C and 330 mm, and the 85% hydrate at 90°C and $p_{N_2H_4}$ = 78 mm.

$$F_{78mm} - F_{330mm} - \int_{330}^{78} vdp = RT \ln\left(\frac{78}{330}\right) \qquad (4)$$

$$= 1.987 \times 363 \times (-1.442)$$

$$= -1{,}040 \text{ cal} = -1.04 \text{ Kcal}$$

This free energy loss represents loss in electrical potential.

$$\% \text{ decrease} = \frac{1.04 \times 100}{135.5} = 0.77\%$$

h. Calculation of Free Energy Loss Due to Dissociation of N_2O_4

$$N_2O_4 \rightleftharpoons 2NO_2$$

$$\Delta F = \mu_{NO_2} - \mu_{N_2O_4}$$

where μ is free energy per mole

$$\mu_{N_2O_4} = \mu^{\circ}_{N_2O_4} + RT\ln P_{N_2O_4}$$

$$\mu_{NO_2} = \mu^{\circ}_{NO_2} + RT\ln P_{NO_2}$$

Let x = fraction of one mole of N_2O_4 that dissociates.

Then: 1 - x = moles N_2O_4
2x = moles NO_2
1 + x = total moles

Assume total pressure = 1 atmosphere

$$P_{N_2O_4} = \frac{1 - x}{1 + x}$$

$$P_{NO_2} = \frac{2x}{1 + x}$$

$$K_{eq} = \frac{(P_{NO_2})^2}{P_{N_2O_4}} = \frac{4\,x^2}{1 - x^2} = 8.9 \text{ (from Figure 1)}$$

$$12.9x^2 = 8.9$$

$$x = 0.831$$

$$P_{N_2O_4} = \frac{1 - x}{1 + x} = 0.0923 \text{ atm}$$

$$P_{NO_2} = \frac{2x}{1 + x} = 0.9077 \text{ atm}$$

$$-\Delta F^\circ = RT\ln K_{atm} = (1.9872)(363)(\ln 8.9) = 1577 \text{ cal/mole}$$

What is free energy change for:

1 mole $N_2O_4 \longrightarrow 2x$ moles $NO_2 + (1-x)$ moles N_2O_4 at 90°C.

$$\Delta F = (1-x)\mu_{N_2O_4} + 2x\mu_{NO_2} - \mu^\circ_{N_2O_4}$$

$$\Delta F = x\Delta F^\circ + 2xRT\ln P_{NO_2} + (1-x)RT\ln P_{N_2O_4}$$

$$= 0.831(-1577) + (1.662)(1.9872)(363)(-0.097) + (0.169)(1.9872)(363)(-2.39)$$

$$= -1310 - 116 - 291$$

$$= -1717 \text{ cal/mole} = -1.717 \text{ Kcal/mole at 90°C}$$

$$\% \text{ decrease in voltage} = \frac{1.72 \times 100}{135.5} = 1.27\%$$

i. <u>I^2R Loss Necessary to Sustain Cell Temperature</u>

Consider the electrochemical reaction:

$$N_2H_{4\,liq} + N_2O_{4\,gas} \longrightarrow N_2 + 2NO + 2H_2O_{gas}$$

Conditions: 90°C, 1 atm.

ΔH = -86.92 Kcal per 4 equivalents

ΔF = -135.61 Kcal per 4 equivalents

$-T\Delta S$ = -48.69 Kcal per 4 equivalents = 36% of ΔF

= -12.17 Kcal/per equivalent

If $-T\Delta S = I^2R$, what is R/cm^2 ?

Assume $I = 0.1 \text{ amp/cm}^2 = \frac{0.1 \text{ coulomb}}{\text{sec-cm}^2}$

$$\left(\frac{0.1 \text{ coulomb}}{\text{sec-cm}^2}\right)\cdot\left(\frac{1}{96{,}500}\ \frac{\text{eq}}{\text{coulomb}}\right)\cdot\left(12.17\ \frac{\text{Kcal}}{\text{eq}}\right)\cdot\left(4{,}186\ \frac{\text{watt sec}}{\text{Kcal}}\right)$$

$$= 0.0528\ \frac{\text{watt}}{\text{cm}^2}$$

$0.0528 = I^2R \qquad I^2=0.01$

$\therefore \quad R = 5.28\ \frac{\text{ohm}}{\text{cm}^2}$

j. Voltage Decrease and Heat Generated Due to Spontaneous Decomposition of Hydrazine at Catalyst Surface

Equation:

$$N_2H_4 \longrightarrow N_2 + 2H_2$$

$$\Delta H_{decomp} = \frac{-12.278 \text{ Kcal}}{4 \text{ equivalents}} = \frac{-3.07 \text{ Kcal}}{\text{equivalent}} \quad \text{(exotherm)}$$

The subsequent reaction is:

$$2H_2 + N_2O_4 \longrightarrow 2NO + 2H_2O_{gas} \quad \text{at 90°C and 1 atm}$$

$\Delta F_{H_2O} = 2(-53.933)$	$S_{H_2O} = 2(46.767)$
$\Delta F_{NO} = 2(20.527)$	$S_{NO} = 2(51.747)$
	$-S_{H_2} = -2(32.57)$
$-\Delta F_{N_2O_4} = -28.146$	$-S_{N_2O_4} = -75.935$

$\Delta F = -94.958\ \frac{\text{Kcal}}{4 \text{ eq.}} = -nFE \qquad T\Delta S = \frac{(55.95)(363.16)}{1000} =$

$20.319\ \frac{\text{Kcal}}{4 \text{ eq.}}$

$E = 1.03$ volts

The net endothermic heat effect/4 eq. $= T\Delta S + \Delta H = 20.319 - 12.278$

$= 8.041$ Kcal/4 eq.

$$\frac{T\Delta S + \Delta H_{decomp}}{\Delta F} = 8.467\%$$

$$\frac{0.1 \text{ coulomb}}{\text{sec cm}^2} \times \frac{1 \text{ equiv.}}{96{,}500 \text{ coulomb}} \times \frac{8.041 \text{ Kcal}}{4 \text{ equiv.}} \times \frac{4{,}186 \text{ watt sec}}{\text{Kcal}} = I^2R$$

$$0.00871 = I^2R$$

$$R = 0.871 \text{ ohms/cm}^2$$

$$\% \text{ Decrease in voltage} = \frac{1.47 - 1.03}{1.47} \times 100 = 29.9\%$$

2. Electrode Preparation

a. Electrochemically Plated Catalysts

The electrodes were solid 1/8-inch cylinders of the various base metals, tightly wrapped with Teflon tape. The bottom part was bared to expose a total area of 1 cm^2, which was plated according to the following procedures.

(1) Platinum

(a) On Carbon

Plate for 2 minutes at 30 ma/cm^2 with 3% chloroplatinic acid solution containing 0.3% lead acetate.

(b) On Stainless Steel (SS)

Pt/SS electrodes are now produced by first plating for 4 minutes at 5 ma/cm^2 with Rhodex plating solution, and then for 2 minutes at 20 ma/cm^2 with 3% chloroplatinic acid solution.

(c) On Nickel

Plate for 4 minutes at 5 ma/cm^2 with Rhodex plating solution, then plate for 2 minutes at 20 ma/cm^2 with the 3% chloroplatinic acid solution.

(2) Gold

(a) On Carbon

Plate for 2 minutes at 20 ma/cm^2 with the 3% gold chloride plating solution ($HAuCl_3 \cdot 3H_2O$).

(b) On Stainless Steel and Nickel

Plate for 4 minutes at 5 ma/cm^2 with Rhodex plating solution, and then for 2 minutes at 20 ma/cm^2 with 3% gold chloride solution.

(3) Rhodium

For all substrates plate for 4 minutes at 5 ma/cm^2 with Rhodex plating solution, and then for 2 minutes at 20 ma/cm^2 with the 0.1M rhodium plating solution.

b. Chemically Precipitated Catalyst Electrodes

Porous FC-14 carbon cubes 1/2 cm on an edge were used as the substrate upon which the catalyst was plated. The particular salts of the catalyst or catalyst combination were dissolved in distilled water at specific concentration as outlined in the following procedure:

1. The carbon cubes (uncatalyzed) were washed with distilled water and placed under reduced pressure in a vacuum oven at 80°C to dry.

2. Immediately the cubes were weighed on a precision analytical balance in the dry state.

3. The cubes were then impregnated with distilled water, under reduced pressure and a lot of 25 were weighed.

4. The number of ml of H_2O taken up by the cubes is calculated and from this value the catalyst-salt solution is prepared in such concentrations as to leave the required weight of catalyst black in the carbon cube. In some cases when salts have a limited solubility, two or more separate impregnations and reductions must be made.

5. The impregnated electrode was dropped in a 1% $NaBH_4$ solution, which rapidly reduced them to the metal.

6. The reduced electrode was dried at 80°C in a vacuum to remove water, and reduce any nonreduced catalyst. When dry the electrode was weighed to find the increase in weight due to catalyst. The per cent catalyst was then calculated.

The carbon cubes had a fine hole drilled in by the Pure Carbon Company, of the right size to make a force fit to a platinum wire which was used as the electrical contact lead.

c. Porous Teflon Vapor Electrodes Preparation

Figure A-1 shows the best method of construction found to date for the Teflon vapor electrode.

Item	Description
1.	Tantalum holder chosen for compatibility with reactants and electrolytes which are expected to be used.
2.	Teflon gasket 1 mil thick treated with sodium in liquid NH_3 to make it easily adhered to for reduction of side leakage.
3.	Electrolytically perforated 316 stainless steel plate 4 mils thick containing 65% open area, used to retain catalyst before impregnation, and as current collector for catalyst when in use.
4.	Catalyst powder plus 10% Teflon powder for binding purposes.
5.	Porous Teflon membrane.
6.	Coarse mesh tantalum screen used to impart mechanical stability and to prevent the porous Teflon from sticking to the stainless steel block used for applying pressure.
7.	Stainless steel block for pressure application.

Components 1, 2 and 3 are preformed at 10,000 psi pressure, using a stainless steel block with a raised die the same diameter as the exposed electrode surface. This forms a special pocket for catalyst to be contained. The catalyst is then evenly spread into this pocket, and components 5, 6 and 7 are put into place. A clean platinum plate is used in the press at the catalyst-stainless steel side of the electrode. The assembly is then pressed at a specific pressure and temperature for a specific time.

3. Experimental Apparatus

a. Half Cells

Three designs of half cell: A, B, and C, were used for the polarization studies. Type A was a general purpose cell (Figure A-2) for soluble or liquid reactants. Type B was a gas cell (Figure A-3) used when porous flow-through electrodes are desirable or required. Type C was used for porous Teflon vapor diffusion electrodes.

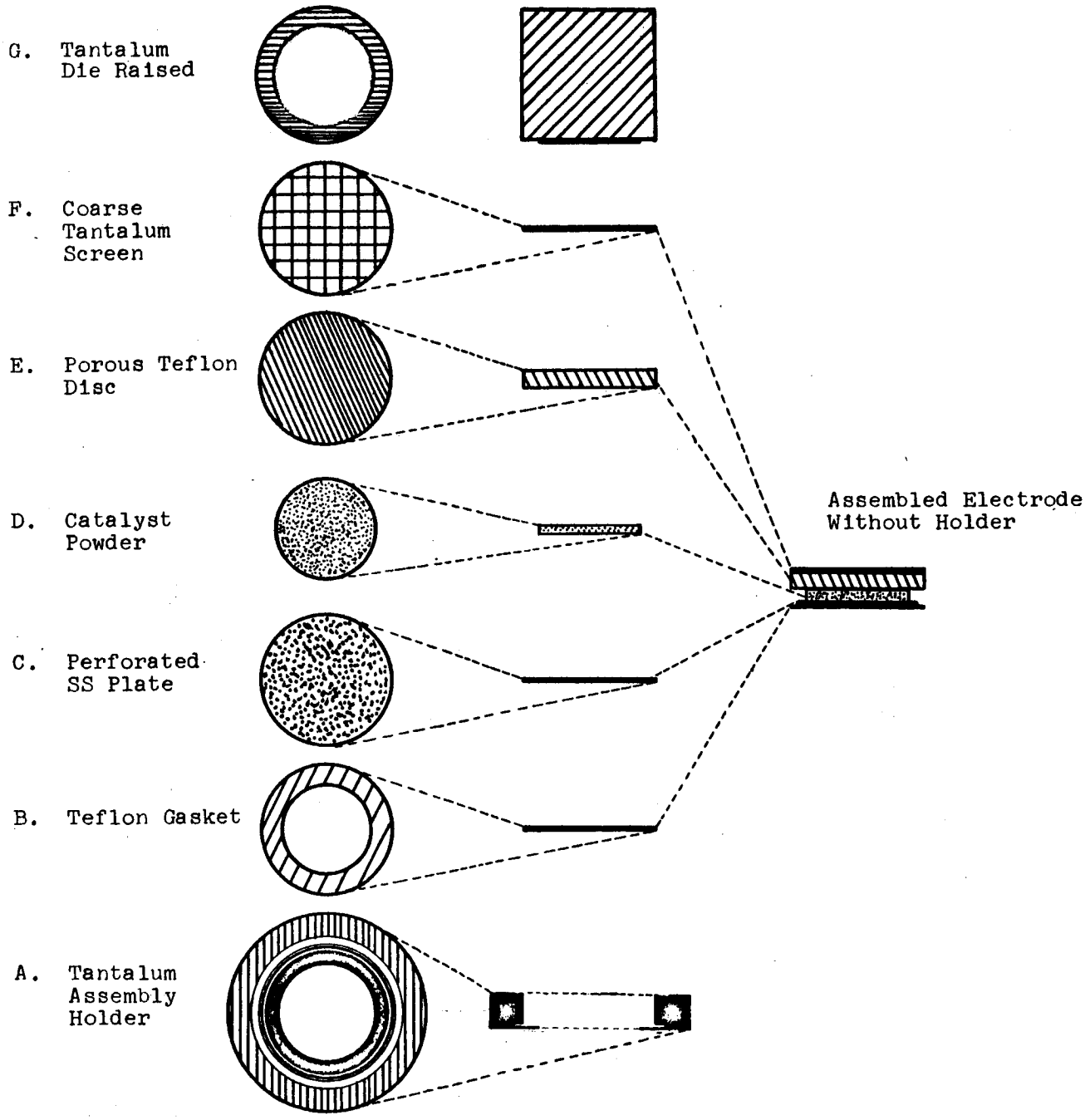

Figure A-1. Exploded View of Porous Teflon Vapor Diffusion Electrode

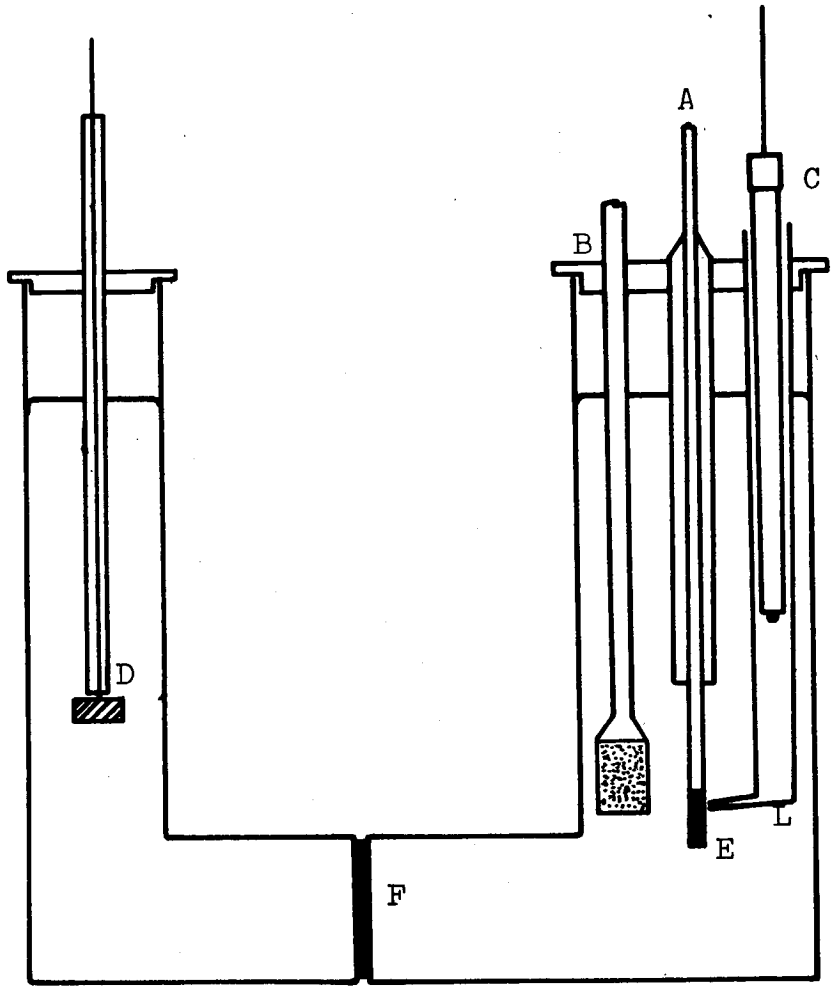

Figure A-2. H-Cell for Short Term Polarization Studies

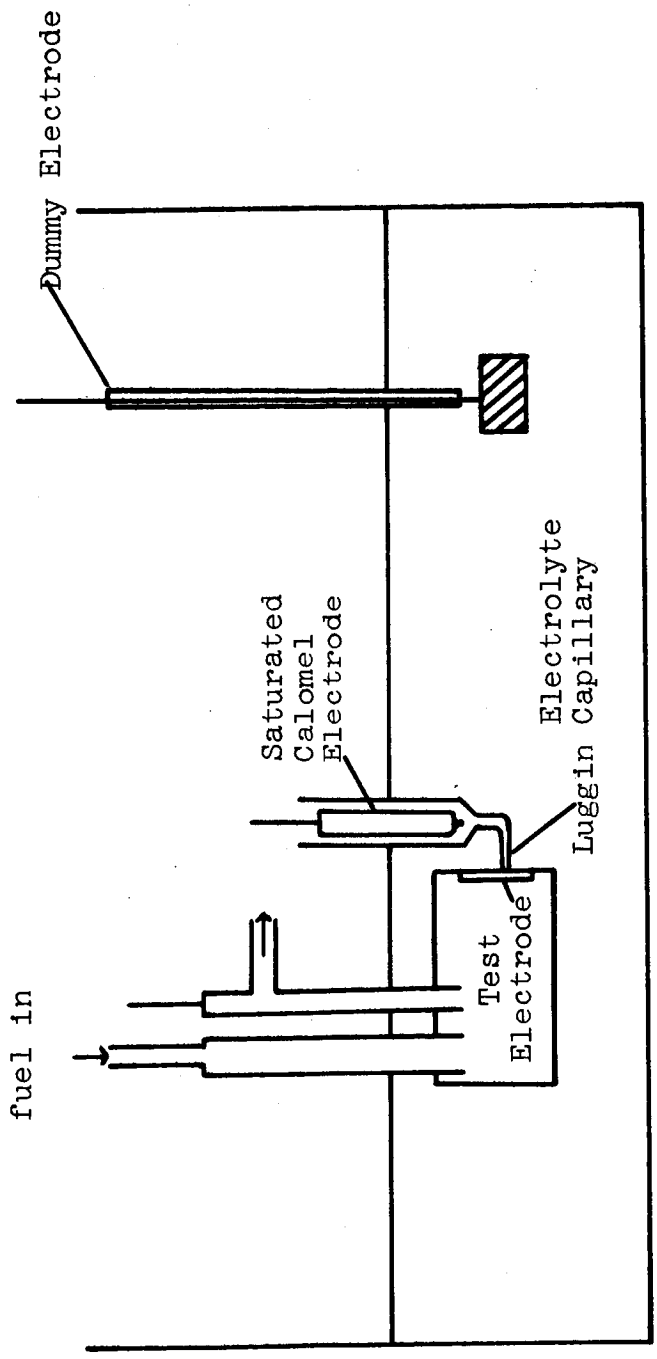

Figure A-3. Gas Half Cell

(1) Type A

Type A was a Pyrex H-cell with Teflon stoppers supporting the dummy electrode, D, the working electrode, E, and the Luggin capillary, L. A reference electrode (C) was immersed in the well above the Luggin capillary. A glass frit (F) prevented gross mixing between the anode and cathode compartments. Provisions (B) were made to stir and purge the system. The working electrode was a cylinder of the base material insulated with a tightly wrapped Teflon tape for most of its length. Both ends were bare; the top for making the electrical connection, the bottom for supporting the catalyst. The cells were immersed in a thermostatically controlled water bath. The cell was also used for tests with precipitated electrode catalyst.

(2) Type B

Type B cell consisted of a Teflon holder for the porous electrode, a Luggin capillary, L, and a dummy electrode, D. One side of the electrode faced the electrolyte; the other side was exposed to the gas stream (Figure A-3). The excess gas and the gaseous reaction products are exhausted through the gas outlet. The static pressure on the electrode gas side can be adjusted by a bypass valve (not shown). It is possible, then, to establish a balanced operation without flooding the electrode or bubbling the gas through it.

Figure A-4 shows the construction details of the electrode holder.

(3) Type C

Figure A-5 shows system used for testing of half-cell porous Teflon vapor electrodes. It features separate glass compartments for fuel or oxidant in the pure state, and for the electrolyte used. Between the two compartments, and connecting them is the tantalum holder into which is built the Teflon vapor electrode. A Kordesch-Marko bridge is always used with this particular system due to distance of Luggin from the test electrode.

b. Testing Apparatus

Three types of testing apparatus were used for half cell measurements, all manually operated.

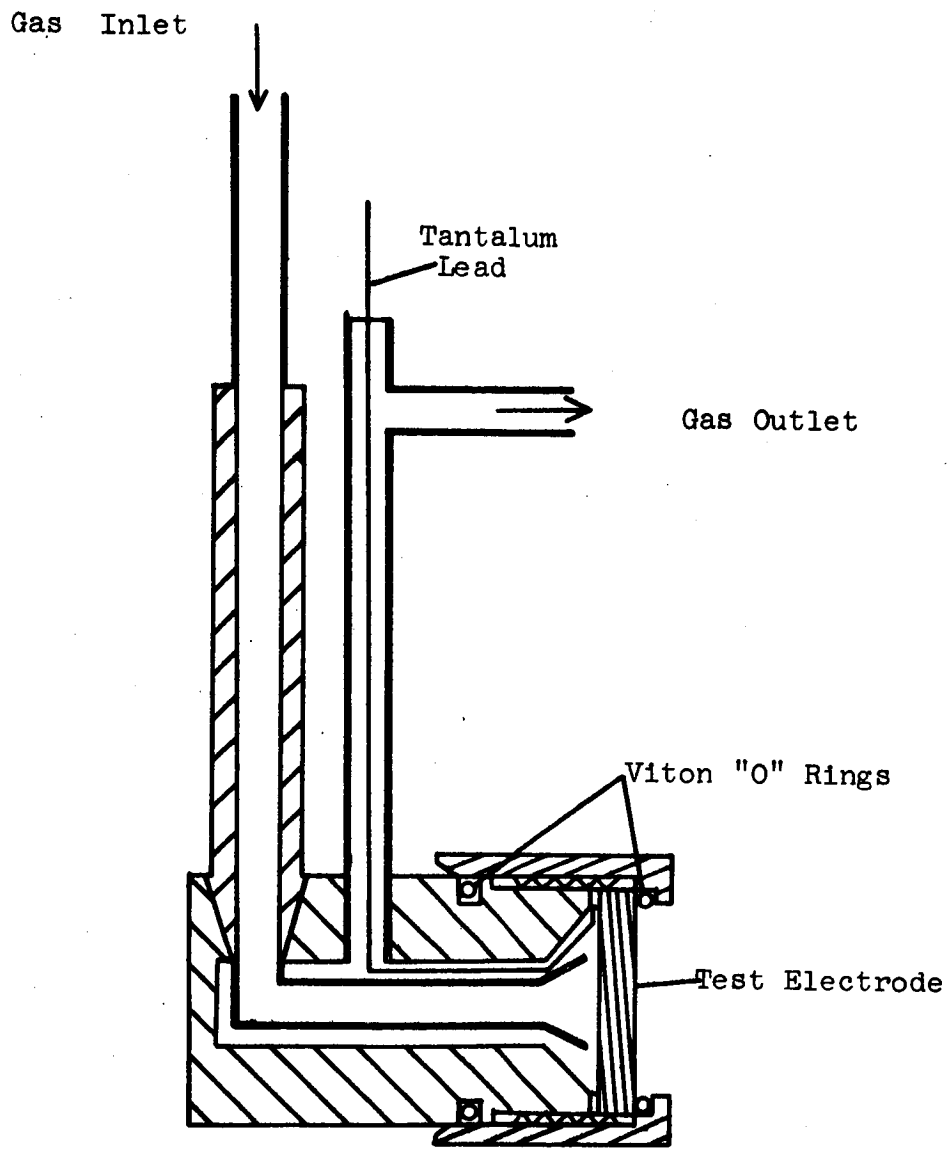

Figure A-4. All-Teflon Gas Cell Electrode Holder

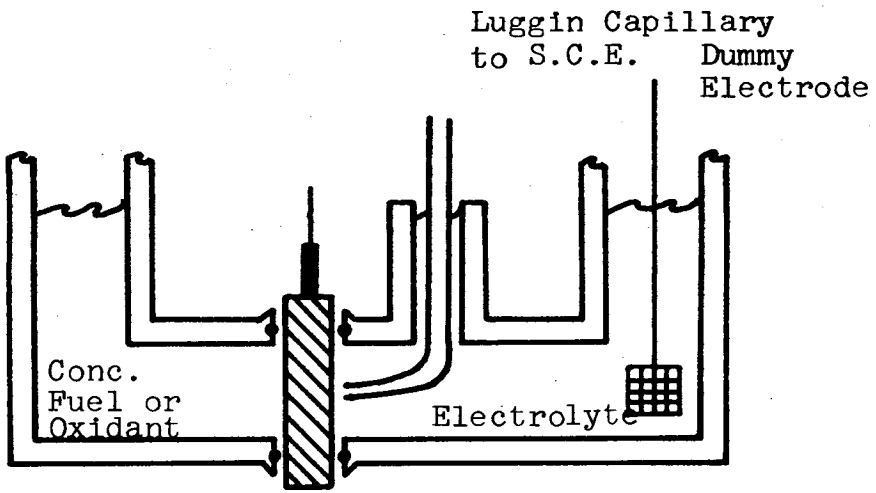

Figure A-5.- Half Cell Construction for Testing Porous Teflon Vapor Diffusion Electrodes

(1) Manual Apparatus

Figure A-6 is a schematic drawing of the manually operated device employed in half cell studies. The apparatus consisted of two five-decade resistance boxes and the relative switching circuits. The current through each of the two cells can be varied independently and accurately measured by a precision milliammeter. The potential vs the reference cells are measured with high resistance electrometers.

(2) Constant Current Programable Power Supply

The second method for half cell polarization tests was a Harrison Laboratories Model 6200A constant current power supply. It can deliver, over time ranges, up to 1.5 amperes with less than 0.5 ma ac ripple. It has a voltage output maximum of 40 volts up to 750 ma, and 20 volts on the 1.5-ampere ranges. In addition the instrument can be programed at the supply output with a 10-turn precision resistor, thus gaining very fine control of current in manual polarization tests.

(3) Kordesch-Marko (K-M) Bridge

Two of these instruments were built for use in polarization studies where IR drop might not be able to be easily eliminated by Luggin capillaries. The circuit diagram of the bridge in use in our laboratory is shown in Figure A-7. It is essentially a simplified version of the original bridge as reported in the Journal of Electrochemical Society by its developers (ref. 20).

4. Analytical Apparatus

There are three main features to the cell design and manifold system pictured in Figures A-8 and A-9. These are:

(1) Take-off for gas volume measurements.

(2) Take-off for gas sample collection, or direct connection to VPC.

(3) Take-off for liquid samples.

The main problem associated with these functions is maintaining an air-tight system. Volume is measured by collecting gas from the gas outlet tube, with the manifold set so that stopcock 1 diverts the gas to a volume measurement apparatus consisting of a graduated gas collection buret with water as the atmospheric balance. When a gas sample is to be collected, the gas inlet system sweeps

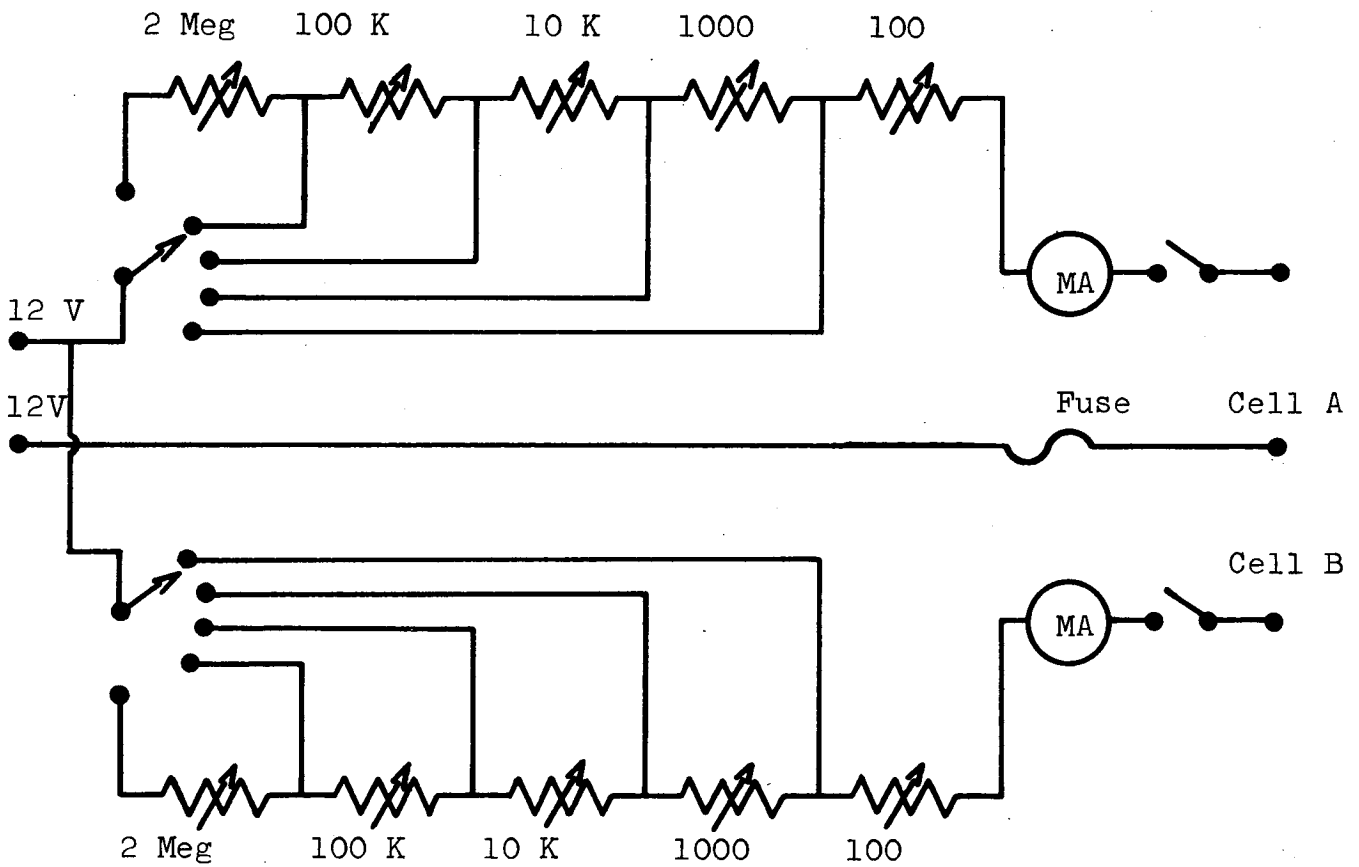

Figure A-6. Schematic of the Manually Operated Testing Apparatus

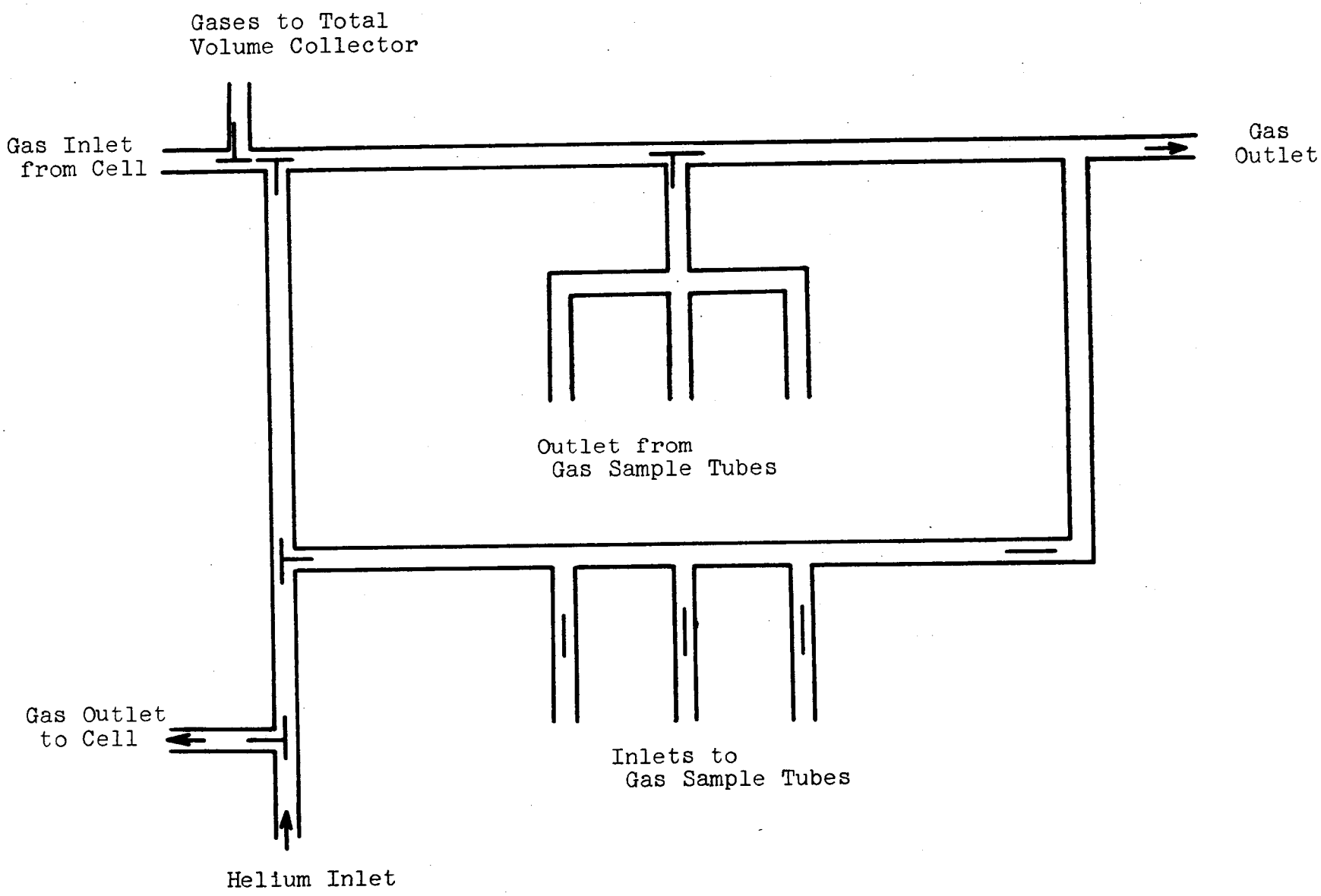

Figure A-9 Analytical Control System

helium at such a rate as to leave 10 to 50% of the product gas in the collection buret. The manifold is then set to allow gas to fill the gas sample tube. Liquid samples are obtained with a syringe through the rubber plug on the capillary tubing. At all times a slight positive pressure is kept on the cell, either by a helium sweep or with water pressure when volume measurements are being made. The manifold system also allows flushing of the cell and manifold system before starting test, and direct flushing of just the manifold system or individual gas sample tubes at any time without involving the cell. Also the VPC can be directly connected to the gas outlet on the manifold for continual monitoring of the gas produced.

The tops of the liquid sample capillary, the electrode, the calomel, and the Luggin capillary are sealed with pressure-sensitive Teflon tape. No air leaks have been detected, even with NO gas evolution, which would react to turn brown with oxygen. The dummy or counterelectrode is vented to the atmosphere to prevent pressure buildups from forcing material from the dummy to the test compartments. Some diffusion occurs in spite of this, and the dummy compartment solution is analyzed along with the test compartment solution.

The electrochemical features of the cell otherwise are the same as the H cell described in Figure A-2.

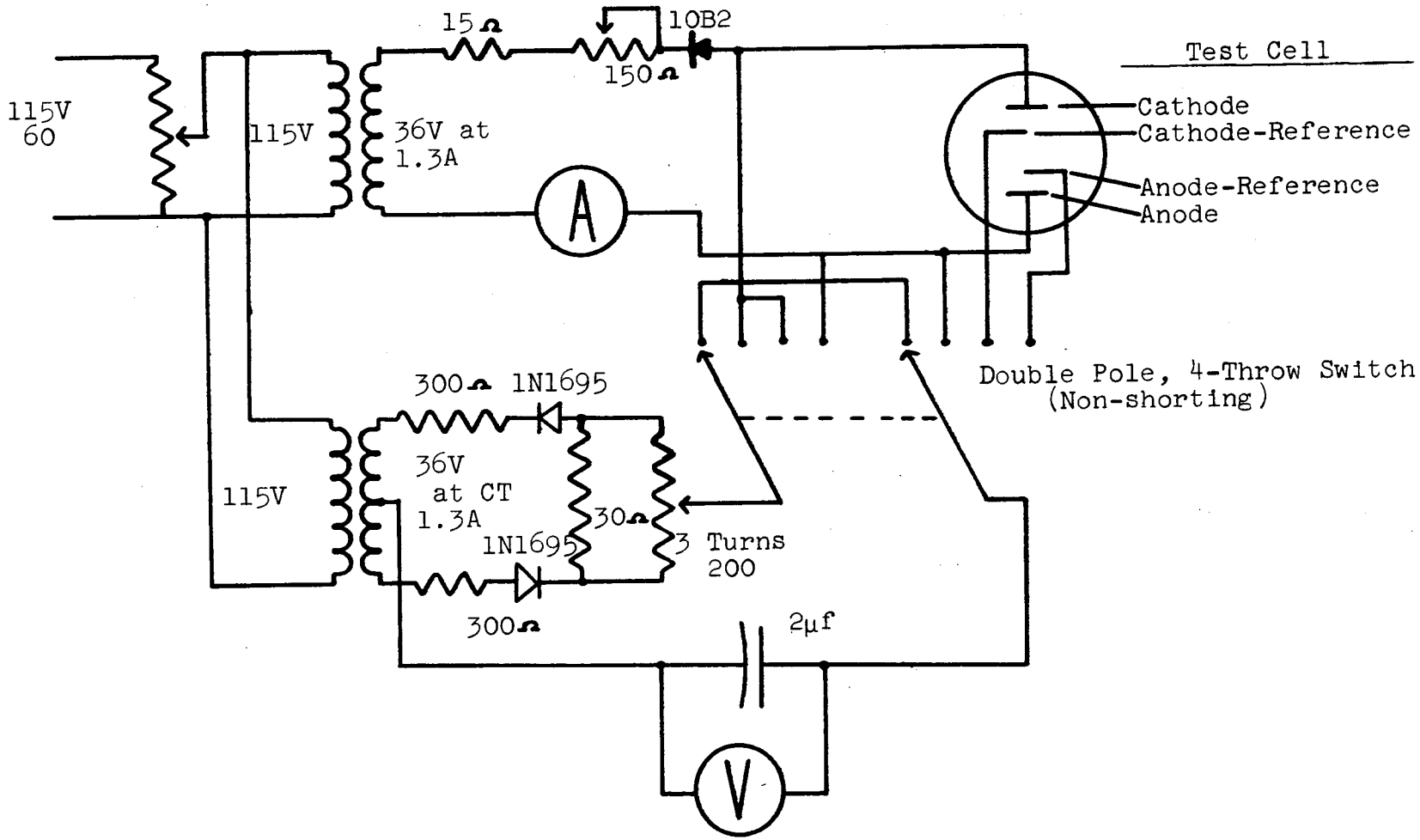

Figure A-7 Kordesch-Marko Bridge

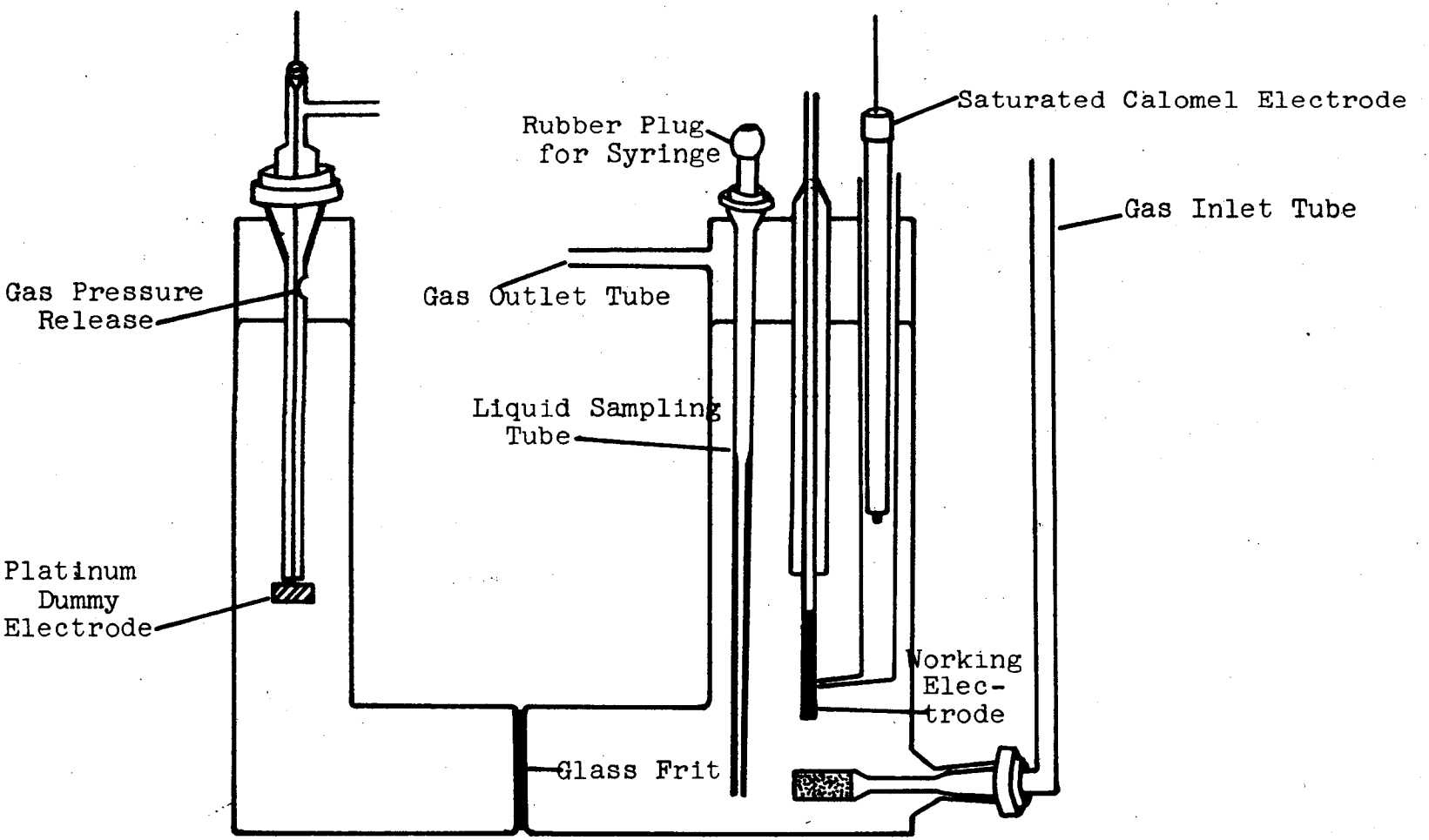

Figure A-8 Analytical Cell

B. ANHYDROUS HYDROGEN FLUORIDE SYSTEMS

1. Preparation of Solid Platinum Electrodes for Use in Fluoride Solutions

Rectangular electrodes, 0.5 cm by 1.0 cm, were cut from 0.005-cm thick platinum foil. A lead wire of 0.05-cm diameter platinum was spot welded to the foil. The foil was degreased in ethylene trichloride vapor and immersed in hot aqua regia until the surface had an etched appearance. After washing in distilled water, the foil was electroplated in one of the following solutions at 20 ma/cm^2 for 2 minutes for each side:

Catalyst	Plating Solution
Platinum	3% $H_2PtCl_6 \cdot 6H_2O$ with 0.03% $Pb(OAc)_2 \cdot 3H_2O$
Gold	3% $HAuCl_4 \cdot 3H_2O$
Rhodium	3% $RhCl_3 \cdot xH_2O$ (40% Rh)
Ruthenium	7% $RuCl_4 \cdot 5H_2O$ (41% Ru)
Iridium	3% $IrCl_4$ (48.3% Ir)

2. Preparation of Hydrazine Dihydrogen Fluoride

Anhydrous hydrazine (AH) reacted explosively with liquid anhydrous hydrogen fluoride (AHF) on direct mixing between -78 and 0°C. For this reason, the hydrazine dihydrogen fluoride (HDHF) salt, $N_2H_4 \cdot 2HF$, was prepared for solution in AHF.

HDHF was synthesized by slowly mixing stoichiometric quantities of the aqueous reactants at 0°C. Excess water was removed by vacuum pumping, and the solid was dried over concentrated sulfuric acid in a vacuum desiccator for three days. The solubility of HDHF in AHF was 2.09 molar at 0°C and 3.13 molar between 15 and 20°C. Long, needle-like crystals precipitated from the latter solution when it was cooled to 0°C. The HDHF salt dissolved smoothly in both AHF and in molten $KF \cdot 3HF$ for anodic polarization studies.

3. Chlorine Trifluoride Solutions in Anhydrous Hydrogen Fluoride

Solutions of CTF in AHF were prepared by direct mixing of the condensed liquids. The components were miscible in all proportions. CTF and AHF form an azeotropic mixture at about 65 mole-% AHF. (ref. 24). A 69% mole-% mixture of AHF in CTF had a vapor pressure of 645 mm Hg at 0°C.

Literature conductivity values are listed in Table 26 for the above system. These values compare very favorably with conductivities determined in our laboratory on an unrelated project.

The purity of the CTF was checked by comparing its vapor pressure to the theoretical value. The agreement was good.

Liquid hydrogen fluoride was used directly from commercial cylinders. CTF solutions in AHF are only slightly ionized ($HClF_4 = H^+ + ClF_4^-$), so salts such as sodium fluoride and potassium fluoride must be added to increase the conductivity. Solubilities of fluoride salts in AHF, given by Fredenhagen and Candenbach (ref. 25) and Jacke (ref. 26) are given in Table 33.

Table 33

SOLUBILITIES IN LIQUID HYDROGEN FLUORIDE

Salt	Solubility g salt/100 g HF	Temperature °C	Reference
LiF	10.33	12.2	26
	10.31	-3.3	
	10.30	-23.0	
NaF	30.1	11.0	26
	25.1	-9.8	
	22.1	-24.3	
KF	38	0	25
Hg_2F_2	0.877	11.8	26
	0.811	-4.5	
	0.789	-22.5	

4. Constant Current Polarization Sequence

The polarization sequence was (1) to record the open-circuit potential of the working electrode vs the $Pb-PbF_2$ reference, (2) to polarize for two minutes (either anodically or cathodically) and to record the polarized potential, (3) to allow the cell to remain on open-circuit for one minute, and (4) then proceed with the next polarization at twice the current density of the previous polarization. This schedule was repeated until a polarization in excess of 0.5 volt from the original open-circuit potential occurred.

5. Reference Electrodes in Anhydrous Hydrogen Fluoride

When conducting electrode polarizing experiments by the half cell method, a stable and reproducible unpolarized electrode is required as a reference potential plateau. Koeber and DeVries (ref. 27) have demonstrated the silver, cadmium, and lead fluoride systems in anhydrous hydrogen fluoride (AHF). These electrodes, prepared by anodizing each of the metals in AHF, were used as references as was the hydrogen electrode.

a. Silver-Silver Fluoride Reference Electrode

A silver-silver fluoride reference electrode was prepared by anodizing a clean silver wire in a solution of 0.5M NaF in AHF at a current density of 12 ma/cm^2 for 5 minutes. Diffusion of oxidizing or reducing materials into the reference electrode compartment was minimized by enclosing the electrode in a Teflon tube with a 0.01-inch hole for solution contact with the working electrode. Two electrodes prepared by this procedure had potentials within 5 mv of each other. After momentary cathodic or anodic polarization at 0.1 ma/cm^2, the electrodes returned to their original open-circuit potentials.

b. Cadmium-Cadmium Fluoride Reference Electrode

Cadmium-cadmium fluoride reference electrodes were prepared by a similar anodizing procedure, starting with the clean stick of cadmium metal. Since cadmium is the more active metal, it is preferred to silver as a reference electrode. Unlike silver ion, traces of cadmium ion that might diffuse to a hydrazine electrode would not be reduced and the electrode surface would be altered. Potentials of the above electrodes, compared with that of a hydrogen electrode in AHF are given in Table 34.

Table 34

POTENTIALS OF REFERENCE ELECTRODES IN ANHYDROUS HYDROGEN FLUORIDE 0.5 M IN NaF AT 3°C

Electrode	Potential, Volts	
	Assigned	Experimental
Hydrogen at Rhodinized Platinum	0.00	-
Cd/CdF_2	-	-0.50
Ag/AgF	-	+0.05

c. Lead-Lead Fluoride Reference Electrode

In molten KF·3HF mixtures, the Pb-PbF_2 electrode was used as a working reference. In this case a length of pure lead wire was anodized at 12 ma/cm^2 for 5 minutes. After both anodic and cathodic polarization at 0.1 ma/cm^2, the potential of the fluorinated lead electrode returned to the same open-circuit value. The potential of the lead-lead fluoride electrode was measured against that of the hydrogen-rhodium-palladium electrode (see Table 35), and polarization data in the KF·3HF melt were reported with reference to the hydrogen electrode. Lead is an active metal in the AHF-KF melts and, like cadmium, will not be reduced at the hydrogen electrode potential.

Table 35

POTENTIALS OF REFERENCE ELECTRODES IN MOLTEN KF·3HF AT 85°C

Electrode	Potential, Volts	
	Assigned	Experimental
Hydrogen at Rhodinized Platinum	0.00	-
Pb/PbF_2 2½ HF	-	-0.32
Ag/AgF	-	-0.02

d. Hydrogen Reference Electrode

It is well known that palladium absorbs hydrogen until a saturation ratio of 0.69 atoms of hydrogen per atom of palladium is reached. At this concentration, the "gas-charged alloy" has the same potential as the platinized platinum electrode (ref. 28).

Two palladium electrodes were made by spot welding 0.001-inch palladium foil on platinum wire and mounting in a Teflon holder.

The potential of the hydrogen electrode in AHF solution in the AHF·KF melt was established by cathodically polarizing a palladium electrode at 5 ma/cm² for one hour and until the open-circuit potential of the electrode became steady. This steady hydrogen potential was recorded against a silver-silver fluoride and a cadmium-cadmium fluoride electrode. The metal reference electrodes were more convenient than the hydrogen electrode for polarization experiments, but polarization results are reported with reference to the hydrogen electrode in the AHF solution being investigated. Reference electrodes were separated from current-carrying electrodes by a porous Teflon disk with a 0.01-inch hole as shown in Figure 25.

5. Palladium Membrane Electrodes in Anhydrous Hydrogen Fluoride

Solid palladium is an interesting electrode material for use as a potential reference or for the anodic oxidation of hydrogen gas or materials that can be reformed into hydrogen, such as hydrazine. The palladium serves the dual role of a conducting electrode and a solid separator between the fuel and oxidant compartments. The use of palladium as a hydrogen electrode has been reported by Hoare and Schuldiner (ref. 29), and a palladium-hydrogen anode in aqueous solution has been described by Oswin and Chodosh (ref. 30).

A 0.001-inch thick palladium foil was electroplated with rhodium on both sides and mounted in a Teflon holder. The assembly was immersed in liquid AHF at 3°C and hydrogen gas was purged through the electrode gas compartment as shown in Figure A-10. The potential of the palladium electrode as a function of purging time is shown in Figure A-11. The potential dropped suddenly during the first minute's purging to a plateau. After an hour's purging, the potential decreased to 0.50 volt positive to the lead-lead fluoride electrode. This behavior is similar to that reported by Flanagan and Lewis (ref. 31). The initial potential plateau corresponds to a partial hydrogen saturation and the formation of an "alpha" palladium-hydrogen phase. After complete saturation the electrode assumes the same potential as the hydrogen-platinized platinum electrode (ref. 32). The hydrogen-palladium electrode is of interest in AHF solutions both as an anode candidate and as a reference electrode for assigning potentials to other electrode systems.

The anodic and cathodic polarizations of the hydrogen-saturated palladium electrode in AHF at 3°C are shown in Figure A-12. An anodic current of about 10 ma/cm^2 could be carried with 0.5 volt polarization, while cathodic currents up to 50 ma/cm^2 could be carried with very little polarization. The limiting anodic current was low at 3°C, but subsequent work will be concerned with improving the palladium membrane as a fuel cell component.

C. NEW TECHNOLOGY

The reportable items considered to have been developed during the term of the contract are as follows:

1. Method of fuel cell construction and operation using a porous Teflon electrode by which transmission of feedstocks to the catalytic electrode surface is limited to vapor phase. This development is described in the present Final Report. It is considered an invention: a patent disclosure has been submitted and a patent application is being prepared.

2. Method of heat transfer in which heat energy is absorbed from a low temperature (50-100°C) source by a fuel cell which operates with an endothermic electrochemical reaction, such as the electrochemical reaction of hydrazine with nitric acid or with dinitrogen tetroxide,

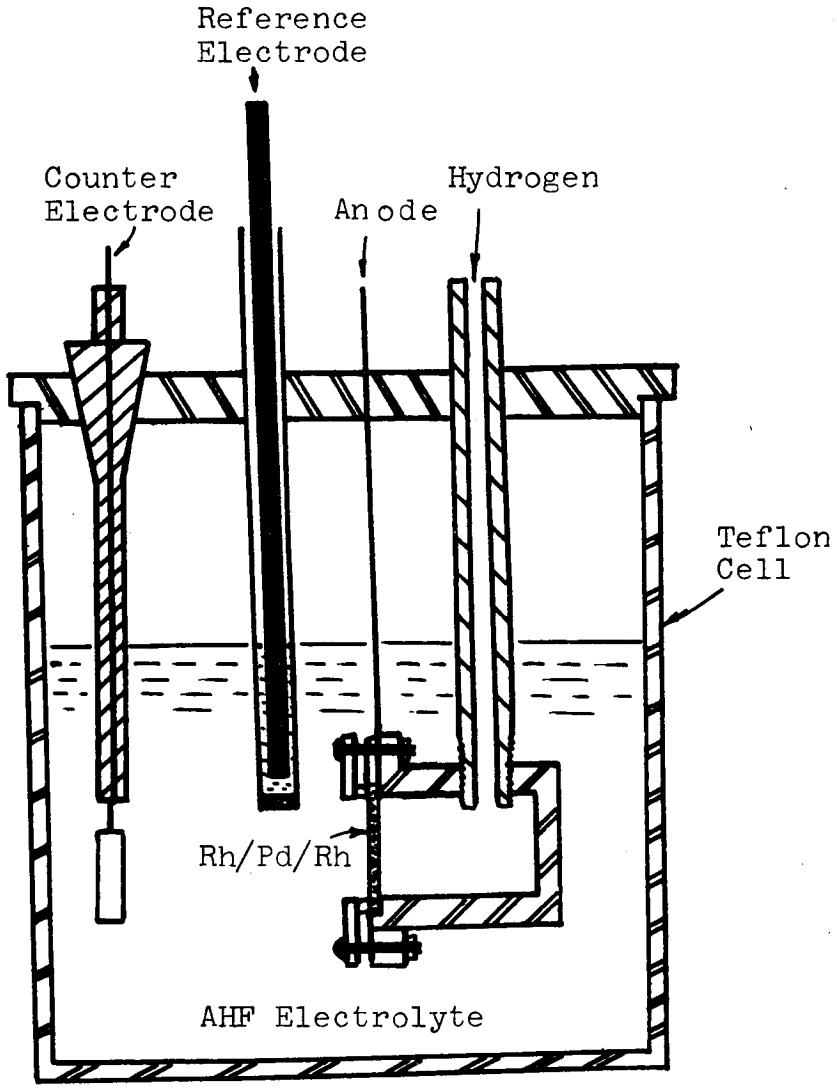

Figure A-10. Half Cell for Evaluating the Hydrogen-Palladium Anode in Anhydrous Hydrogen Fluoride

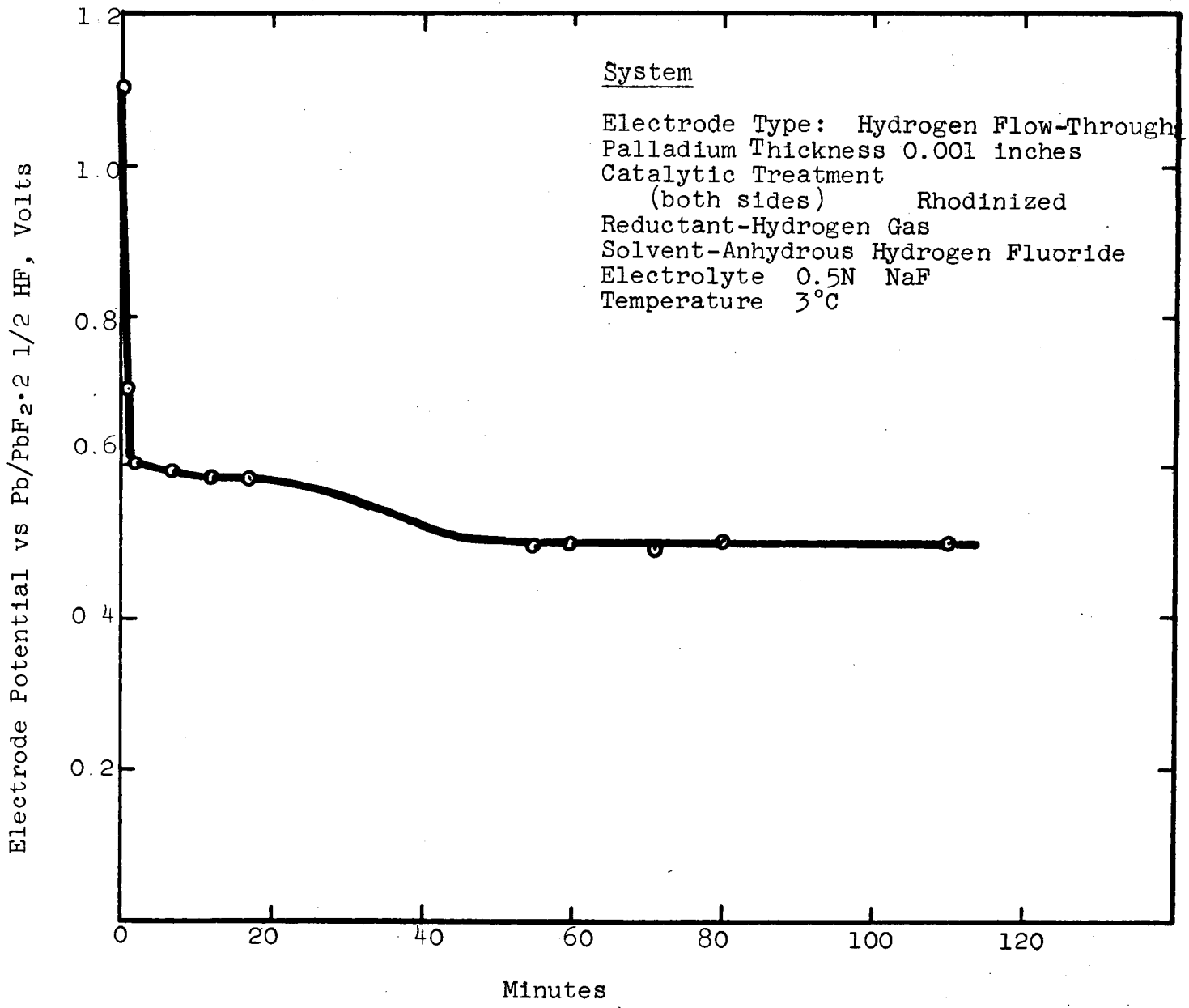

Figure A-11. Open-Circuit Potential of Rhodinized Palladium Electrolyte in Contact with Hydrogen Gas.

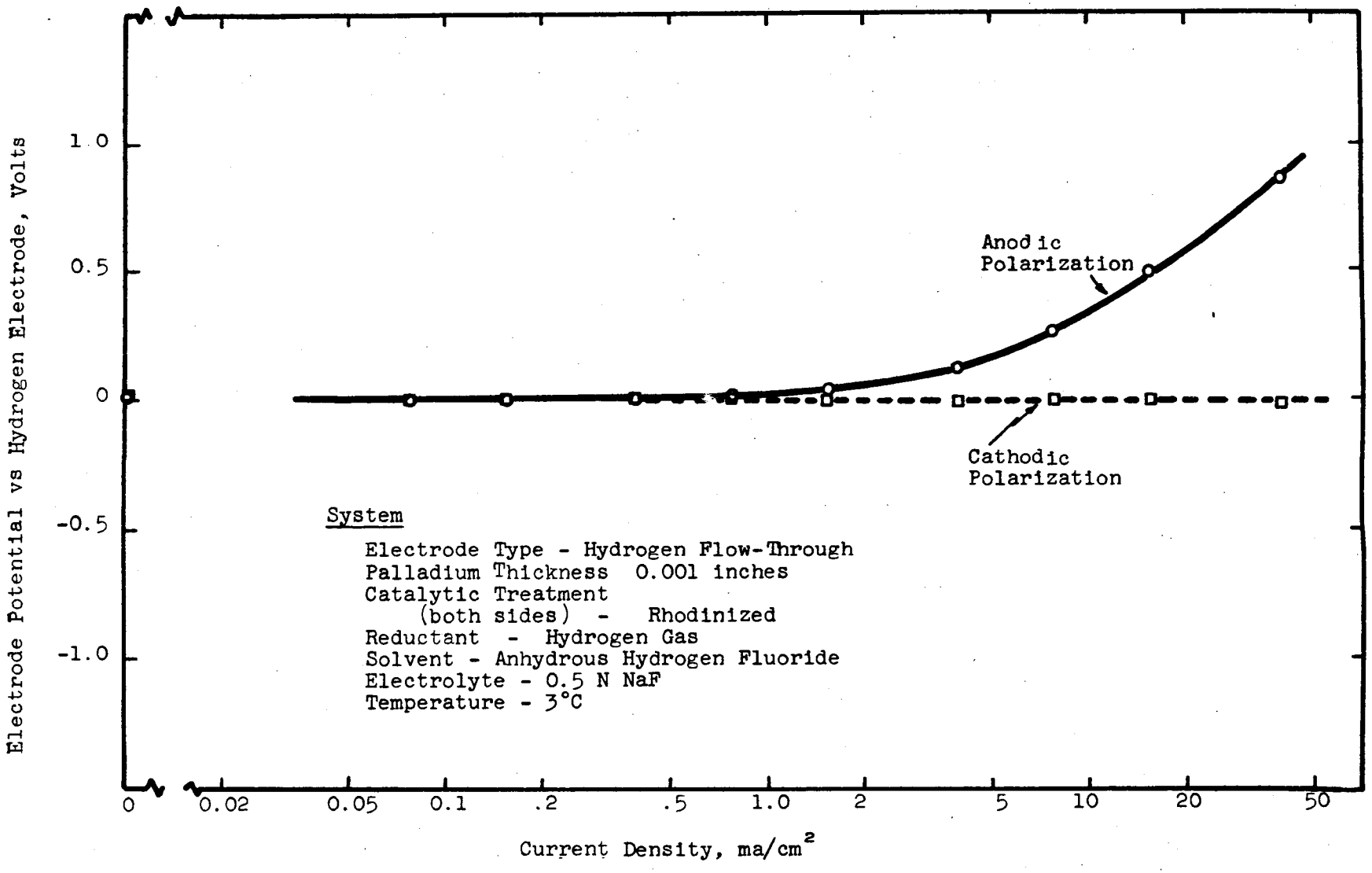

Figure A-12. Anodic and Cathodic Polarization of Palladium Hydrogen Electrode

and sending the electrical output of the cell through a resistor which radiates heat energy at a high temperature into a heat sink. The method is applicable to cooling a space capsule, with the heat exhausted into space. This concept and the thermodynamics of operation of the cell are described in the present report. The method is considered inventive at the present time, and a patent disclosure has been submitted.

3. Method of fuel cell operation in which the oxidant is chlorine trifluoride. The present report describes the experimental work done to date on this concept. It is considered an invention at present.

Monsanto Research Corporation will file a petition for waiver on the above-identified inventions in due course.